

Discovering the Potential of Microalgae-Bacterial Consortia for New Strategies in Fighting off Bacterial Biofilms

Dissertation

For achieving the degree of
Doctor rerum naturalium (Dr. rer. nat.)

Department of Microbiology and Biotechnology
Subdivision at the Faculty of Mathematics, Informatics and Natural Science
Universität Hamburg

Submitted by
Lutgardis Bergmann

Hamburg 2025

The following evaluators recommend the admission of the dissertation:

Prof. Dr. Wolfgang R. Streit

PD Dr. Ines Krohn

Day of oral defense: 28.08.2025

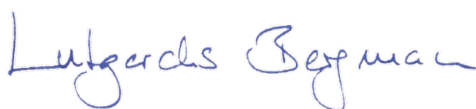
Affidavit

I hereby declare and affirm that this doctoral dissertation is my own work and that I have not used any aids and sources other than those indicated. If electronic resources based on generative artificial intelligence (gAI) were used in the course of writing this dissertation, I confirm that my own work was the main and value-adding contribution and that complete documentation of all resources used is available in accordance with good scientific practice. I am responsible for any erroneous or distorted content, incorrect references, violations of data protection and copyright law or plagiarism that may have been generated by the gAI.

Eidesstattliche Versicherung

Hiermit versichere ich an Eides statt, die vorliegende Dissertationsschrift selbst verfasst und keine anderen als die angegebenen Hilfsmittel und Quellen benutzt zu haben. Sofern im Zuge der Erstellung der vorliegenden Dissertationsschrift generative Künstliche Intelligenz (gKI) basierte elektronische Hilfsmittel verwendet wurden, versichere ich, dass meine eigene Leistung im Vordergrund stand und dass eine vollständige Dokumentation aller verwendeten Hilfsmittel gemäß der Guten wissenschaftlichen Praxis vorliegt. Ich trage die Verantwortung für eventuell durch die gKI generierte fehlerhafte oder verzerrte Inhalte, fehlerhafte Referenzen, Verstöße gegen das Datenschutz- und Urheberrecht oder Plagiate.

Hamburg, 26.06.2025



Lutgardis Bergmann

Contribution to published scientific research

Lutgardis Bergmann, Simone Balzer Le, Gunhild Hageskal, Lena Preuss, Yuchen Han, Yekaterina Astafyeva, Simon Loevenich, Sarah Emmann, Pablo Perez-Garcia, Daniela Indenbirken, Elena Katzowitsch, Fritz Thümmeler, Malik Alawi, Alexander Wentzel, Wolfgang R. Streit, Ines Krohn, **New diene lactone hydrolase from microalgae bacterial community - Antibiofilm activity against fish pathogens and potential applications for aquaculture** (2024), scientific reports, <https://doi.org/10.1038/s41598-023-50734-9>.

- Participation in planning, performance and evaluation of all experimental work
- Participation in evaluation and illustration of the bioinformatic data
- Participation in the design of the study and co-writing of the manuscript

Yekaterina Astafyeva, Marno Gurschke, Minyue Qi, Lutgardis Bergmann, Daniela Indenbirken, Imke de Grahl, Elena Katzowitsch, Sigrun Reumann, Dieter Hanelt, Malik Alawi, Wolfgang R. Streit and Ines Krohn, **Microalgae and bacteria interaction – Evidence for division of diligence in the alga microbiota** (2022), ASM Microbiology Spectrum, <https://journals.asm.org/doi/10.1128/spectrum.00633-22>

- Participation in planning and performance of experimental work
- Participation in co-writing and proof reading of the manuscript

Jascha F.H. Macdonald, Yuchen Han, Yekaterina Astafyeva, Lutgardis Bergmann, Marno Gurschke, Philipp Dirksen, Patrick Blümke, Yannik K. H. Schneider, Malik Alawi, Sebastian Lippemeier, Jeanette H. Andersen, and Ines Krohn, **Exploring Tetraselmis chui microbiomes - functional metagenomics for novel catalases and superoxide dismutases** (2025), Applied Microbiology and Biotechnology, <https://link.springer.com/article/10.1007/s00253-024-13395-w>

- Participation in planning and performance of experimental work
- Participation in co-writing and proof reading of the manuscript

Ines Krohn, Lutgardis Bergmann, Minyue Qi, Daniela Indenbirken, Yuchen Han, Pablo Perez-Garcia, Elena Katzowitsch, Birgit Hägele, Tim Lübcke, Christian Siry, Ralf Riemann, Malik Alawi and Wolfgang R. Streit, **Deep (Meta)genomics and (Meta)transcriptome Analyses of Fungal and Bacteria Consortia from Aircraft Tanks and Kerosene Identify Key Genes in Fuel and Tank Corrosion**, frontiers in Microbiology, <https://doi.org/10.3389/fmicb.2021.722259>

- Participation in planning and evaluation of all experimental work

- Participation in evaluation and illustration of the bioinformatically evaluated metagenome and transcriptome data
- Participation in the design of the study and co-writing of the manuscript


In work:

Lutgardis Bergmann, Pablo Perez-Garcia, Simone Balzer Le, Gunhild Hageskal, Yuchen Han, Sebastian Lippemeier, Malik Alawi, Alexander Wentzel, Wolfgang R. Streit & Ines Krohn (expected 2025), **Antimicrobial and Biofilm Inhibition Potentials in Microalgae-Bacteria Community Metagenomes - Highly Effective Candidates for Aquaculture Health Management**

- Participation in planning and evaluation of all experimental work
- Participation in evaluation and illustration of the bioinformatically evaluated metagenome data
- Participation in the design of the study and co-writing of the manuscript

Draft

Julia Gebert, Stefanie Böhnke-Brandt, Florian Zander, Daniela Indenbirken, Lutgardis Bergmann, Ines Krohn and Mirjam Perner (expected 2025), **Linking microbial community composition, microbial biomass and extracellular polymeric substances to organic matter liability gradients in the tidal Elbe River**, Science of the Total Environment, manuscript number: STOTEN-D-25-06894

Hamburg, 26.06.2025,  _____

Prof. Dr. Wolfgang R. Streit (Supervisor)

1 Table of Contents

2	Abstract.....	1
3	Zusammenfassung.....	3
4	Introduction	6
4.1	Biofilm architecture.....	6
4.2	Life cycle of biofilms	7
4.3	Key biofilm regulatory pathways	10
4.3.1	Two-component system	10
4.3.2	Quorum sensing.....	13
4.4	Challenges in medicine, industry and farming	15
4.5	Importance of the growing sector of aquaculture	16
4.5.1	Global production and consumption of aquatic animals.....	16
4.5.2	Development of aquaculture.....	17
4.5.3	Aquaculture systems	20
4.6	Ecologic and economic encounters in aquaculture	21
4.6.1	Land and freshwater restrictions.....	21
4.6.2	Water deterioration.....	21
4.6.3	Bacterial infections of farmed aquatic animals.....	22
4.6.4	Abuse of antibiotics in aquaculture	23
4.7	Alternatives to antibiotics in aquaculture.....	23
4.7.1	Vaccines	24
4.7.2	Bacteriophages	25
4.7.3	Quorum quenching.....	25
4.7.4	Bacteriocins	25
4.7.5	Probiotics	25
4.7.6	Chicken egg yolk immunoglobulin	26
4.7.7	Medicinal plant and immunostimulants	26
4.8	Microalgae and microalgae-bacterial consortia.....	27
4.9	Intention of this study	29
5	Material and methods.....	30
5.1	Bacterial and algal strains and cultivation conditions	30
5.2	Media and medium additives	30
5.2.1	Microalgae growth media	30
5.2.2	Bacteria growth media.....	33
5.2.3	Agar Plates	34
5.2.4	PBS.....	34
5.3	Storage and cultivation of bacteria and microalgae	34
5.3.1	Long term storage of bacteria.....	34

5.3.2	Cultivation of bacteria and microalgae.....	34
5.4	Molecular biological and bioinformatic methods	35
5.4.1	Vectors and primers used in this study.....	35
5.4.2	Total DNA extraction of microalgae for establishing metagenomes	37
5.4.3	Processing and analysis of DNA-seq reads - Sequencing and assembly	37
5.4.4	Cloning of <i>E. coli</i> DH5 α and <i>E. coli</i> Rosetta gami <i>pLysS</i> (DE3) for protein overexpression.....	38
5.4.5	Recombinant enzyme production in <i>E. coli</i> Rosetta gami 2 (DE3) and purification.....	41
5.4.6	RNA extraction for transcriptome establishment.....	42
5.5	Laboratory approaches to evaluate effects on bacterial growth and biofilm formation	43
5.5.1	Growth curves of bacterial pathogens incubated with microalgae supernatants	43
5.5.2	Static anti-biofilm assay.....	43
5.5.3	Laser scanning confocal microscopy	43
5.5.4	Observation of biofilm growth in oCelloScope™	44
5.5.5	Toxicity assays.....	44
6	Results and discussion.....	46
6.1	Microalgae supernatants	48
6.1.1	Static anti-biofilm assays.....	48
6.1.2	Effect of microalgae supernatants on growth curves of pathogenic bacteria....	50
6.1.3	Effect of microalgae supernatants on mature biofilms	51
6.1.4	Effects of microalgae supernatants visualized by LSCM	53
6.1.5	Composition of the microalgae supernatants.....	56
6.1.6	Current use of microalgae in fish farming	57
6.2	Metagenomic exploration of microalgae-bacterial consortia	59
6.2.1	Phylogenetic composition of microalgae-bacterial consortia.....	59
6.2.2	General key features of microalgae-bacterial consortia	62
6.2.3	Potential of highly interesting enzyme candidates for antibiofilm and quorum quenching agents in microalgae metagenomes.....	63
6.3	Novel dielactone hydrolase (Dlh3) from <i>Scenedesmus communis</i> metagenome	64
6.3.1	Quorum quenching.....	64
6.3.2	Characterization of the novel Dlh3.....	67
6.3.3	Effect of Dlh3 on biofilm formation of various fish pathogens.....	71
6.3.4	Transcriptome analysis of <i>E. anguillarum</i> in the presence of Dlh3.....	74
6.3.5	Inhomogeneous cell layers of <i>E. anguillarum</i> in the presence of Dlh3	76
6.3.6	Cell toxicity assays show no influence on fish cell line CHSE-214.....	79
6.4	Putative anti-biofilm enzymes from <i>T. chui</i> metagenome.....	80

6.4.1	5-methylcytosine-specific restriction endonuclease 28-84 McrA	81
6.4.2	8-oxoguanine deaminase 28-08 OxoD	84
6.4.3	Dienelactone hydrolase 28-50 Dlh.....	89
6.4.4	Toxicity assay with <i>Galleria mellonella</i>	94
6.5	Outlook.....	95
7	References.....	96
8	Supplemental	109
9	Acknowledgements	116

2 Abstract

Bacterial biofilms are comparable to organs complex structures that provide protection and nutrition to their inhabitants. The biofilm matrix shields embedded bacteria by trapping antibiotics, toxins and agents of the host immune system at the surface while inside the biofilm bacteria enhance their endurance through genetic exchange, physiological heterogeneity and metabolic reduction. Due to their highly resilient character, biofilms cause severe and costly problems in industry, farming and health care, with this study focusing particularly on challenges of the fast-growing sector of aquaculture. Facing the limited number of available antibiotics and in contrast the constantly growing antibiotic resistance in bacteria, new strategies are inevitable to address pathogenic bacteria and their sheltering surrounding.

Microalgae are small, unicellular organisms that successfully inhabit all kinds of aquatic environments displaying a worldwide distribution. Their cooperative lifestyle with beneficial bacteria shelters their survival in challenging environments and protects them efficaciously from pathogenic threads. Up to date little is known about the composition and the intrinsic potential of these microalgae-bacterial consortia. Hence, the present study focused on the potential of microalgae-bacterial consortia to influence biofilm formation of pathogenic bacteria. This question was addressed by data mining of newly established metagenomes and by practical application. First approaches made use of the total supernatant of various microalgae cultures to find out if there is any effect on bacterial biofilms proved by static anti-biofilm assay and, as effects were measurable, which microalgae's supernatant showed the highest inhibiting effect in terms of biofilm reduction. Of 17 marine and freshwater microalgae cultures (data not entirely shown) the six candidates with the highest inhibitory results on bacterial biofilms of *Pseudomonas aeruginosa* PA14, *Burkholderia cenocepacia* K56-2, *Stenotrophomonas maltophilia* K279a, *Stenotrophomonas maltophilia* SM454 and *Klebsiella pneumoniae* WT1617 were chosen for further investigation. The supernatant of the marine microalgae *Tetraselmis chui* reduced biofilm in all tested bacteria significantly by an average of 57.2%. Biofilm inhibition, if only for certain bacterial species each, was also observed for the supernatants of the marine microalgae *Nannochloropsis salina*, *Isochrysis galbana* and *Isochrysis* spec. as well as for the freshwater microalgae *Chlorella vulgaris*, and *Scenedesmus acuminatus*. The inhibitory potential of the total supernatants of microalgae cultures on the biofilm of *P. aeruginosa* PA14 was explored more deeply by laser scanning confocal microscopy (LSCM). Calculations of total cell numbers within a defined biofilm area revealed a decrease of 25% of *P. aeruginosa* cells after treatment with *T. chui* supernatant and alterations in biofilm architecture towards lower biofilm density.

Metagenomes of the six effective microalgae were prepared to first enlighten the phylogeny of the bacterial communities encompassing the individual microalgae and second to elucidate their enzymatic potential. Though all of the microalgae-bacterial consortia showed a prevalent

fraction of proteobacteria with an emphasis on alphaproteobacteria, particularly apparent in *T. chui*, *I. galbana* and *C. vulgaris*, the composition of the consortia on genus level occurred highly divers. Only the marine bacteria *Roseobacter*, *Roseovarius*, *Muricauda* and *Marinobacter* appeared repeatedly within the metagenomes. Promising enzyme classes were explored and quantified for current and future use. Since bacterial biofilms promote virulence and decrease antibiotic susceptibility a multifaceted approach seems to be required to either alter the biofilm architecture for better access of classic antibiotics to the embedded pathogens or to weaken and ideally inhibit the process of biofilm formation. Hence, the metagenome data of the six microalgae-bacterial consortia should serve as a valuable toolbox for advances to interfere with key points in biofilm formation such as quorum sensing, initial attachment or accumulation of EPS (extracellular polymeric substances) with special regard to the role of extracellular DNA. First experiences with a microalgae-metagenome-derived enzyme were gained with a putative quorum quenching diene lactone hydrolase (Dlh3). Due to its intended application in aquaculture, Dlh3 was administered to the fish pathogens *Edwardsiella anguillarum*, *Aeromonas salmonicida*, *P. aeruginosa*, *Flavobacterium columnare* and *Flavobacterium psychrophilum*. Interactions of Dlh3 and the fish pathogens were analyzed in static anti-biofilm assays, LSCM, and oCelloScope, revealing decreased biofilm formation, e.g., for *E. anguillarum* of up to 54.4% in static anti-biofilm assay and alterations in biofilm construction in optical approaches. Encouraged by these impressions more target-specific enzymes were chosen from the newly prepared metagenome data of microalgae-bacterial consortia. The successfully overexpressed enzymes, a methylcytosine-specific restriction endonuclease, that cleaves DNA in a specific, modified context, an 8-oxoguanine deaminase, that alters external DNA and a second diene lactone hydrolase were characterized by phylogenetic and structural attributes. First applications of the enzymes on fish pathogens, analyzed by LSCM, had considerable effects on the viability and structure of the observed biofilms. Considering the harmlessness of the enzymes stated in toxicity assays, this study might be a path-breaking approach for a versatile attack on pathogenic biofilms to avoid bacterial adaptation and resistance to antibiotic treatment and simultaneously, by harboring a wide-range enzymatic toolbox, maintaining the flexibility to react to changing demands e.g. in the context of high-density farming as for aquaculture.

3 Zusammenfassung

Bakterielle Biofilme weisen vergleichbar mit Organen komplexe Strukturen auf, die den innewohnenden Bakterien Schutz und Nahrung gewähren. Die Biofilm Matrix schützt die Bakterien im Biofilm indem sie Antibiotika und Angriffe des Wirts' eigenen Immunsystems abfängt, während die Bakterien im Biofilm ihre Lebensfähigkeit durch genetischen Austausch, physiologische Heterogenität und Reduzierung des metabolischen Umsatzes steigern. Durch ihren starken protektiven Charakter verursachen Biofilme große Schäden und hohe Kosten in Industrie, Tierzucht und im Gesundheitswesen. Ein besonderes Augenmerk legt diese Studie auf die Herausforderungen im schnell wachsenden Sektor der Aquakultur. Im Bewusstsein der begrenzten Verfügbarkeit von und der stetig wachsenden Resistenz gegen die angewandten Antibiotika, ist es unerlässlich, neue Strategien gegen krankheitserregende Bakterien und ihre schützende Umgebung zu entwickeln.

Mikroalgen sind kleine, einzellige Organismen, die mit ihrer weltweiten Ausbreitung erfolgreich alle Arten von aquatischen Lebensräumen bewohnen. Die Kooperation mit Bakterien sichert ihr Überleben in herausfordernden Lebensräumen und schützt sie weitgehend vor Pathogenen. Über die Zusammensetzung der Mikroalgen-Bakterien-Gemeinschaften ist bisher wenig bekannt. Diese Studie untersucht daher eingehend das Potential von Mikroalgen-Bakterien-Gemeinschaften, Einfluss auf die Bildung von Biofilmen pathogener Bakterien zu nehmen. Dafür wurden Daten von neu etablierten Mikroalgen-Metagenomen analysiert und verschiedene praktische Anwendungen erprobt. Zunächst wurde der komplette Überstand von Mikroalgenkulturen genutzt um festzustellen, ob ein Effekt auf die Biofilmbildung pathogener Bakterien in einem statischen Anti-Biofilm-Assay messbar wäre, und welche Mikroalgenkulturen die stärkste biofilmreduzierende Wirkung erzielten. Von 17 getesteten marinen und Süßwasser Mikroalgenkulturen (Daten nicht vollständig dargestellt) wurden die sechs Kulturen mit der stärksten inhibitorischen Wirkung auf die Biofilme der Bakterien *Pseudomonas aeruginosa* PA14, *Burkholderia cenocepacia* K56-2, *Stenotrophomonas maltophilia* K279a, *S. maltophilia* SM454 und *Klebsiella pneumoniae* WT1617 für weitere Untersuchungen ausgewählt. Der Überstand der Mikroalge *Tetraselmis chui*, zeigte eine biofilmreduzierende Wirkung auf alle getesteten Bakterien mit einer durchschnittlichen Verminderung um 57.2%. Biofilminhibition, wenn auch jeweils nur für einzelne Pathogene, zeigten darüber hinaus die marinen Mikroalgen *Nannochloropsis salina*, *Isochrysis galbana* und *Isochrysis spec.* sowie die Süßwasser Mikroalgen *Chlorella vulgaris* und *Scenedesmus acuminatus*. Das inhibitorische Potential der kompletten Überstände von Mikroalgenkulturen auf den Biofilm von *P. aeruginosa* PA14 wurde tiefergehend mittels Laser scanning confocal microscopy (LSCM) ermittelt. Eine 25%ige Reduktion der absoluten Zellzahlen innerhalb eines definierten Bereichs eines *P. aeruginosa* Biofilms konnte nach Zugabe des Überstands der

Mikroalge *T. chui* berechnet werden. Gleichzeitig veränderte sich die Architektur des *P. aeruginosa* Biofilms in Richtung einer geringeren Dichte.

Von den sechs wirkungsvollen Mikroalgen wurden Metagenome angefertigt, um die Phylogenie der kooperierenden Bakterien zu ergründen, sowie Einblicke in das enzymatische Potential der Mikroalgen-Bakterien-Gemeinschaften zu gewinnen. Trotzdem sich in allen Metagenomen ein hoher Anteil an Proteobakterien, vor allem Alpha Proteobakterien zeigte, insbesondere bei *T. chui*, *I. galbana* und *C. vulgaris*, herrschte auf Genus-Level hohe Diversität. Einzig die marinen Bakterien *Roseobacter*, *Roseovarius*, *Muricauda* und *Marinobacter* waren in mehreren Metagenomen nachweisbar. Des Weiteren wurden mögliche wirkungsvolle Enzyme in den Metagenomdaten für aktuelle und zukünftige Anwendungen klassifiziert und quantifiziert. Da Biofilme bakterielle Virulenz verstärken und die Empfindlichkeit gegenüber antibakteriellen Substanzen verringern scheint nur ein breitgefächelter Ansatz erfolgsversprechend, um entweder die Biofilmarchitektur aufzubrechen und klassischen Antibiotika den Zugang zu den Bakterien zu erleichtern oder um den Prozess der Biofilmbildung zu schwächen, im besten Falle sogar zu unterbinden. Die Metagenomdaten sollten daher als Werkzeugkasten dienen, Schlüsselstellen in der Biofilmbildung wie das Quorum Sensing, die initiale Anheftung oder die Anreicherung von EPS (extracellular polymeric substances) anzugreifen. Ein besonderes Augenmerk sollte auf die Rolle der extrazellulären DNA gerichtet werden.

Erste Erfahrungen mit einem Enzym, das auf Grundlage eines Mikroalgenmetagenoms entwickelt wurde, konnten mit einer Dienlacton Hydrolase (Dlh3) gewonnen werden, die wahrscheinlich im Sinne des Quorum Quenchings wirkt. Im Hinblick auf deren Anwendbarkeit im Aquakultur-Sektor wurde Dlh3 an den Fischpathogenen *Edwardsiella anguillarum*, *Aeromonas salmonicida*, *P. aeruginosa*, *Flavobacterium columnare* und *Flavobacterium psychrophilum* erprobt. Die Wirkung der Dlh3 auf die Fischpathogene wurde in statischen Anti-Biofilm-Assays, LSCM und dem oCelloScope getestet. Um bis zu 54.4% konnte die Biofilmbildung z.B. in *E. anguillarum* reduziert werden, einhergehend mit Veränderungen der Biofilmarchitektur, die in den optischen Verfahren deutlich wurden. Ermutigt durch die gewonnenen Erkenntnisse, wurden weitere zielgerichtete Enzyme in den neu etablierten Metagenomdaten der Mikroalgen-Bakterien-Gemeinschaften gesucht. Die erfolgreich überexprimierten Enzyme, eine Methylcytosin-spezifische Restriktionsendonuclease, die DNA an spezifisch modifizierten Basen schneidet, eine 8-Oxoguanin Deaminase, die extrazelluläre DNA modifiziert und eine zweite Dienlacton Hydrolase wurden phylogenetisch und strukturell charakterisiert. Erste Anwendungen der Enzyme auf Fischpathogenen zeigten deutliche Effekte auf die Überlebensfähigkeit der bakteriellen Zellen im Biofilm und auf die Strukturen der Biofilme im LSCM. In Anbetracht der Unschädlichkeit der untersuchten Enzyme für eukaryotische Zellen, die in Toxizitätstests bewiesen wurde, könnte diese Studie ein

wegweisender Ansatz für einen vielfältigen Angriff auf bakterielle Biofilme sein, der die Gefahr der Resistenz vermindert und gleichzeitig, durch den Charakter eines variablen Werkzeugkastens die Flexibilität erhält, auf wechselnde Bedürfnisse zu reagieren, wie sie in Tierzucht mit hoher Dichte, wie der Aquakultur, zu erwarten sind.

4 Introduction

Life on earth is an ongoing fight for colonizing habitats. Bacteria invading living organisms can have various outcomes from beneficial to deathly. Consequently, host and bacteria are in enduring competition for the most successful mechanisms to ensure their survival. The invention of antibiotics in 1929 (Fleming, 1929) was a milestone in fighting off pathogenic bacteria but conclusively only enlarged the bacterial strategic arsenal. Their plasticity allowed bacteria to adapt to the antibiotic threat by developing e.g. enzymes that either modify or degrade antibiotics, mechanisms to reduce drug uptake or to enhance drug export, as well as efforts to modify and protect the target of the antibiotic drug (Sionov & Steinberg, 2022). This protective potential is even extended by the bacterial capacity to build up and live in biofilms. This work aims to highlight some advantageous traits of biofilm lifestyle and tries to figure out weak points to address with the intention of supporting or replacing the challenging work of antibiotics.

4.1 Biofilm architecture

Biofilms are structurally and dynamically complex biological systems providing homeostasis and survival in hostile environments. First evidence for biofilm formation dates early in the fossil record. Putative biofilm colonies have been identified in the 3.3-3.4-billion-year-old South African Kornberg formation as well as in the 3.2-billion-year-old deep-sea hydrothermal rocks of the Pilbara Craton, Australia (Hall-Stoodley, Costerton, & Stoodley, 2004; Rasmussen, 2000). The emergence of primitive biofilms appears to have coincided with the first evidence of the transition from unicellular to multicellular organization, which suggests that bacteria, transformed into a biofilm lifestyle, might have been the first multicellular life forms (de la Fuente-Nunez, Reffuveille, Fernandez, & Hancock, 2013). The transition from planktonic to biofilm growth might have happened as an adaptation to environmental stress, enabling a greater ability to withstand the harsh conditions of the primitive earth (de la Fuente-Nunez et al., 2013). Biofilm formation therefore appears as an environmentally driven development that increases resistance to exogenous stresses, providing bacterial survival under unfavorable conditions (de la Fuente-Nunez et al., 2013), which could be nowadays the immune system of an infected host or the use of antimicrobial drugs. What kind of extracellular cue drives attachment is highly dependent on the individual species. Factors like nutrient deprivation, cation availability or a mucin-rich environment may enhance attachment for one species while impeding it for others (Petrova & Sauer, 2012).

The complex architecture of biofilms includes sessile bacteria concentrated at an interface (usually solid-liquid, air-liquid or solid-air), surrounded by a self-produced matrix of extracellular polymeric substances (EPS) which is mainly composed of polysaccharides, proteins, and extracellular deoxyribonucleic acid (eDNA) (Flemming et al., 2024; Jahn, 1999). The whole biofilm structure is interspersed with open water and nutrition channels (de Beer, Stoodley,

Roe, & Lewandowski, 1994; Lawrence, Korber, Hoyle, Costerton, & Caldwell, 1991). Unlike an inert mass, it represents a highly hydrated, open system in constant interaction with its environment, like a sponge, sequestering dissolved and particulate matter. Even more, the matrix acts as a recycling yard by keeping the components of lysed cells available. eDNA represents a reservoir of genes for horizontal gene transfer and particulate substrates can be degraded by extracellular enzymes after being trapped owing to the sticky properties of the biofilm matrix (Flemming et al., 2024; Flemming & Wingender, 2010). Finding potential attack points needs a profound knowledge of the development of biofilm formation, the very specific bacterial behavior inside the biofilm, and the challenging but favorable biofilm conditions.

4.2 Life cycle of biofilms

The original model of biofilm formation, based on studies of *P. aeruginosa* by Flemming in 2008 proposed a cyclic process that occurs in a five-stage-specific and progressive manner, as depicted in Figure 1 (Flemming, 2008; Sauer et al., 2022).

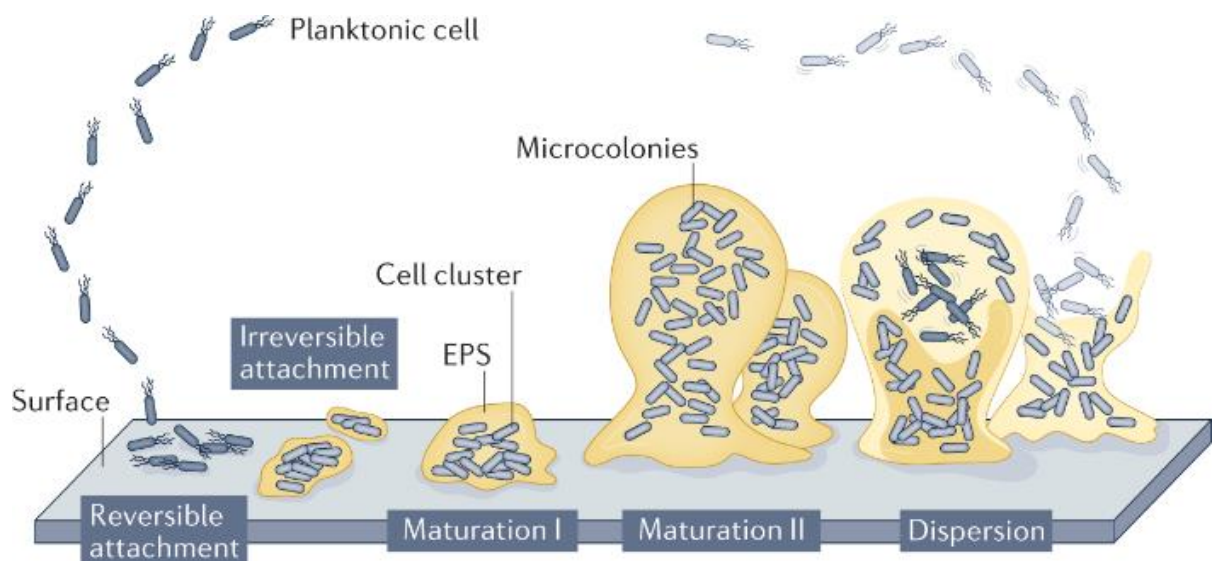
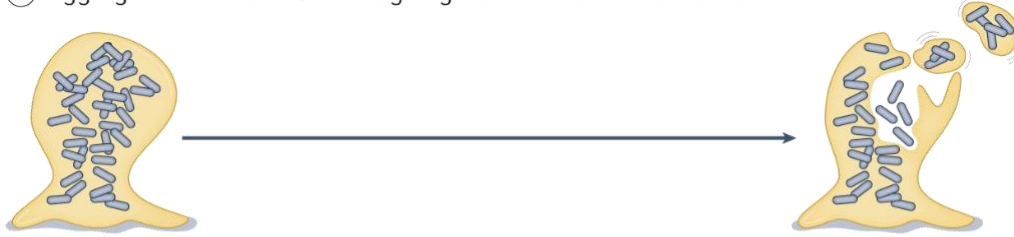


Figure 1: Original five-step model of biofilm development. Based on investigations of *P. aeruginosa* the model proposed a cyclic process initiated by surface contact by single planktonic cells. Transition from reversible to irreversible attachment coincided with a reduction in flagella gene expression and the production of matrix components. Maturation stages I and II were characterized by the appearance of smaller cell clusters and larger microcolonies, respectively. Dispersion was related to degradation of matrix components and regained motility of dispersed bacterial cells (Flemming, 2008; Sauer et al., 2022).

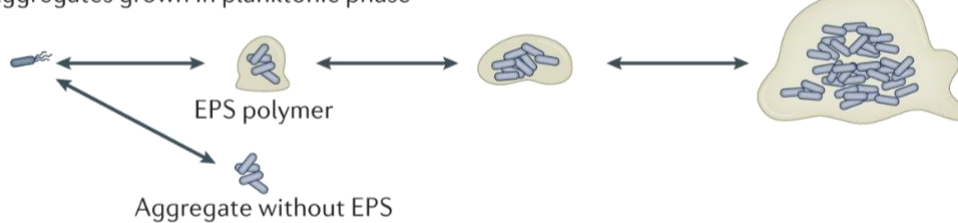
The first stage of reversible attachment was characterized by cells attaching to a surface by a single pole, while detachment and returning to the planktonic phase were still observed. A more stable surface existence constituted once rod-shaped cells attached via their longitudinal axis, ceased mobility and started the production of EPS, referred to as irreversible attachment,

the second stage. Maturation stages I and II are characterized by development from monolayer to multilayer architecture, structured organization with microcolonies, interspersed by fluid-filled channels and adaptation of the bacterial metabolism to changes in their microenvironment driven by cellular crowding as well as chemical, nutritional and pH gradients (Stewart & Franklin, 2008). Flemming defined maturation I with clusters growing thicker than 10 μm and maturation II, the penultimate stage, with clusters reaching approximately 100 μm . Finally, due to degradation of matrix components, single cells left the biofilm structure and returned to planktonic mode by a process referred to as dispersion (Flemming, 2008; Rumbaugh & Sauer, 2020). Using the term seeding dispersal implied that the disseminated bacteria started the colonization of new locations (Purevdorj-Gage, Costerton, & Stoodley, 2005). Due to its intuitive simplicity, this model was quickly accepted as a base for scientific research but needs a closer and more differentiated look for adaptations to real-world environments beyond the petri dish, like wounds or industrial components and for understanding biofilm formation of microbes other than *P. aeruginosa*. The proposed mushroom shape of biofilms, derived from observations of the growth of *P. aeruginosa* in flow cells, must be expanded to a wide variety of biofilm architectures up to microbial mats, which can be highly stratified along horizontal layers (Prieto-Barajas, 2018). Even the shapes of *P. aeruginosa* biofilms vary highly from flat to streamer-formed surfaces, depending on growth medium and flow rate conditions (Sauer et al., 2022). Either way, the original five-step model obligatory presents biofilms attached to a surface. This motivated researchers to investigate antibacterial and anti-adhesive surfaces or to use biofilm attachment structures as a target to attack biofilm formation. However, the surface-attached biofilm is not a mandatory form of appearance. Biofilms in the environment are often free-floating, form aggregates, granules or fluid-embedded aggregates as apparent in wastewater treatment processes (Trego, 2020) or present in marine, lake and river habitats (Flemming & Wuertz, 2019). Examples of embedded aggregates include bacteria in host material such as mucus from the lungs of patients with cystic fibrosis or slough in the chronic wound bed. (Sauer et al., 2022). Even the conceptual separation between planktonic growing bacteria in shaken liquid cultures and bacteria growing in static biofilms is merely a theoretical approach, as bacteria can grow as a mixture of planktonic and aggregate cells in liquid batch cultures (Schleheck et al., 2009). Currently, five mechanisms are proposed for the formation of floating aggregates as shown in Figure 2 (Sauer et al., 2022).

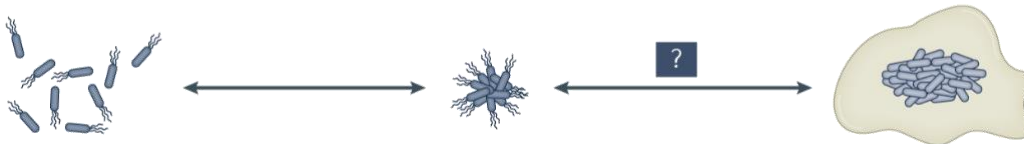
① Aggregates formed due to sloughing from surface-attached biofilm



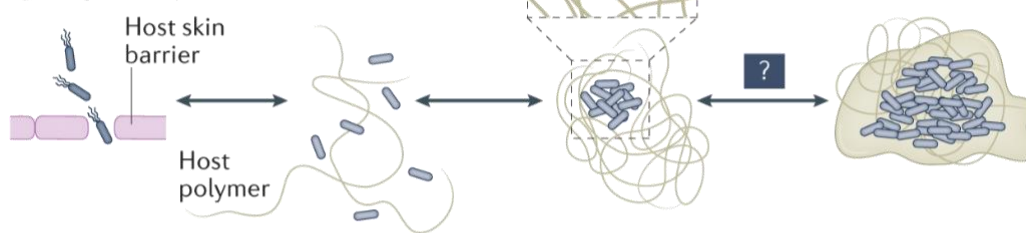
② Aggregates grown in planktonic phase



③ Aggregate formation initiated through cell surface components of single cells



④ Polymer depletion



⑤ Polymer bridging

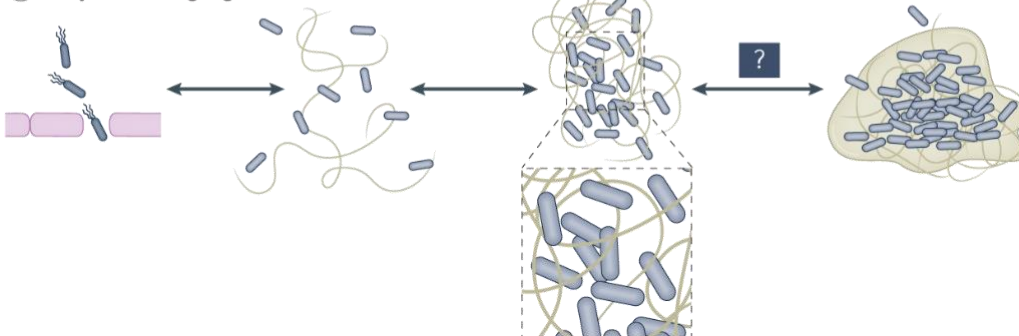


Figure 2: Different mechanisms for generating free-floating biofilm-like aggregates. (1) Sloughing detachment of aggregates from attached biofilms. (2) Clonal growth in the liquid, with or without facilitation by bacterially produced EPS. (3) Auto- or co-aggregation (single species or multiple species, respectively), whereby bacteria attach to each other through mutual attraction of surface molecules, such as adhesins or EPS bridging interactions, followed by clonal growth and EPS production. (4) Polymer depletion-driven aggregation. Under high concentrations of polymers, phase separation occurs and the polymers and cells separate out such that the polymers surround groups of aggregated cells. In the case of bacteria entering a wound, the polymers can be produced by the host as is the case for hyaluronic acid (Gilbertie et al., 2019; Secor, Michaels, Ratjen, Jennings, & Singh, 2018). (5) Polymer bridging aggregation occurs when polymers in the liquid environment form bridges that connect individual cells, such as fibronectin in synovial fluid (Macias-Valcayo et al., 2021; Sauer et al., 2022).

The first mechanism of aggregate formation is the detachment of pieces of an attached biofilm due to physical abrasion, nutrient reduction, hydrodynamic shear or endogenously produced dispersal agents, a process often referred to as ‘sloughing’ (Hall-Stoodley & Stoodley, 2005). The second and third mechanisms face growth in the planktonic phase. After cell division, the daughter cells remain with the mother cell rather than dispersing, presumably through interactions of self-recognizing cell surface adhesion molecules or simultaneous production of EPS, respectively (Kragh et al., 2018). Aggregates then recruit further planktonic cells, which results in larger aggregates that eventually seed smaller aggregates which again recruit planktonic cells resulting in a so-called ‘snowball effect’ of aggregate formation (Kragh et al., 2018). The fourth mechanism refers to ‘depletion aggregation’, which occurs as an entropically driven interaction between polymers and bacteria (Dorken, Ferguson, French, & Poon, 2012). Highly abundant at chronic infection sites, polymers cause single bacterial cells in suspension to ‘push out’ polymers between the bacterial cells, driven by entropy gains that become realized, when the space available for polymer movement is enlarged. Rod-shaped bacteria like *P. aeruginosa* were found to typically align laterally as they come close together to maximize space and entropy gains. The fifth mechanism for aggregation is that bacteria bind to molecules in host fluids through surface adhesion interactions as an interaction between bacterial factors, such as adhesin proteins, and host factors like fibrinogen, fibronectin and hyaluronic acid. Host fluids like synovial fluid and human serum can induce rapid bacterial aggregation by forming these bridging connections (polymer bridging) (Macias-Valcayo et al., 2021). Clonal growth of trapped bacteria leads to a continually increasing aggregate size (Sauer et al., 2022). Formation of free-floating bacterial aggregates was observed in several conditions and probably will modify the search of targets for prevention or elimination, as there are signs that the formation of aggregates does not require the entire change in gene expression for biofilm formation but it still does cause bacteria to become less susceptible to antibiotics (Beloin & Ghigo, 2005; Secor et al., 2018). Certainly, it is worth taking a glance at the inner regulation systems of the bacterial cell to understand how bacteria can perceive and react to environmental signals.

4.3 Key biofilm regulatory pathways

4.3.1 Two-component system

The developmental progression from first surface attachment by planktonic bacteria leading to a mature biofilm not only coincides with observable phenotypic changes but also requires alterations in gene expression affecting e.g. protein production and resistance to the host immune system or antimicrobial agents (Petrova & Sauer, 2012). Since initiation of biofilm formation is assumed to depend on environmental stimuli it is worth reflecting how bacteria perceive their surroundings. In general, bacteria use two-component systems (TCSs), which

were intensively studied in *P. aeruginosa*, to translate external signals into adaptive responses by a variety of mechanisms (Mikkelsen, Sivaneson, & Filloux, 2011) (Figure 3).

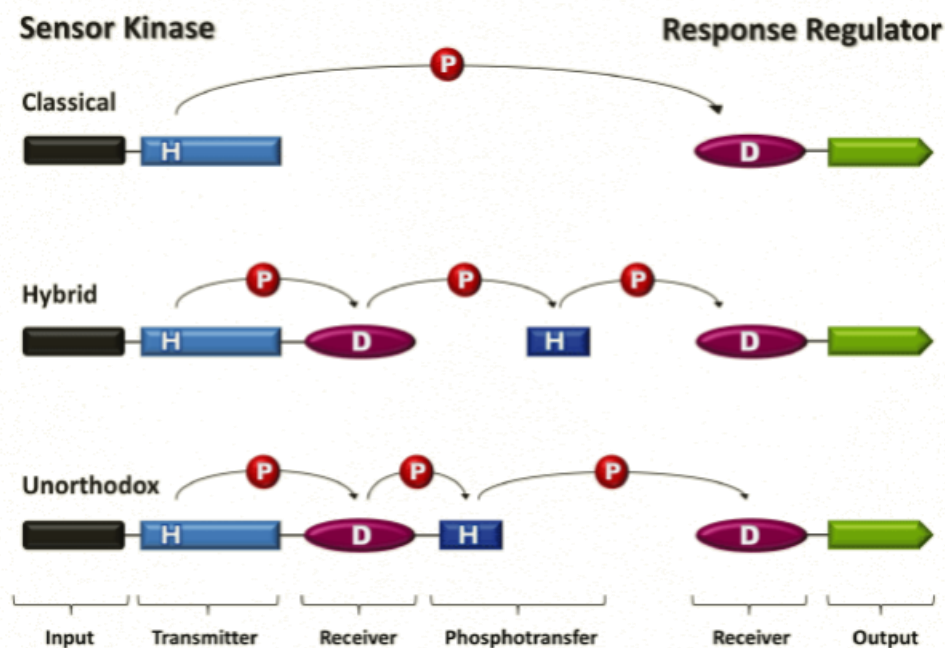


Figure 3: Domain organization of two-component regulatory systems in *P. aeruginosa*. Histidine sensor kinases can be divided into three groups: classical, hybrid and unorthodox (Rodrigue, Quentin, Lazdunski, Mejean, & Foglino, 2000). A classical sensor consists of an N-terminal input domain (dark brown), followed by a transmitter domain (light blue) with a conserved histidine (H) that can be auto-phosphorylated. The phosphoryl group (P) can then be transferred onto a conserved aspartate residue (D) in the receiver domain (purple) of the response regulator. This activates the output domain (green), which is commonly a DNA binding domain. Hybrid and unorthodox sensors contain an additional C-terminal receiver domain and therefore require an external phosphotransfer (Hpt) module (dark blue) in order to phosphorylate the response regulator. In the unorthodox sensor, the Hpt module is an integral part of the protein, while hybrid sensors require an independent Hpt protein in order to phosphorylate the response regulator (Rodrigue et al., 2000).

TCSs consist of a sensor kinase and a response regulator and are considered to be the predominant signaling mechanism in most bacteria. Sensor kinases that enable bacteria to monitor environmental conditions, such as nutrients, temperature, pH, osmolarity or the presence of toxic substances are often membrane-bound, but can also be cytosolic (Mikkelsen et al., 2011). They consist of a variable N-terminal input domain (dark brown) and a conserved C-terminal transmitter domain (light blue) located in the cytosol (Rodrigue et al., 2000). Response regulators have a conserved N-terminal receiver domain (purple), which is most often followed by a C-terminal output domain (green) with a helix-turn-helix (HTH) motif that is able to bind DNA (Stock, Robinson, & Goudreau, 2000). Upon detection of a signal, the sensor kinase auto-phosphorylates on a conserved histidine (H) residue in the transmitter domain, and the phosphoryl is transferred onto a conserved aspartate (D) residue in the receiver domain of the response regulator, thereby activating it as a transcription factor (R. Gao & Stock, 2009). While the classical TCS transfers the phosphoryl directly to the response regulator, the hybrid and the unorthodox TCS require an additional phosphotransfer (Hpt)

module to phosphorylate the response regulator. Several hallmarks of changing gene expression towards biofilm formation are considered to be under the regulation of TCSs (Mikkelsen et al., 2011). One intensively studied example is the GacS/GacA-RsmA system which was found to orchestrate the transition between acute infection and chronic infection, of *P. aeruginosa* in patients with cystic fibrosis (CF) (Bhagirath et al., 2017). While acute infection was associated with motility and release of toxic effector proteins, chronic infection was associated with biofilm formation as depicted in Figure 4.

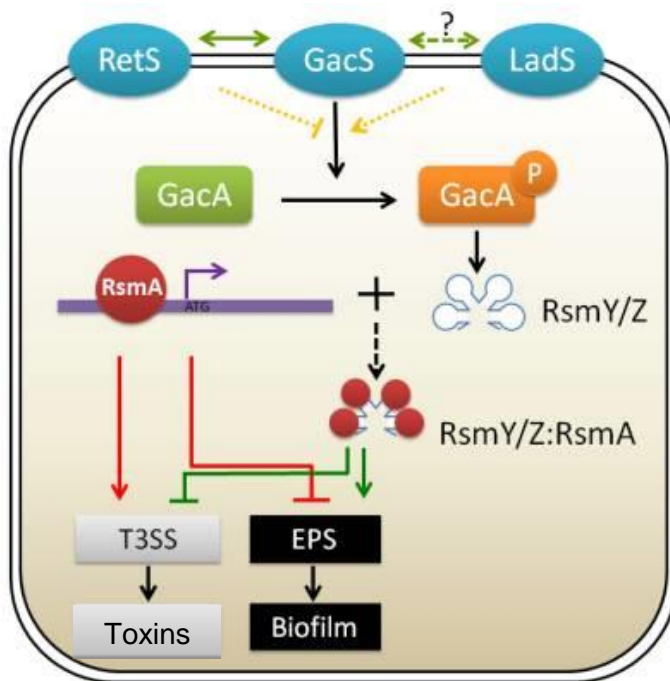


Figure 4: Schematic diagram of the two-component system regulation of biofilm formation in *P. aeruginosa* (Wei & Ma, 2013). Environmental cues received by the input domains of the three membrane-associated sensor kinases (GacS, LadS and RetS) activate or repress the expression of genes necessary for acute or chronic infection. Free regulatory protein RsmA binds to mRNAs, thus repressing translation of biofilm-associated mRNAs and enhancing T3SS and bacterial motility (Red lines) during acute infection. When the response regulator GacA is phosphorylated by the upstream sensor kinase GacS, the production of small regulatory RNAs *rsmZ* and *rsmY* are stimulated, followed by sequestration of RsmA protein, which ultimately de-represses the expression of biofilm-related genes and represses the production of acute-phase related factors (Green lines). The signaling cascade going through RetS generates more free RsmA, resulting in T3SS activation and biofilm repression (Red lines). T3SS, type III secretion system. P, phosphorylated state of GacA. Dark red circle indicates RsmA protein (Wei & Ma, 2013).

GacS functions as a sensor kinase, receiving environmental information, GacA serves as a cognate response regulator. Once GacS is autophosphorylated, the phosphorelay from GacS to GacA activates the production of small RNAs RsmY and RsmZ, which are antagonists of the mRNA-binding regulator RsmA. RsmA regulates the Type III secretion system (T3SS), the bacterial secretion system for toxic effector proteins, motility, and biofilm formation post-transcriptionally by inhibiting translation in a dose-dependent manner. Free RsmA binds to mRNA hence, positively controls motility and the expression of genes in T3SS, a hallmark of acute infection, while RsmA which was sequestered by the small RNAs RsmY and RsmZ

enhances the production of exopolysaccharides and biofilm formation (Brencic & Lory, 2009; Wei & Ma, 2013). Moreover, TCS drive the important trait of bacterial communication, as elucidated in the following.

4.3.2 Quorum sensing

The background of quorum sensing in Gram-negative bacteria was originally detected in 1970 by Nealson, Platt and Hastings in an attempt to better understand the phenomenon of bioluminescence and the control of luciferase synthesis in *Photobacterium fischeri* (today *Aliivibrio fischeri*) (Nealson, Platt, & Hastings, 1970). The authors assigned the control of luciferase to the level of transcription, discussed an underlying operon system, and created the term 'autoinduction'. 'Quorum' was later defined as the minimum behavioral unit of bacteria, as it was described, that certain bacterial behaviors could be performed efficiently only by a sufficiently large population (Fuqua, Winans, & Greenberg, 1994). Today quorum sensing is understood as a cell-to-cell communication process, enabling orchestrated, collective behavior including bioluminescence (Bassler, Wright, & Silverman, 1994), virulence factor production (Bronesky et al., 2016), secondary metabolite production (Barnard et al., 2007), competence for DNA uptake (Kleerebezem, Quadri, Kuipers, & de Vos, 1997; Okada et al., 2005) and biofilm formation (Mukherjee & Bassler, 2019). In general quorum sensing is mediated by the production, release, accumulation and group-wide detection of extracellular signaling molecules called autoinducer (AI), allowing bacteria to count their population density and control their behavior in response to variations in cell numbers (Bassler & Losick, 2006). Gram-negative bacteria use small molecules as autoinducers and two types of receptors, cytoplasmic transcription factors or transmembrane two-component histidine sensor kinases, while Gram-positive bacteria use oligopeptides as autoinducers and transmembrane two-component histidine sensor kinases as receptors (Novick & Geisinger, 2008). Autoinducers of Gram-negative bacteria were first identified by Eberhard et al. in 1981 as *N*-(3-oxo-hexanoyl)-3-aminodihydro-2(3*H*)-furanone, commonly called acyl homoserine lactones (AHLs), isolated from cell-free supernatant of a *P. fischeri* culture. AHLs were found to be produced by LuxI-type autoinducer synthases and detected by cognate LuxR proteins, which were initially discovered in *Vibrio fischeri* as part of the light-producing *lux* operon (Engebrecht, Nealson, & Silverman, 1983; Engebrecht & Silverman, 1984). The AI molecule is secreted into the extracellular environment of a bacterial cell. At a low cell density, AI levels remain low and pathways for individual behaviors are activated (Mukherjee & Bassler, 2019). With growing population density, the AI molecules accumulate and diffuse back into the bacterial cells where they bind to and induce the LuxR-type response regulator to transcribe genes of the *lux* operon in a positive circuit manner, logarithmically enhanced by auxiliary promoting the synthesis of AI. After a threshold concentration is reached, the entire bacterial group reacts with a population-wide alteration in gene expression, leading to a function mode as a multicellular

organism, with minute exceptions discussed below (Bassler & Losick, 2006). While the *lux* operon controls the production of light in *V. fischeri*, in many pathogenic bacteria such as *P. aeruginosa*, virulence and biofilm-associated genes are under the control of homologous operons, as part of the quorum sensing feedback loop (Pearson et al., 1994). It turned out that in general bacteria try to keep their quorum sensing conversations private, hence, species of Gram-negative bacteria produce and detect a huge variety of structures of AHLs, differing e.g., in chain length or number of carbonyl groups (Bassler & Losick, 2006). Examples of signaling molecules are shown in Figure 5. *P. aeruginosa* e.g., uses AHLs of the type butyryl-homoserine lactone (C4-HSL) and 3-oxo-dodecanoyl-homoserine lactone (C12-HSL) which are produced and detected by the LuxRI homologs LasRI as illustrated in Figure 6. The virulence response of Gram-positive bacteria such as *Staphylococcus aureus* was shown to be analogously regulated by a density-sensing system. The *agr* locus produces and is induced by the cyclic signaling octapeptide AIP, which varies slightly in amino acid composition among different *S. aureus* strains (G. Ji, Beavis, & Novick, 1995; Malone, Boles, & Horswill, 2007).

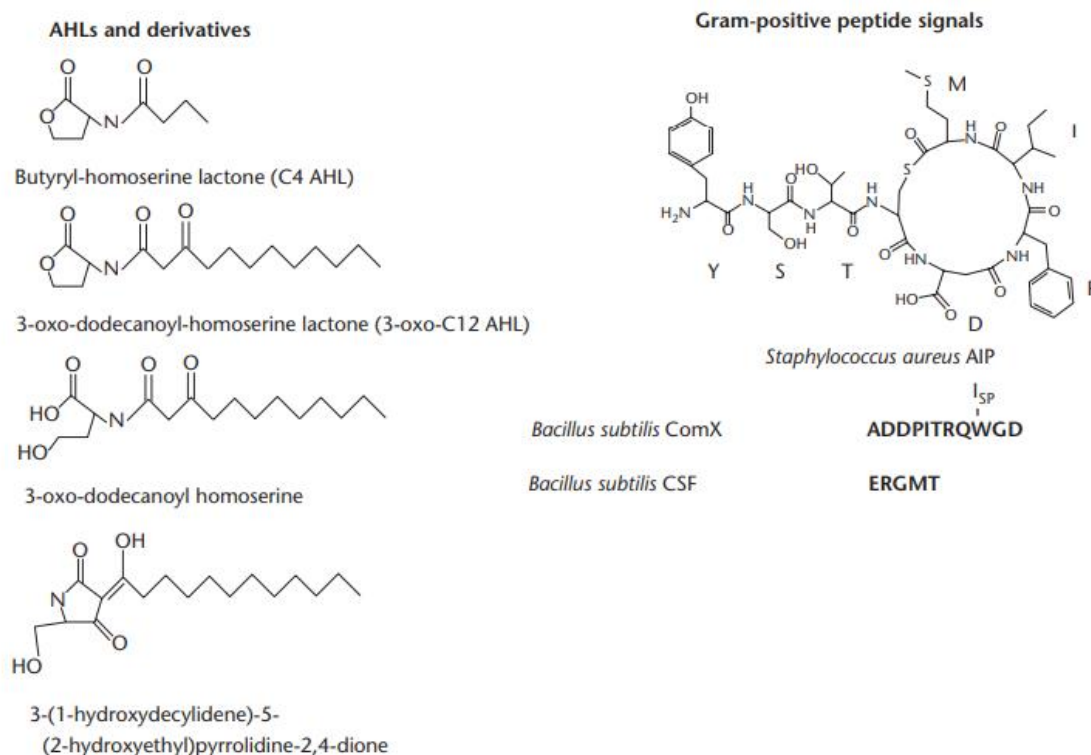


Figure 5: Structures of quorum-sensing signals and their derivatives. Left: Autoinducer of Gram-negative bacteria, AHLs of different chain length, carbonylation and lactone ring structure used e.g., by *P. aeruginosa*. Right: Signal peptides of Gram-positive bacteria, letter indicate amino acids. Figure adapted from (Flemming, 2008; Horswill, Stoodley, Stewart, & Parsek, 2007).

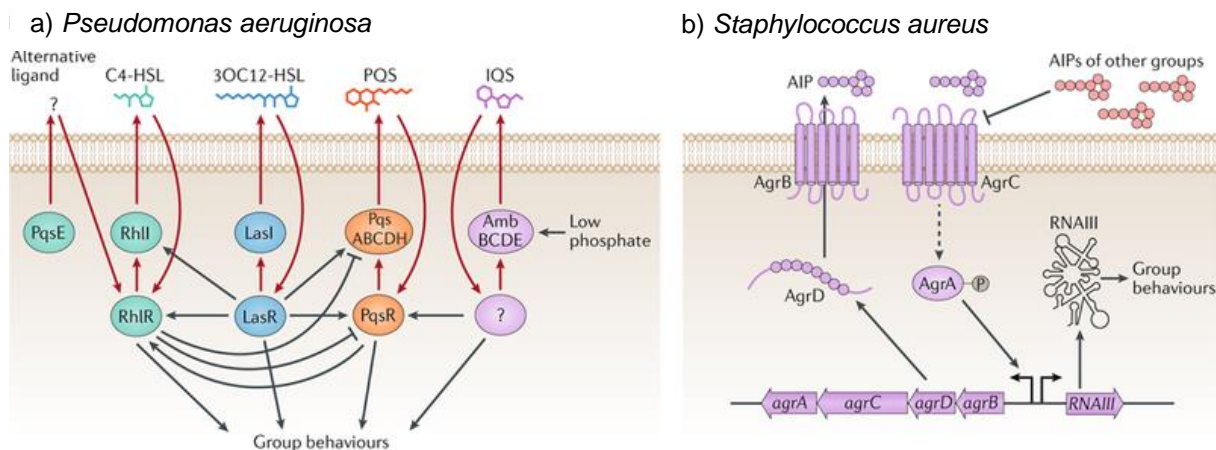


Figure 6: Bacterial quorum sensing. Networks of autoinducers, autoinducer synthases and receptors, downstream signal transduction components that convert the autoinducer signal into changes in gene expression. a) *Pseudomonas aeruginosa* employs four interwoven quorum-sensing loops using LasI and LasR, RhlI, PqsE and RhIR, PqsABCDH and PqsR, AmbBCDE and an unknown receptor as the synthases and receptors of the autoinducers 3OC12-HSL, C4-HSL, unknown (PqsE), PQS and IQS, respectively. b) At high cell densities, AgrB from *Staphylococcus aureus* processes the AgrD precursor peptide and exports the autoinducing peptide AIP, which in turn signals through the AgrC receptor and the downstream transcription factor AgrA. Phosphorylated AgrA induces the production of a regulatory RNA that controls group behaviors. sRNA, small RNA. Dashed lines represent phosphorylation and dephosphorylation. Solid lines represent gene regulation or protein production or small molecule production. Figure adapted from (Eickhoff & Bassler, 2018; Mukherjee & Bassler, 2019)

Quorum sensing is usually described as the population-wide behavior with synchronized function, comparable to a multicellular organism and a boost of AI production after sensing a threshold population density, as described above. Surprisingly, some heterogeneity was observed in both, target gene activation and AI production in high cell density conditions. This strategy allows some cells in the population to perform individual behaviors while others engage in collective activities, maintaining a balance between the fitness advantage gained by the nonproducers who avoid the costly production of AI and the endurance of producers that engage in the autoinduction loop (Bauer, Knebel, Lechner, Pickl, & Frey, 2017; Bettenworth et al., 2019).

4.4 Challenges in medicine, industry and farming

Plenty of biofilm research is attributed to medical environments since biofilm-associated microorganisms have been shown to colonize a wide variety of medical devices and have been implicated in over 80% of chronic inflammatory and infectious diseases including chronic otitis media, native valve endocarditis, gastrointestinal ulcers, urinary tract and middle ear infections, as well as chronic lung infections in cystic fibrosis (CF) patients (Costerton, Stewart, & Greenberg, 1999).

Similarly, biofilms play a significant role in an industrial context. Biofilms are associated with microbially induced plugging of pipes, fouling of ship hulls creating drag and increased fuel

costs, reductions in heat transfer in cooling towers and soiling of manufacturing lines resulting in product contamination (Krohn et al., 2021; Vishwakarma, 2020). Biofilms in aircraft tanks, composed of fungal and bacterial consortia cause economic losses by corrosion of the thin tank shell. Moreover, severe safety risks arise due to clogging of the fuel quantity indicator (Krohn et al., 2021).

Alongside the harm biofilms cause in medical and industrial environments, huge losses are caused by biofilm-forming pathogens in food production and farming, while fish and other aquatic animals or plants are fundamental to feeding the growing global population.

4.5 Importance of the growing sector of aquaculture

4.5.1 Global production and consumption of aquatic animals

According to 'The State of World Fisheries and Aquaculture 2024' published by FAO (Food and Agriculture Organization of the United Nations) the global consumption of aquatic animals increased from 28 million tonnes in 1961 to an estimated 162 million tonnes in 2021 with an emphasis on consumption increase in Asian countries, such as China, Indonesia and India. From 1961 to 2021, consumption of aquatic animal foods per capita increased worldwide at an average rate of about 1.4% per year, while Asia experienced consumption growth rates of 3.7% per capita and year as shown in Figure 7 (all following data of the 2024 report refer to statistical survey of 2021 and 2022).

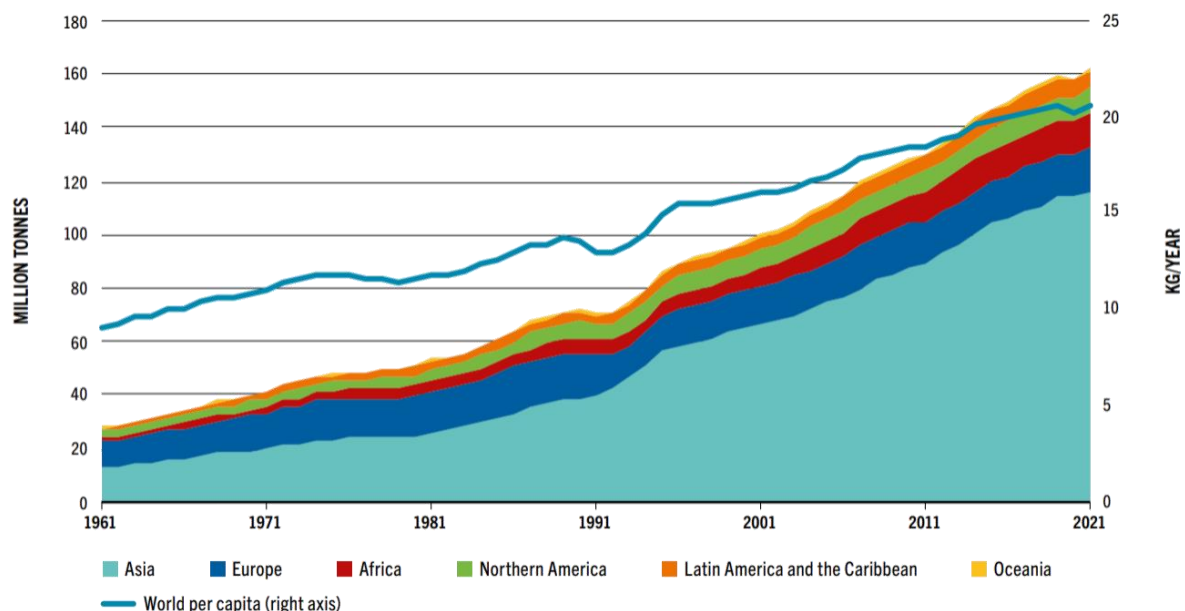


Figure 7: Consumption of aquatic animal foods by region, 1961-2021 (FAO, 2024). Dramatic increase of consumption of aquatic animals. Within the last 60 years the worldwide consumption increased fivefold, mainly driven by Asian countries, experiencing growth rates of 3.7% per capita and year.

Of the 185.4 million tonnes (live weight equivalent) of aquatic animals (algae excluded) harvested globally in 2022, about 89% (164.6 million tonnes) were used for direct human consumption. The remaining 11% (20.8 million tonnes) were destined for non-food purposes,

such as reduction to fishmeal and oil, usage as bait, in pharmaceutical applications or for pet food. Beyond the nutrition of the global population, fisheries contribute to economic independence. In 2022, an estimated 61.8 million people were engaged as full-time, part-time or occasional workers in the primary sector of commercial fisheries. At present, half of the world's fish and aquatic animals supply derives from aquaculture. In 2022, farmed aquatic animals for the first time exceeded captured aquatic animals by volume, counting for 51%, which corresponds to 94.4 million tonnes. An overview of the aquatic animal production in 2022 and an estimation for 2032 is represented in Figure 8).



Figure 8: World aquatic animal production. a) World aquatic animal production in 2022 b) estimation for 2032, *Farmed aquatic animals for the first time exceeded captured aquatic animals by volume in 2022, algae excluded (FAO, 2024).

An outlook for aquatic animal production by 2032 suggests an increase of another 10%, resulting in 205 million tonnes of harvested animals with emphasis on aquaculture, counting for 54% by then.

4.5.2 Development of aquaculture

Global capture fisheries production has been relatively stable since the late 1980s and includes fisheries in marine areas and inland waters like lakes and rivers. Aquaculture on the other hand has grown significantly during the same period, in a region-specific intensity. Aquaculture is located either in marine areas using net cage cultures or land-based in pond cultures of highly diverging technological levels. Exemplary for the deviation in developing aquaculture capacities, China is compared to Europe in Figure 9.

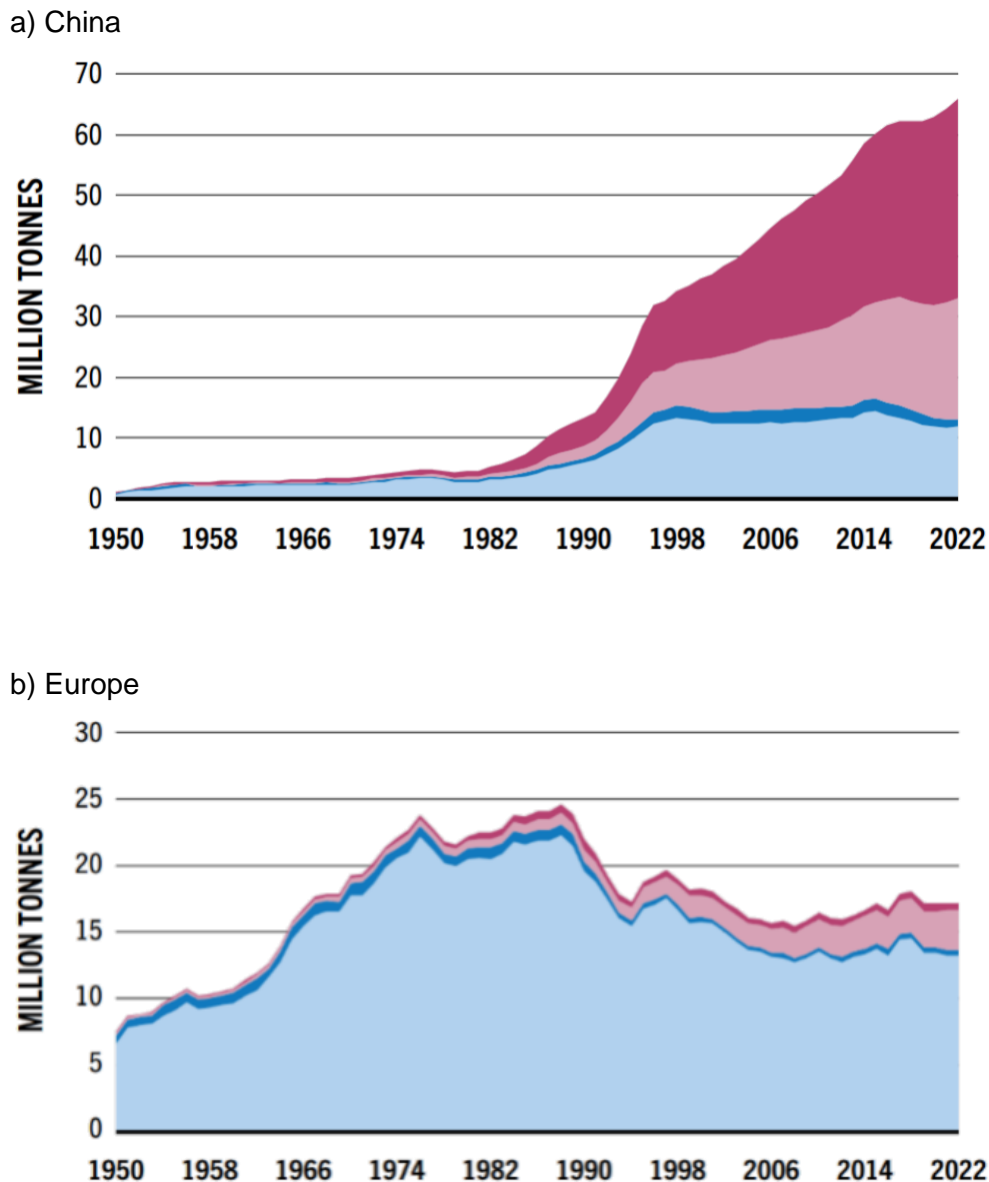


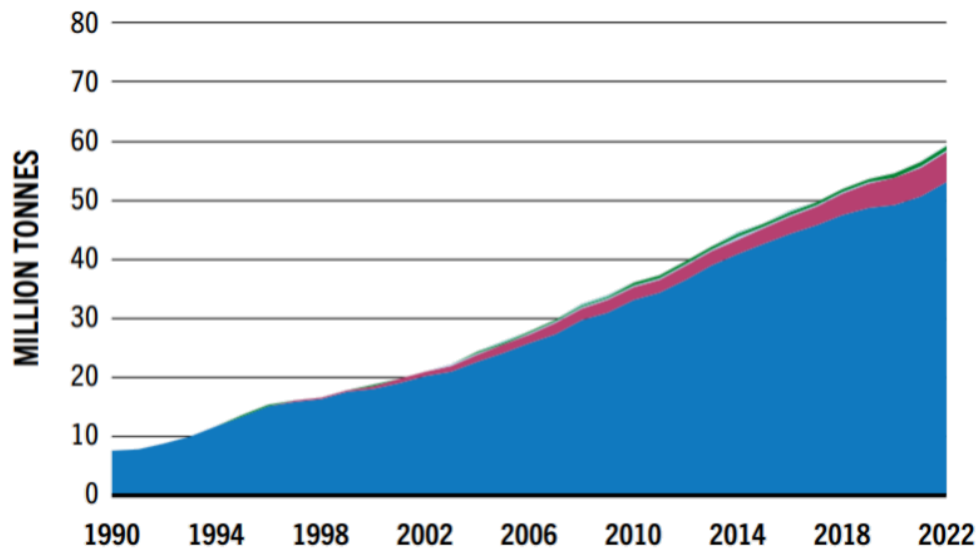
Figure 9: World fisheries and aquaculture production of aquatic animals, 1950-2022. a) China, b) Europe, light blue: Capture fisheries marine areas, dark blue: Capture fisheries inland waters, light pink: Aquaculture marine, dark pink: Aquaculture inland, algae excluded.

China underwent a substantial expansion of its marine and even more of its land-based aquaculture capacities beginning from the late 1980s on, while Europe experienced a gradual decrease in its global harvesting of aquatic animals in the same period, due to overfishing induced depletion of fish stocks and stricter regulations by the European Commission's Common Fisheries Policies (CFP). From the late 2000s on Europe recovered slightly and enhanced its capacity building in marine aquaculture, while land-based aquaculture is still of minor significance.

Worldwide aquaculture production in 2022 achieved a record of 130.9 million tonnes, comprising 94.4 million tonnes of aquatic animals and 36.5 million tonnes of algae (seaweed

and microalgae). Of interest is the specification of inland and marine aquaculture for farmed organisms as depicted in Figure 10.

a) Inland aquaculture



b) Marine aquaculture

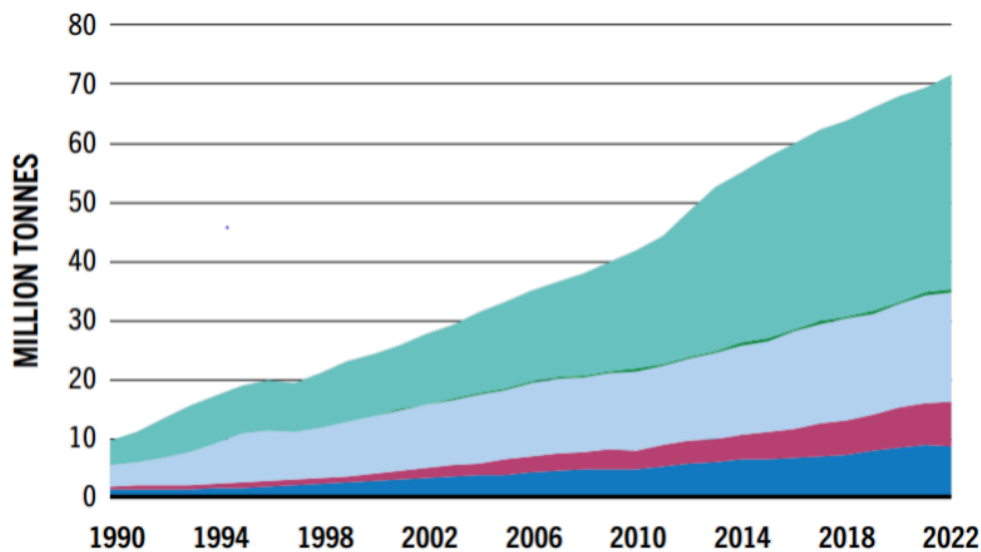


Figure 10: World aquaculture production, 1990–2022. Distribution of farmed animals and algae in a) inland aquaculture and b) marine and coastal aquaculture. Dark blue: Finfish, pink: Crustaceans, light blue: Molluscs, dark green: Other aquatic animals, light green: Algae (wet weight).

Inland aquaculture produced mainly finfish (89.7% of global inland production), while marine and coastal aquaculture produced 36.4 million tonnes of algae and about 24% of Molluscs and Crustaceans.

4.5.3 Aquaculture systems

World inland aquaculture comprises a diverse range of culture methods and technologies. It varies greatly in terms of input intensity, level of technological and management complexity and degree of integration with other economic activities. Globally, raising finfish and other species in constructed earthen ponds remains the most widely adopted culture method as represented in Figure 11.



Figure 11: Land-based tank aquaculture in Canada (Chopin, 2009)

Raceway systems, built in artificial concrete channels, provide continuous water flow, allowing for higher stock density of the farmed animals and thereby increasing production levels and efficiency (<https://propas.iita.org/en/> 27.03.2025).

Mariculture – or marine aquaculture – takes place offshore in cage culture (Figure 12), while coastal aquaculture, typically is practiced in ponds in intertidal zones. On a global scale, Seaweed farming and mollusk culture are overwhelmingly dominated by production in the sea, while Crustaceans are primarily raised in coastal brackish water ponds and tanks.



Figure 12: Marine aquaculture in net-cage system (<https://www.akvagroup.com>)

To prevent a global negative impact resulting from the anticipated growth of the aquaculture sector, the FAO developed the first-ever Guidelines for Sustainable Aquaculture (GSA) in 2017. Following a multidisciplinary and participatory process, FAO has developed the Aquaculture Legal Assessment and Revision Tool (ALART), a framework for methodic scoping of the aquaculture sector of a given country in terms of cultured species, geographic areas and socioeconomic effects. Objectives for sustainable aquaculture development include enhancing food security and nutrition; improving socioeconomic conditions for aquaculture-dependent communities; and promoting the sustainable use of aquatic resources. Developing GSA in 2017 appears to happen rather late facing the huge environmental impact aquaculture had in recent years.

4.6 Ecologic and economic encounters in aquaculture

4.6.1 Land and freshwater restrictions

Intensifying fish farming comes with considerable challenges. Although traditional aquaculture made a great contribution to the supply of aquatic products in times when the wild fishery resource was depleted, the environmental impact of aquaculture is of concern. Increased aquaculture production will probably result in substantial resource constraints due to limited land and freshwater. An estimated 44 million ha (hectare) will be occupied in 2050 by inland and coastal aquaculture, with additional land use impacts for ingredients of aquafeed if fishmeal and fish oil were replaced by crop-based ingredients like soy and other protein and oil-rich alternatives (Waite, 2014). Unregulated coastal aquaculture caused widespread mangrove deforestation in the tropics and subtropics (Ahmed, Thompson, & Glaser, 2019). Competition for freshwater use between agriculture and aquaculture will rapidly increase. Globally, aquaculture is estimated to use 469 km³ in 2050 with possible additional water requirement for aquafeed. Water shortages in several parts of the world as a result of climate change will exacerbate the situation by raising water demand for agricultural food production and decreasing freshwater availability (Waite, 2014).

4.6.2 Water deterioration

Inland aquaculture is highly susceptible to water deterioration. Residual uneaten aquafeed would be converted by bacteria to soluble nutrients which in turn contribute to eutrophication (nutrient over-enrichment) of the water body (Han, 2019). Together with the excretions of the farmed animals the nutrition-rich water accelerates microbial reproduction and causes harmful algal bloom. Previous studies identified cyanobacteria as harmful algal bloom species, consuming oxygen and producing a variety of toxic secondary metabolites (e.g. cyanotoxins) while blooming (Paerl & Otten, 2013). Owing to oxygen depletion, bacterial reproduction and toxin accumulation, the survival and health of aquatic animals would be seriously threatened (Han, 2019). Moreover, high levels of excreted NH₄⁺ (Ammonium) in particular in high stocking density may induce diseases or even death in farmed animals. One of the key mechanisms is

that NH_4^+ at elevated levels gets transported into animal cells and displaces K^+ , causing the depolarization of neurons and the activation of the N-methyl-D-aspartate (NMDA) type glutamate receptor, which leads to an influx of excessive Ca^{2+} and subsequent cell death in the central nervous system (Randall, 2002).

4.6.3 Bacterial infections of farmed aquatic animals

Low water quality and reduced oxygen supply may weaken the immunologic defense of the farmed animals and increase their vulnerability to bacterial infection (Bergmann et al., 2024). Outbreaks of bacterial fish diseases are a major cause of mortality and economic loss in aquaculture (Lafferty et al., 2015). Especially in land-based recirculating aquaculture systems (RAS), biofilms on tanks, pipes and filtration systems can serve as reservoirs for bacterial pathogens that can be difficult to eradicate. Over the years, the number of bacterial species associated with fish disease has increased steadily (Austin, 2011). One of the oldest described pathogens is *Aeromonas salmonicida* (Lehmann & Neumann, 1896), the bacterium causing furunculosis in salmonids (Charette, 2021). Other examples are *F. columnare* (synonymous *Flexibacter columnaris* (Bernardet, 1986)), the bacterium responsible for columnaris disease in various wild and freshwater fish species such as Carp, Salmonids and Eel (Declercq, Haesebrouck, Van den Broeck, Bossier, & Decostere, 2013), *F. psychrophilum* (synonymous *Flexibacter psychrophilum* (Bernardet, 1986)) leading to bacterial cold-water disease (BCWD) in Salmonids (Knupp, Soto, & Loch, 2024), as well as *P. aeruginosa* (synonymous *Bacterium aeruginosum* (Schroeter, 1872) which can cause septicemia and gill necrosis under certain stress conditions (Algammal et al., 2020). Beyond this, *P. aeruginosa* plays a prominent role in the field of pathogens due to its significant impact on human health, particularly in the context of anti-microbial resistance (AMR). *P. aeruginosa* is implicated in a wide range of infections, including urinary tract and pulmonary infections, which pose a major challenge for clinical management (Newman, Floyd, & Fothergill, 2022; Nickerson, Thornton, Johnston, Lee, & Cheng, 2024). In addition to the bacteria mentioned above, the bacterial genus of *Edwardsiella* (Ewing, 1965) (*E. tarda*, *E. ictaluri*, *E. hoshinae*, *E. piscicida* and *E. anguillarum*) is harmful to fish and humans, causing edwardsiellosis, characterized by septicemia, a generalized inflammation (Katharios, Kalatzis, Kokkari, Pavlidis, & Wang, 2019). *E. anguillarum* (Shao et al., 2015) was isolated from various aquatic species including Groupers, Seabream species, Channel catfish, Hybrid catfish and Tilapia (Armwood et al., 2019; Griffin et al., 2014). Investigating the pathogenicity of *E. anguillarum* isolated from a Nile tilapia, Oh et al. (Oh et al., 2020) found multi-focal necrotic lesions throughout the entire liver, severe congestion and signs of vasculitis and septicemia. It is well known that several bacteria including *Edwardsiella* are affiliated with an increasing resistance to common antibiotics making them a major concern for aquaculture (Bergmann et al., 2024).

4.6.4 Abuse of antibiotics in aquaculture

As depicted in the section above, most bacterial pathogens in aquatic animals are aerobic, gram-negative rods and, for this reason, most antibiotics used in aquaculture are effective against gram-negative bacteria (Yanong, 2021). According to a survey conducted by the FAO in 2012, Tetracyclines (Oxytetracycline), Amphenicols (Florfenicol), Trimethoprim and Sulfonamides (Sulfadiazine) are the most commonly used antibiotics for controlling diseases on farms (Alday-Sanz, 2012). Availability and application of antibiotics vary widely between highly controlled regions like Europe, North America and Japan or lower controlled use in many developing countries. Since it is not practical to treat individual animals in aquaculture, metaphylactic use of antibiotics is common to treat the entire population (Bondad-Reantaso, 2023). Exposure to antimicrobials, either during treatment or at sub-therapeutic, preventive levels would select resistant mutants. Once a bacterial strain is resistant, this resistance can be transferred to other bacterial species and strains via horizontal gene transfer (W. Li & Zhang, 2022). Environmental conditions can be favorable for the growth and transmission of resistant bacterial strains from farmed to wild fish, in particular in marine net cage systems (Ahmed et al., 2019). Zoonotic pathogens, such as *Aeromonadaceae*, *Vibrionaceae* (Véron, 1965), *Pseudomonadaceae* may carry anti-microbial resistance (AMR) genes (ARGs) and can be transmitted by contact with or consumption of aquatic animals to humans (Ziarati et al., 2022). Antibiotic residues in food have received major attention, posing potential challenges to food safety and public health. Possible implications to public health include the widespread of AMR, allergies (Penicillin), carcinogenicity (Sulfamethazine, Oxytetracycline, Furazolidone), anaphylactic shock, nephropathy (gentamicin), teratogenicity, bone marrow depression and disruption of normal intestinal flora (Arsene et al., 2022; Okocha, Olatoye, & Adediji, 2018). Unlike in terrestrial environments, where individual animals can be treated or antibiotics can be delivered by injection, treatment of aquatic animals is predominantly administered through food. Uneaten medicated food may end up in sediments or wastewater, where further selection to AMR bacteria can occur (Bondad-Reantaso, 2023).

4.7 Alternatives to antibiotics in aquaculture

Facing the threat posed by careless or incorrect use of antimicrobial agents, Bondad-Reantaso in cooperation with the FAO reviewed in 2023 a number of alternatives to antimicrobials in aquaculture. These included vaccination strategies, phage therapy, quorum quenching, probiotics, prebiotics, chicken egg yolk antibody (IgY) and plant therapy (Figure 13) (Bondad-Reantaso, 2023; FAO, 2024).

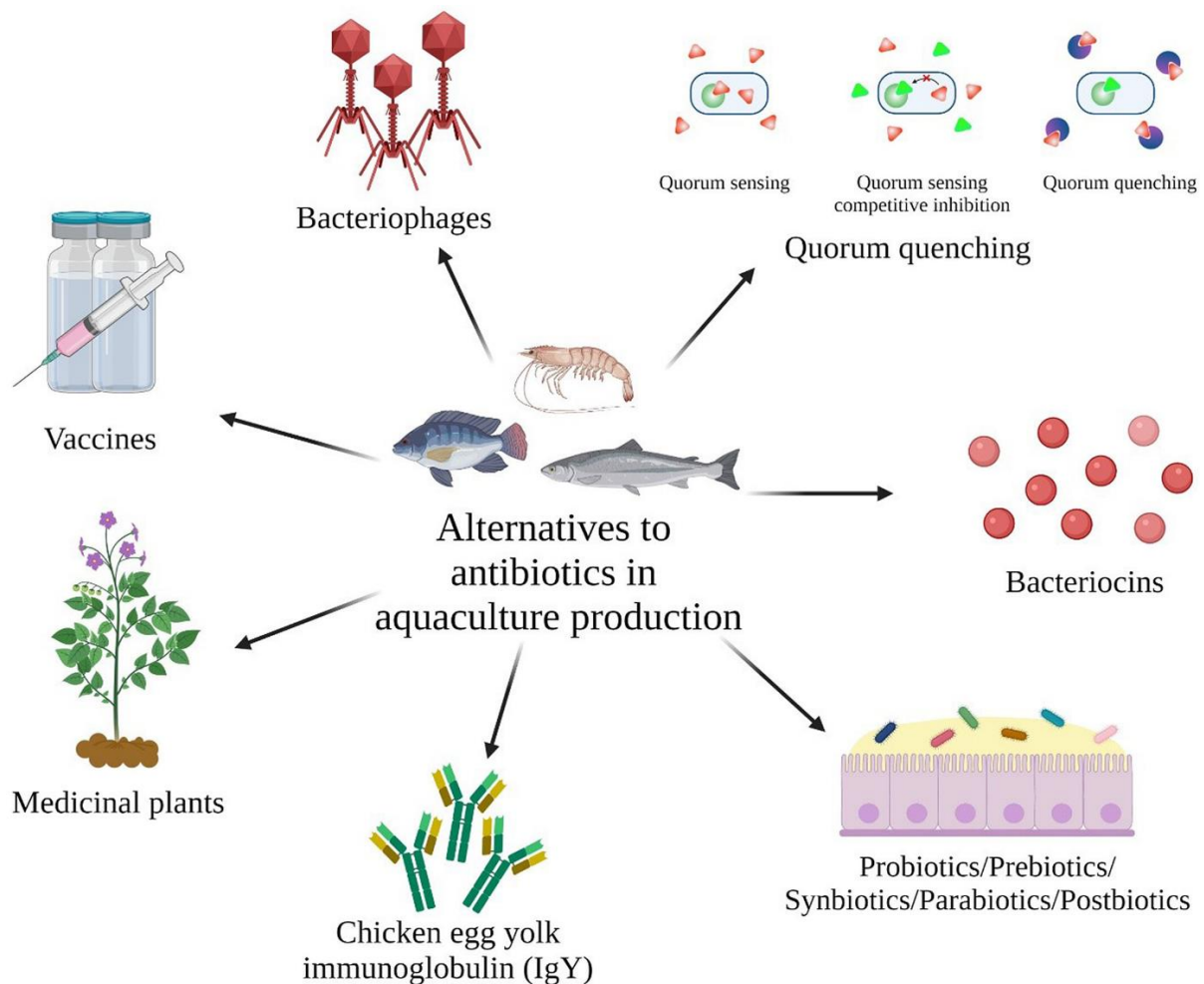


Figure 13: Alternative approaches to reduce the use of antimicrobials in aquaculture. Possible examples are depicted as vaccines, bacteriophages, quorum quenching, bacteriocins, chicken egg yolk immunoglobulin, medicinal plants and microbiomes (Bondad-Reantaso, 2023).

The proposed approaches showed promising advantages while facing various challenges.

4.7.1 Vaccines

The easy-to-apply fish immersion vaccines based on formalin-inactivated broth cultures had proven to be effective against some pathogens like *Vibrionaceae* in the 1970s but ineffective against newly arising pathogens like *A. salmonicida*. Injectable vaccines containing adjuvants were developed in the early 1990s, leading to a significant reduction of antibiotic use in salmon farming (Evelyn, 1997; Sommerset, Krossoy, Biering, & Frost, 2005). Cost-effectiveness was an essential limitation to commercial vaccine development for all species of farmed fish for decades. Fish generally need a large antigen dose compared with terrestrial animals and cost-effective inactivated viral vaccines have proven difficult to develop. Moreover, some species were too small, other species were too vulnerable to handle the stress induced during injection, or developed severe side effects post vaccination (Sommerset et al., 2005). However, developing oral vaccination included in food to replace the labor-intensive process of injecting

every single fish, remained ineffective due to poor and inconsistent responses. In recent years, nucleic acid vaccines of DNA or RNA encoding antigens have been developed, which appear to be cost-competitive, but only a limited number of these have been commercialized yet (Ma, Bruce, Jones, & Cain, 2019).

4.7.2 Bacteriophages

Phages are bacterial viruses that invade bacterial cells and, in the case of lytic phages, disrupt bacterial metabolism and cause the bacterium to lyse. Successful cases of phage therapy for preventive and therapeutic purposes in aquaculture have been reported, using phages targeting *Aeromonadaceae*, *Vibrionaceae*, *Pseudomonadaceae* and *Flavobacteriaceae*. Due to the complexity of application scenarios and the interaction of phages with their hosts, there are still many questions to be answered to permit commercial application (Liu et al., 2022).

4.7.3 Quorum quenching

Several *Bacillus* species were isolated from marine or aquaculture environments and demonstrated their capacities to suppress communication molecules produced by *Vibrionaceae* (Defoirdt, 2011; Müller, Spiers, Tan, & Mujahid, 2023). As bacilli are common gut microbiota possible applications include co-cultivation or feed supplementation (Müller et al., 2023). With their targeted anti-virulence approach, QQ probiotics (QQPs) have substantial promise as a potential alternative to antibiotics. The application of QQPs in aquaculture, however, is still in its early stages and requires additional research. Key challenges include determining the optimal dosage and treatment regimens, understanding the long-term effects, and integrating QQPs with other disease control methods in diverse aquaculture systems (Lubis et al., 2024).

4.7.4 Bacteriocins

Bacteriocins are bioactive compounds produced by bacteria. They are ribosome synthesized, low molecular weight bactericidal peptides, encoded either in chromosome or extrachromosomal elements, usually 20-60 amino acids in length. Many of the bacteriocins tested for food-related applications were isolated from lactic acid bacteria (LAB) and lead to bacterial death via pore formation, prevention of cell wall synthesis, damage to genetic material and protein synthesis (Pereira et al., 2022). Several bacteriocins have been investigated for pharmaceutical applications. Application for aquaculture is still in *in vitro* testing (Pereira et al., 2022).

4.7.5 Probiotics

Beyond the renowned beneficial microbes such as LAB, *Bifidobacteria* and *Saccaromyces* spp. to maintain a healthy gut microbiome and immunologic defense in aquatic animals, some unconventional microorganisms including additional *Bacillus* spp., different yeasts, *Escherichia coli*, and *Weissella* spp. were suggested as probiotics referred to as next-

generation probiotics (NGPs) (Fei et al., 2023). Proper selection of the optimal probiotics for aquaculture is essential to ensure effectiveness and safety. Criteria for suitability in aquaculture comprise non-pathogenicity, acid tolerance, rapid regeneration, robustness, antigenotoxicity, genetic stability, survival during technical procedures, as well as lack of resistance toward antibiotics (Puri, Sharma, & Singh, 2022). Additional beneficial effects were expected from prebiotics which were initially described as non-digestible nutrient substances that affect the host by selective stimulation of the growth of colonic bacteria, thus improving host health (Gibson & Roberfroid, 1995). Combinations of probiotics and prebiotics called synbiotics are under investigation for safe and viable delivery in the host (Todorov et al., 2024). Drawbacks occurred when in 2017 the US FDA (Food and Drug Administration) revealed serious violations such as misidentification of bacterial strains or contamination of supplements in more than 50% of the visited establishments (Cohen, 2018). Transfer of resistance gene is despite all caution a growing concern as it was observed that a *Lactobacillus* strain was able to transfer a resistance gene to host microbiota and that a probiotic product, approved by FDA contained a strain with tetracycline resistance (Pereira et al., 2022).

4.7.6 Chicken egg yolk immunoglobulin

Chicken egg yolk immunoglobulin (IgY) is an antibody for passive immunization. High titers of pathogen-specific IgY are produced after the immunization of hens and cost and labor-effective methods have been developed for IgY extraction from egg yolk (Bondad-Reantaso, 2023). IgY are stable in a pH-value range of 4-9 and up to 65 °C (Schade et al., 2005). Specific antibodies have been developed for the treatment and prevention of certain fish diseases such as white spot syndrome in shrimp, vibriosis, enteric redmouth disease and edwardsiellosis (Baloch, 2015). The specific IgY antibody binds to the bacterial cell, induces agglutination, thus, inhibits bacterial growth, while simultaneously enhancing phagocytosis by macrophages (Qin et al., 2018). It can be administered through a variety of different routes, including, intraperitoneal injection, immersion or oral administration (Bondad-Reantaso, 2023). Obvious limitations are caused by the susceptibility of IgY antibodies to proteolysis. Even if certain IgY antibodies are resistant against digestive factors, their activity ceases at pH <4, if administered as oral passive immunotherapy. Since the primary target of IgY antibodies lies in the small intestine it is essential to find an effective method to protect IgY antibodies from the acidic environment of stomach and peptic digestion. Methods such as microencapsulation have been proposed but are difficult to implement at the commercial level due to cost-intensiveness (Baloch, 2015).

4.7.7 Medicinal plant and immunostimulants

Medicinal plants and their derivatives have received attention as immunoprophylactics or immunostimulants. Active ingredients, including polysaccharides, alkaloids, organic acids, flavonoids, and phenols are supposed to act antibacterially and in addition, to promote the body's immune function and resistance to diseases (Nik Mohamad Nek Rahimi et al., 2022).

Despite numerous studies on the discovery and characterization of new plant-derived compounds, their successful on-site farm application is limited and their effective performance is inconsistent (P. T. Lee, Yamamoto, Low, Loh, & Chong, 2021). Translation of *in vitro* tests into *in vivo* application in aquaculture is challenging due to dosage-dependent toxicity of several of the plant-derived compounds (W. Liao et al., 2022).

Overall, the numerous approaches for enhancing the health of farmed aquatic animals and reducing the use of antibiotics as summarized above are encouraging and it is to be hoped, that promising methods will find their way into *in vivo* application. However, little was proposed for directly addressing biofilm formation in aquaculture, yet. Since this study intended to explore the potential of microalgae-bacterial consortia in fighting off bacterial biofilms, the microalgae used in this study will be briefly introduced in the following.

4.8 Microalgae and microalgae-bacterial consortia

Algae are photosynthetic organisms that inhabit aquatic environments including lakes, rivers, oceans and even wastewater. They are generally classified as Rhodophyta (red algae), Phaeophyta (brown algae), Chlorophyta (green algae) and categorized by size as macroalgae which are multicellular large-sized algae and microalgae, the tiny unicellular microorganisms. Microalgae occasionally are prokaryotic (cyanobacteria) but typically are eukaryotic, unicellular and photosynthetic or mixotrophic microorganisms. As phytoplankton, microalgae are the main primary producers in their aquatic habitats, providing energy and organic matter, such as omega-3 fatty acids for zooplankton and fish (Thore, Muylaert, Bertram, & Brodin, 2023). Recently, it has become clear that microalgae and their associated microbiota harbor a large and diverse set of genes for the biosynthesis of enzymes, that have an impact on bacterial pathogens (Krohn et al., 2022). For this study, six different microalgae strains were chosen for further investigation based on previous approaches testing the effects of supernatants of microalgae cultures on biofilm formation of pathogenic bacteria (see Results and Discussion). The green algae *Tetraselmis chui* (Butcher, 1959) (CCAP (Culture collection of algae and protozoae, Scotland, United Kingdom) 8/6), which belongs to the class of Chlorodendrophyceae (Schoch et al., 2020), is a unicellular organism with a flattened elliptical morphology, equipped with four equal flagella and is located mainly in marine but also in freshwater environments in Europe and North America (Moser, 2022). *T. chui* is generally reported as rich in polyunsaturated fatty acids (PUFAs), antioxidants like carotenoids and phenolic compounds, which makes it a valuable nutritional source but also a potential treatment of inflammatory and degenerative diseases. The total supernatant of *T. chui* showed the highest defeating effects on bacterial biofilms, determined within this study. *Nannochloropsis salina* (Hibberd, 1981) (SAG (Sammlung von Algenkulturen, Göttingen, Germany) 40.85) also named *Microchloropsis salina* (Fawley, 2015) belongs to the class of Eustigmatophyceae. The tiny (2-8 µm) unicellular green microalga with cylindrical shape lives

in marine habitats in Scandinavia, Britain and Ireland, India and North America (Guiry, 2023). It is currently under research for biofuel (Fisher, Fong, Lane, Carlson, & Lane, 2023; Vinoth Arul Raj, Praveen Kumar, Vijayakumar, Gnansounou, & Bharathiraja, 2021) and β -glucan (Ocaranza et al., 2022) production. *Isochrysis galbana* (Parke, 1949) (CCAP 927/14) also named *Tisochrysis lutea*, is a flagellated marine brown microalgae belonging to the class of Coccolithophyceae. It is distributed in European and North American coastal waters and is currently under investigation as nutraceutical for humans due to its high fucoxanthin content, an oxygenated carotenoid with potential anti-inflammatory, anti-obesity and anti-oxidant effects (D. Chen et al., 2022). The three marine microalgae *T. chui*, *N. salina* and *I. galbana* were provided by BlueBioTech International GmbH (24568 Kaltenkirchen, Germany) and cultivated in marine F/2 medium. A second *Isochrysis* species (SAG 927-3) was investigated as part of this study, referred to as *Isochrysis* spec., but was cultivated in 1/2 SWES growth medium instead of marine growth medium as instructed by the provider of the microalgae (Culture Collection of Algae at the University of Göttingen, Germany). *Chlorella vulgaris* (Beijerinck, 1890) (MZCH (Microalgae and Zygnematophyceae Collection Hamburg, 2609 Hamburg, Germany) 10162, provided by MZCH) is a small (2-10 μm) spherically shaped green freshwater species belonging to the class of Trebouxiophyceae. It is widely distributed from the Arctic to the Antarctic on all continents (Guiry, 2023). *C. vulgaris* was intensively investigated e.g., for municipal wastewater treatment (X. Ji, Li, Zhang, Saiyin, & Zheng, 2019) and for use in photobioreactors as part of a bioregenerative life support system in spacecraft cabins (Niederwieser, Kocielek, & Klaus, 2018) *C. vulgaris* was cultivated in Kessler and Czygan medium. *Scenedesmus acuminatus* (Chodat, 1902) (SAG 38.81, provided by SAG) synonymously named *Tetradesmus lagerheimii* is a green freshwater microalgae of typically curved semicircular cells that form colonies of two or four cells. Apart from Arctic regions *S. acuminatus* is widely distributed on all continents (Guiry, 2023). It was shown to enhance water quality in aquaculture (Yuan et al., 2023) and to contribute to the recovery of nutrients such as nitrogen and phosphorus from wastewater (Mubashar et al., 2024). *S. acuminatus* was cultivated in BG11 medium.

Microalgae live in close relationships with bacteria, forming microalgae-bacterial consortia (Abd-El-Aziz et al., 2025). The interconnected evolutionary history of algae and bacteria created a wide spectrum of associations defined by orchestrated nutrient exchange, mutual support with growth factors and quorum sensing mediation (Cirri & Pohnert, 2019). Studies showed, that for use in biotechnology co-cultured consortia of bacteria and microalgae can result in improved performance compared with monocultures of algae (Abate, Oon, Oon, & Bi, 2024).

Still, compared to the large number of microalgal species, our knowledge remains sparse, and further research requires a focused and more systematic approach to better explore this promising resource with a special emphasis on human, animal and plant health and well-being.

4.9 Intention of this study

The present study focused on the potential of microalgae-bacterial consortia to influence biofilm formation of pathogenic bacteria. A better understanding should be provided of the underlying characteristics of microalgae-bacterial consortia. Possible applications either of the microalgae cultures or of enzymes derived thereof should be elucidated in the context of aquaculture, aiming to contribute to a more sustainable and ecofriendly rearing of aquatic animals through fewer use of antibiotics and better health and robustness of the farmed fish. Providing a wide-range enzymatic toolbox might be a path-breaking approach for a versatile attack on pathogenic biofilms to avoid bacterial adaptation and resistance to the treatment and simultaneously, maintain the flexibility to react to changing demands e.g., in high-density farming as for aquaculture.

5 Material and methods

5.1 Bacterial and algal strains and cultivation conditions

The bacterial and algal strains, vectors and primers used in this study are listed in the tables below.

Table 1: Bacterial strains, characteristics and cultivation conditions

Bacterial strains	Characteristics	Cultivation conditions
<i>E. coli</i> Rosetta gami <i>pLysS</i> (DE3)	F- <i>opmt hsdSB(r_B-m_B-)</i> <i>gal dcm</i> (DE3) <i>pLysSRARE2</i> (Cam ^R)	37 °C, LB medium overnight
<i>Edwardsiella anguillarum</i> (DSMZ No: ALM26)	Wildtype	28 °C, TSB medium, 48 h
<i>Aeromonas salmonicida</i> (DSMZ No. A1)	Wildtype	28 °C, NB medium, 48 h
<i>Pseudomonas aeruginosa</i> PA14	Wildtype	37 °C, LB medium overnight
<i>Flavobacterium columnare</i> (strain B185R)	Wildtype	22 °C, TYES medium, 72 h
<i>Flavobacterium psychrophilum</i> (strain NCIMB 13384)	Wildtype	22 °C, TYES medium, 72 h

Table 2: Algal strains, characteristics and cultivation conditions

Algal strains	Collection number	Characteristics	Cultivation conditions
<i>Tetraselmis chui</i>	CCAP 8/6	Wildtype	20 °C, F/2 medium
<i>Nannochloropsis salina</i>	SAG 40.85	Wildtype	20 °C, F/2 medium
<i>Isochrysis galbana</i>	CCAP 927/14	Wildtype	20 °C, F/2 medium
<i>Isochrysis spec.</i>	SAG 927-3	Wildtype	20 °C, ½ SWES medium
<i>Chlorella vulgaris</i>	MZCH 10162	Wildtype	20 °C, KC medium
<i>Scenedesmus acuminatus</i>	SAG 38.81	Wildtype	20 °C, BG11 medium

All microalgae were grown at static conditions with light/dark cycle of 16/8 h.

5.2 Media and medium additives

5.2.1 Microalgae growth media

Table 3: Composition of KC medium (Kessler & Czygan, 1970)

Component	Stock solution [g/L]	Volume of stock for 1L [mL]
KNO ₃	81	10
MgSO ₄ *7H ₂ O	25	10
NaCl	47	10
NaH ₂ PO ₄ *H ₂ O	47	10
Na ₂ HPO ₄ *H ₂ O	36	10
Micronutrient solution ¹		1 of each Micronutrient stock solution
H ₂ O _{bidest.} ad 1 L		

Adjust pH to 6.5

Table 4: Composition of ¹Micronutrient stock solutions

Component	Stock solution [g/100 mL of H ₂ O _{bidest}]
ZnSO ₄ *7H ₂ O	0.02
CaCl ₂ *2H ₂ O	1.5
H ₃ BO ₃	0.05
MnCl ₂ *4H ₂ O	0.05
FeSO ₄ *7H ₂ O	0.6
EDTA (Triplex III)	0.8
(NH ₄) ₆ Mo ₇ O ₂₄ *4H ₂ O	0.02

The stock solutions and 1 L H₂O_{bidest} were autoclaved for 20 minutes at 121 °C by pressure sterilization at 2 bar before use and combined at sterile conditions to get 1 L of KC medium.

Table 5: Composition of Brackish Water Medium (=1/2 SWES) (According to „Sammlung von Algenkulturen“, Göttingen, Version 10.2008)

Component	Stock solution [g/100 mL]	Volume of stock for 1L [mL]
KNO ₃	1	20
K ₂ HPO ₄	0.1	20
MgSO ₄ *7H ₂ O	0.1	20
Soil extract ¹		30
Micronutrient solution ²		5
H ₂ O _{bidest}		450
Filtered seawater		455

¹Preparation of soil extract: A 6 L flask was filled one third with garden or leaf soil. Success of soil extract depends on selection of suitable soils preferably with low clay content. De-ionized water was added until 5 cm above the soil. Sterilization by heating in a steamer for one hour twice in a 24 h interval. The decanted extract was separated from particles by centrifugation. Aliquots were autoclaved for 20 min at 121 °C and stored in the refrigerator.

Table 6: Components of Micronutrient stock solutions, final ²Micronutrient solution

Component	Stock [g/100 mL]	Volume of stock for 1L of Micronutrient solution [mL]
ZnSO ₄ *7H ₂ O	0.1	1
H ₃ BO ₃	0.2	5
MnSO ₄ *4H ₂ O	0.1	2
Co(NO ₃) ₂ *6H ₂ O	0.02	5
Na ₂ MoO ₄ *2H ₂ O	0.02	5
CuSO ₄ *5H ₂ O	0.0005	1
FeSO ₄ *7H ₂ O		add 0.7 g
EDTA		add 0.8 g
H ₂ O _{bidest}		981

Soil extract was provided by MZCH. The stock solutions and 1 L H₂O_{bidest} were autoclaved for 20 minutes at 121 °C by pressure sterilization at 2 bar before use and combined at sterile conditions to get 1 L of ½ SWES medium, vitamin B₁₂ (5 x 10⁻⁶ g/l) was added in sterile solution after cooling.

Table 7: Composition of BG11 medium (Stanier, Kunisawa, Mandel, & Cohen-Bazire, 1971)

Component	Stock solution [g/L]	Volume of stock for 1L [mL]
CaCl ₂ *2H ₂ O	19	2
MgSO ₄ *7H ₂ O	1.5	50
K ₂ HPO ₄ *3H ₂ O	0.82	50
NaNO ₃	30	50
Na ₂ CO ₃	40	1
Citric acid	3	2
C ₆ H ₈ O ₇ ·nFe·nH ₃ N	3	2
EDTA (Triplex III)	0.5	2
Hepes buffer	119.15	40
Micronutrient solution ¹		1
H ₂ O _{bidest} , ad 1 L		

Adjust pH to 7.5

Table 8: Composition of ¹Micronutrient stock solution

Component	Stock [g/100 mL]
CuSO ₄ *5H ₂ O	0.0079
Co(NO ₃) ₂ *6H ₂ O	0.0049
H ₃ BO ₃	0.29
MnCl ₂ *4H ₂ O	0.18
Na ₂ MoO ₄ *2H ₂ O	0.039
ZnSO ₄ *7H ₂ O	0.022

The stock solutions and 1 L H₂O_{bidest} were autoclaved before use for 20 minutes at 121 °C by pressure sterilization at 2 bar and combined at sterile conditions to get 1 L of BG11 medium.

Table 9: Composition of F/2 medium (Guillard & Ryther, 1962)

Component	Stock solution [g/L]	Volume of stock for 1L [mL]
NaNO ₃	75	1
NaH ₂ PO ₄ *H ₂ O	5	1
Na ₂ SiO ₃ *9H ₂ O	30	50
Micronutrient solution ¹		1
Vitamin solution ²		0.5
Filtered seawater ad 1 L		

Table 10: Composition of ¹Micronutrient stock solution

Component	Stock [g/100 mL]	Quantity for 1 L
CuSO ₄ *5H ₂ O	0.98	1 mL
Na ₂ MoO ₄ *2H ₂ O	0.63	1 mL
ZnSO ₄ *7H ₂ O	2.2	1 mL
MnCl ₂ *4H ₂ O	18.0	1 mL
CoCl ₂ *6H ₂ O	1.0	1 mL
FeCl ₃ 6H ₂ O		3.15 g
Na ₂ EDTA 2H ₂ O		4.36 g
Filtered seawater ad 1 L		

Table 11: Composition of ²Vitamin solution

Component	Stock [g/L H ₂ O _{bidest}]	Quantity for 1 L
Thiamine HCl (vitamin B ₁)		200 mg
Biotin (vitamin H)	0.1	10 mL
Cyanocobalamin (vitamin B ₁₂)	1.0	1 mL
H ₂ O _{bidest} , ad 1 L		

F/2 medium was provided by BlueBioTech International GmbH (24568 Kaltenkirchen, Germany).

5.2.2 Bacteria growth media

Before use all media were autoclaved for 20 minutes at 121 °C by pressure sterilization at 2 bar.

Table 12: Composition of lysogeny broth (LB medium) (Bertani, 1951)

Component	Final concentration [%]
Tryptone	1
NaCl	0.5
Yeast extract	0.5
H ₂ O _{bidest} , ad target volume	

Table 13: Composition of nutrient broth (NB medium) (Fahy, 1983)

Component	Final concentration [%]
Peptone	0.5
Meat extract	0.1
Yeast extract	0.2
NaCl	0.5
H ₂ O _{bidest} , ad target volume	

Adjust pH to 7.0

Table 14: Composition of trypticase soy broth (TSB)

Component	Final concentration [%]
Trypticase Soy Broth Merck	3
H ₂ O _{bidest} , ad target volume	

Adjust pH to 7.3

Table X: Composition of tryptone yeast extract salts (TYES medium) (Cepeda, 2004)

Component	Final concentration [%]
Tryptone	0.4
Yeast extract	0.04
MgSO ₄ *7H ₂ O	0.05
CaCl ₂ *2H ₂ O	0.02
D-glucose (50% stock solution)	0.5
H ₂ O _{bidest} , ad target volume	

Adjust to pH 7.2

5.2.3 Agar Plates

For solid media 1.5% Agar per 1 L (15 g) was added. After autoclaving the plates were prepared at sterile conditions. Antibiotics were added after autoclaving at temperatures below 80 °C.

Table 15: Additives

Component	Solvent	Stock solution	Final concentration
Gentamycin	H ₂ O	10 mg/mL	10 µg/mL
Ampicillin	H ₂ O	100 mg/mL	100 µg/mL
Chloramphenicol	EtOH	25 mg/mL	25 µg/mL
IPTG	H ₂ O	1 M	1 mM

5.2.4 PBS

PBS (Phosphate Buffered Saline, 0.14 M NaCl, 2.7 mM KCl, 10 mM Na₂HPO₄, 2 mM KH₂PO₄) was used from stock solution ROTI®Cell 10x PBS (Carl Roth, Germany), diluted to 1x PBS with H₂O_{bidest.}

5.3 Storage and cultivation of bacteria and microalgae

5.3.1 Long term storage of bacteria

Used bacterial strains were cultivated from a glycerol based cryoculture which was stored at – 70 °C. To create these stocks, 850 µL of a culture grown to early stationary phase were mixed with 150 µL of 99.5% sterile-filtrated glycerol (final concentration 15% (v/v)). All cryocultures were kept on ice during use.

5.3.2 Cultivation of bacteria and microalgae

The cell culture of recombinant *E. coli* Rosetta gami *pLysS* (DE3) was incubated at 37 °C on a shaker with a speed of 160 rpm. To ensure that the plasmid remained in the cells the final concentration of the respective antibiotic was added as listed in Table 15. All other bacteria were cultivated on a shaker with a speed of 160 rpm at conditions according to Table 1. Microalgae were regrown by transfer of 1 mL of microalgae culture to 200 mL of fresh microalgae growth medium according to Table 2, cultivation at 22 °C, static, light cycle of 8 h darkness, 16 h light.

5.4 Molecular biological and bioinformatic methods

5.4.1 Vectors and primers used in this study

Table 16: Vectors used for protein overexpression

Vector	Enzyme	Characteristics
pET21a(+):Dlh_3	Dienelactone hydrolase	Vector with His-Tag, insert Dlh3, Amp ^R
pET21a(+):28-50_Dlh	Dienelactone hydrolase	Vector with His-Tag, insert 28-50_Dlh, Amp ^R
pET21a(+):28-84_McrA	5-methylcytosine-specific restriction endonuclease McrA	Vector with His-Tag, insert 28-84_McrA, Amp ^R
pET21a(+):28-08_OxoD	8-Oxoguanine deaminase	Vector with His-Tag, insert 28-08_OxoD, Amp ^R
pET21a(+):28-97_AhlA	Acyl-homoserine-lactone acylase	Vector with His-Tag, insert 28-97_AhlA, Amp ^R
pET21a(+):28-06_AmiD	1-aminocyclopropane-1-carboxylate deaminase	Vector with His-Tag, insert 28-06_AmiD, Amp ^R
pET21a(+):28-17_McrA	5-methylcytosine-specific restriction endonuclease McrA	Vector with His-Tag, insert 28-17_McrA, Amp ^R
pET21a(+):28-24_McrA	5-methylcytosine-specific restriction endonuclease McrA	Vector with His-Tag, insert 28-24_McrA, Amp ^R
pET21a(+):27-27_McrA	5-methylcytosine-specific restriction endonuclease McrA	Vector with His-Tag, insert 27-27_McrA, Amp ^R
pET21a(+):29-62_McrA	5-methylcytosine-specific restriction endonuclease McrA	Vector with His-Tag, insert 29-62_McrA, Amp ^R
pET21a(+):64-22_FerC	Ferrochelataase	Vector with His-Tag, insert 64-22_FerC, Amp ^R

Table 17: Primers, sequence and characteristics

PCR primer	Sequence	Size (bp)	T _M (°C)	GC-content (%)
pet21_26-80_PksN_TcF	CGCGGATCCATGAGCGGTACGTCGAATGCGTTC	33	64	61
pet21_26-80_PksN_TcR	CCGCTCGAGGTTGGCGGACGGCTTGCG	27	64	74
pet21_29-62_McrA_TcF	CGCGGATCCATGTATCACCCCGACCTGCAAAGGC	34	65	62
pet21_29-62_McrA_TcR	CCGCTCGAGGCTTTCCAGCTCGATATCCCAATATA ACCAG	40	62	53
pet21_28-24_McrA_TcF	CGCGGATCCATGGCCGTTTCACCGGAGGC	29	65	69
pet21_28-24_McrA_TcR	CCGCTCGAGAGGCTCCAGTTCGACGTCCAG	31	66	68
pet21_28-84_McrA_TcF	CGCGGATCCATGCTGAATGCAGACTACCGTCCGC	34	66	62
pet21_28-84_McrA_TcR	CCGCTCGAGCGGCTCCAGCTCGACGTCCC	29	65	76
pet21_27-27_MrcA_TcF	CGCGGATCCATGGACGGTGAATTCAGAACCGAGT TCG	37	65	57
pet21_27-27_MrcA_TcR	CCGCTCGAGCGCCTCCAGTTCGGCATCCC	29	64	72
pet21_28-17_McrA_TcF	CGCGGATCCATGGACGGCGATTTTCAGAACCGGAAT TCAC	38	64	55
pet21_28-17_McrA_TcR	CCGCTCGAGCGCCTCCAGCTCGGCGTCC	28	66	79

PCR primer	Sequence	Size (bp)	T _M (°C)	GC-content (%)
pet21_28-97_AhIA_Tcf	CCGGAATTCATGGTGTGGCGGAGAGGATAAAATAC	36	62	50
pet21_28-97_AhIA_TCr	CCCAAGCTTGGTCCCCCGCACCACCTTG	28	64	68
pet21_29-97_alpA_Tcf	CGCGGATCCATGAAGAAACACATTTTGGCCGCCGC	35	65	57
pet21_29-97_alpA_TCr	CCGCTCGAGCTTGATCCAGACGGCGTAGTTGG	32	62	63
pet21_25-82_Glys_Tcf	CCGGAATTCATGCCGCCGCCGTCGGATA	28	65	64
pet21_25-82_Glys_TCr	CCGCTCGAGTTGCGCTTCCCACACCGCAAAC	31	64	65
pet21_25-10_Glys_Tcf	CCGGAATTCATGCAAGCCTGCACGTGGACC	30	65	60
pet21_25-10_Glys_TCr	CCGCTCGAGCGCCTTCTCCCAGATGGCAAAGTC	33	63	64
pet21_64-43_AlpA_Tcf	CGCGGATCCATGCGCGCCGCCGC	23	66	83
pet21_64-43_AlpA_TCr	CCGCTCGAGGTGCTGGCCCTCCCACACGG	29	66	76
pet21_64-23_AlpA_Tcf	CGCGGATCCATGCCGCCTGCGCTGAC	26	64	73
pet21_64-23_AlpA_TCr	CCCAAGCTTGTTGGTCTTCTCCCACACCGCCC	32	62	63
pet21_64-85_BetA_Tcf	CGCGGATCCATGCCGACCTCGCTGCCC	27	65	74
pet21_64-85_BetA_TCr	CCGCTCGAGCGCCTTGTTCCGCATGCGGTTG	31	66	68
pet21_64-83_GlyP_Tcf	GCTCTAGAATGGGCCCCACCCCGTGC	26	67	69
pet21_64-83_GlyP_TCr	CCGGAATTCCTTCGCCATCAACATCAGCGCCCC	33	66	61
pet21_25-73_FerC_Tcf	CGCGGATCCATGAGTAAAAAAGGAATTCTCTTGGTCAATC	40	58	43
pet21_25-73_FerC_TCr	CCGCTCGAGCAATAACTCCTCTCCCCAAGTTGC	33	59	58
pet21_28-70_FerC_Tcf	CGCGGATCCATGAACATGAAGTCGACCGTCGATC	34	61	56
pet21_28-70_FerC_TCr	CCGCTCGAGCACCCAGCCCTGCAGCTCC	28	64	75
pet21_28-37_FerC_Tcf	CGCGGATCCATGAACATGCAGACGTCGATCGAC	33	62	58
pet21_28-37_FerC_TCr	CCCAAGCTTTCAGATCCAGCCCTGCAGTTC	30	63	63
pet21_28-15_FerC_Tcf	CGCGGATCCATGCCTGACACTCAGACCATTGCCC	34	65	62
pet21_28-15_FerC_TCr	CCGCTCGAGGACCAGCCAGCCGCGCAG	27	65	78
pet21_27-30_FerC_Tcf	CGCGGATCCATGCTTGACGCAAGCACCACC	30	63	63
pet21_27-30_FerC_TCr	CCGCTCGAGGTCCAGCCAGCCTTTGAGGTTGTC	33	63	64
pet21_64-22_FerC_Tcf	GCTCTAGAATGCTTGACGCAAGCACCACCG	30	65	57
pet21_64-22_FerC_TCr	CCGGAATTCGTCCAGCCAGCCTTTGAGGTTGTCGC	35	66	60
pet21_27-61_MgC_Tcf	CGCGGATCCATGGTGGCGCTGGTTCAGACGG	31	66	68
pet21_27-61_MgC_TCr	CCGCTCGAGGTTCCGGGGCGCCTGCC	26	65	81
pet21_27-35_MgC_Tcf	CGCGGATCCATGGTGGCGCTGGTTCAGACGG	31	66	68
pet21_27-35_MgC_TCr	CCCAAGCTTATTGCGCGGCGCTTGCC	26	65	65
pet21_28-25_MgC_Tcf	CGCGGATCCATGATTATCTTAGATAAAGGTACCATTTCTAG	41	55	39
pet21_28-25_MgC_TCr	CCCAAGCTTAGCGGCCCATCCTTCTCTATC	30	61	57
pet21_28-28_MgC_Tcf	CGCGGATCCATGGTCGCACGCGCCTACACC	30	66	70
pet21_28-28_MgC_TCr	CCGCTCGAGCGAGCCGATGGATTGAGGCACGC	32	66	69
pet21_27-02_MgC_Tcf	CCGGAATTCATGGTCACGCGCACCTACACG	30	64	60
pet21_27-02_MgC_TCr	CCCAAGCTTACTGTCGGCTGCCGAAGACAAC	31	64	58
pet21_28-06_AmiD_Tcf	CGCGGATCCATGTCCCTGCTTGATAAATTCGAACGC	36	62	53
pet21_28-06_AmiD_TCr	CCGCTCGAGGCCGTCTTTGTAATAGGACGCATAGC	35	61	57
pet21_28-08_OxoD_Tcf	CCGGAATTCATGAACGACGGCAAGGGGCG	29	65	62
pet21_28-08_OxoD_TCr	CCGCTCGAGGCCGTGCATGAACGCCCGC	28	66	75
pet21_28-50_DIH_Tcf	CGCGGATCCATGAGCTCGATAGAGGTCCAGC	31	60	61
pet21_28-50_DIH_TCr	CCCAAGCTTATATCGGTCCGGTGTTTTTTTATTCTC	36	58	42
pet21_27-21_DIH_Tcf	CGCGGATCCATGACACACCTCGTCTCTTCCACC	34	64	62
pet21_27-21_DIH_TCr	CCCAAGCTTCAGGGTGGCGAGGAAGGCC	28	64	68
pet21_28-01_DIH_Tcf	CGCGGATCCATGACGCCGCGTCTCTTACGG	31	67	68
pet21_28-01_DIH_TCr	CCGCTCGAGGGGGTGGCGTTCGCGCGC	27	69	81

PCR primer	Sequence	Size (bp)	T _M (°C)	GC-content (%)
pet21_28-11_DIH_TCf	CGCGGATCCATGAAAAGCGAAGCATTCAATTACAGCG	37	61	49
pet21_28-11_DIH_TCr	CCGCTCGAGATTCTGCAAGGTCTCGGCCAGAAATC	35	64	57
pET21a(+)_for	ATATAGGCGCCAGCAACC	18	56	56
pET21a(+)_rev	TCCGGATATAGTTCCTC	17	56	47
616 V	AGAGTTTGATYMTGGCTCAG	20	56	40
1492 R	TACGGYTACCTTGTTACGAC	20	56	45

5.4.2 Total DNA extraction of microalgae for establishing metagenomes

Cell pellets of the six microalgae cultures, including the associated microbial community, were used to prepare the metagenome datasets. 30 mL of the respective culture were centrifuged for 30 min at 5000 g. The resulting pellets were resuspended in Elution Buffer, provided by the used kit (NucleoBond High Molecular Weight Genomic DNA-Kit (MACHEREY-NAGEL, Düren, Germany)). The microalgae suspensions were shock-frozen in liquid nitrogen and after thawing pipetted on bashing beads. 40 µL Buffer MG, 0.5 mg proteinase K and 5 mg lysozyme were added before they were bead-bashed on Vortex-Genie®2 (Scientific Industries, New York, NY, USA) four times for 1 min with breaks on ice for 30 sec. After addition of 600 µL Buffer MG the suspensions were incubated at 55 °C for 30 min under static conditions. Finally, the DNAs were eluted in 30 µL of deionized water according to the manufacturer's instructions. DNA concentration and purity were analyzed using a NanoPhotometer® NP80 (IMPLEN, Westlake Village, CA, USA). By measuring the extinction at wavelength $\lambda=260$ nm and 280 nm the purity was detectable by calculation of the quotient of the latter. The quotient of pure DNA is assumed to be about 1.8.

5.4.3 Processing and analysis of DNA-seq reads - Sequencing and assembly

Library preparation and sequencing were performed at the Leibniz Institute of Virology (LIV, Hamburg). 1 ng of DNA was subjected to library preparation with the Nextera XT DNA Library Preparation Kit (Illumina, product number: FC-131-1096) according to the manufacturer's instructions. Illumina short-read sequencing was done on a NextSeq 500 (Illumina, San Diego, CA; USA) sequencer (NextSeq 500/550 High Output Kit v2.5, 300 Cycles, product number: 20022408) with 2 × 151 bp (plus 2 × 8 bp Index reads). Demultiplexing with bcl2fastq (default settings) yielded read numbers sequencing details displayed in supplemental Table S1. Sequence reads were processed with fastp (v0.21.0) to remove sequences originating from sequencing adapters (S. Chen, Zhou, Y., Chen, Y., Gu, J., 2018). Processed reads shorter than 40 bp were discarded. The remaining reads were assembled using IDBA-UD in metagenomic mode (Peng, Leung, Yiu, & Chin, 2012).

5.4.4 Cloning of *E. coli* DH5 α and *E. coli* Rosetta gami *pLysS* (DE3) for protein overexpression

5.4.4.1 Primerdesign

To design primer the gene sequences of the chosen fragments of promising enzyme candidates were added to SnapGene[®]. For each fragment forward and reverse primer were designed using the first and last 18 to 21 nucleotides, depending on the GC-content which should be between 35%-65%. The annealing temperature was calculated with the following formula: $2^{\circ}\text{C} \cdot (\text{A}+\text{T}) + 4^{\circ}\text{C} \cdot (\text{G}+\text{C}) - 5^{\circ}\text{C}$. With the help of the SnapGene[®]-tool “noncutters” the restriction enzymes that don’t cut the fragment could be discovered. The sequence of the required restriction site was added to the primers as overhang to ensure, that the fragments could be ligated into the expression vector. For 5’ and 3’ end different restriction sites had to be chosen to guarantee the proper direction of the enzyme sequence inside the expression vector. Within the reverse primer sequence, the stop-codon was deleted for addition of the His-Tag for protein purification.

5.4.4.2 Polymerase-chain-reaction (PCR)

The DNA sequences of promising enzyme candidates from *T. chui* metagenome were amplified by PCR using the primers listed in Table 17. Within three steps (first denaturation of DNA-double strand, second annealing of respective primers, third elongation of a complementary DNA-strand by DNA polymerase, starting at the primer from 5’ to 3’ end) PCR synthesizes DNA polymers for ligation into protein expression vectors. Reaction cycles and pipetting scheme of practiced PCR are listed in the following Tables 18 and 19.

Table 18: Reaction cycles of PCR

Reaction step	Temperature [°C)	Time	Number of cycles
Initial denaturation	95	3 min	35
Denaturation	95	45 sec	
Annealing	according to length and GC content of respective primers	30 sec	
Elongation	72	15-30 sec/kb	
Final elongation	72	10	
Hold	8	infinite	

Table 19: Pipetting scheme of PCR

Component	volume [μ L] for 20 μ L run	Final concentration
5x Phusion™ HF Buffer	4	1x
10 mM dNTPs	0.4	200 μ M each
Forward primer	1	0.5 μ M
Reverse primer	1	0.5 μ M
Template DNA	0.4	see below ¹
(DMSO, optional)	0.3	1.5%
Phusion™ Hi-Fi DNA Polymerase	0.2	0.02 U/ μ L
H ₂ O _{bidest.} ad 20 μ L		

¹For high complexity genomic DNA, the amount of DNA template should be 50–250 ng per 50 μ L reaction volume

5.4.4.3 Agarose gel electrophoresis

Agarose gel electrophoresis separates nucleic acids according to size and was used for verification of extracted total DNA or the size of the DNA fragments of the enzyme candidates. Due to the negative charge of the nucleic acid strands, DNA-fragments move from cathode to anode within the electric field generated by a voltage source. The assay was done with the Electrophoresis system by *Biometra* (Jena, Germany) and *BioRad* (München, Germany). 0.8% TAE-agarose gel was used, and the chamber was filled with 1x TAE-Buffer. 5 μ L of the sample were mixed with 1 μ L of loading dye (*Thermo Scientific*, Waltham, MA, USA) and loaded onto the gel. Depending on the expected fragment size the 100 bp+ or the 1 kb Ladder (*Thermo Scientific*, Waltham, MA, USA) was used. Unless otherwise noted, gels were run for 45 min at 80 to 100 V. Afterwards the gel was dyed in ethidium bromide solution (10 μ g/mL) for 20 min and subsequently monitored at the GelDoc XR+ by *BioRad* under UV-light at wavelength λ =254 nm.

Table 20: Composition of loading dye and 50x TAE-Buffer

Loading dye	50x TAE-buffer
60% v/v Glycerol	2 mM Tris-HCl
20 mM Tris-HCl	100 mM EDTA
60 mM EDTA	pH value was adjusted to 8.2
0,48% m/v SDS	
0,03% m/v Xylene Cyanole	
0,03% m/v Bromphenole blue	
0,12% m/v Orange G	

5.4.4.4 Restriction

Restriction endonucleases recognize palindromic recognition sites, which were previously added as overhangs to the primers, to cut the DNA-fragment (insert) specifically. By cutting the vector and the insert by the same restriction endonuclease in separate approaches the fragments had the same interface for ligation. The sample was incubated for 1 h at 37 °C and afterward purified with the *Machery-Nagel* Nucleo spin DNA & PCR clean-up Kit according to

the manufacturer's protocol to get rid of salts and enzymes. The DNA was eluted with 20 µl of H₂O_{bidest.}

5.4.4.5 Ligation

After restriction, the vector and insert were ligated with the help of T4-ligase (*Thermo Scientific*, Waltham, MA, USA). For successful ligation, the ng-amount of the insert was applied five times the vector amount. Samples were incubated overnight at 4 °C, finally the ligase was deactivated at 65 °C for 10 min.

5.4.4.6 Heat shock transformation

By heat shock, expression vectors were transformed into competent *E. coli* host cells. First, an aliquot of competent *E. coli* cells was thawed on ice. After addition of the ligated expression vector, the sample was incubated for 30 min on ice, followed by a heating step at 42 °C for 90 sec. The sample was put back on ice for 1 min. After addition of 800 µL of LB-Medium the sample was incubated for 45 min, shaking, at 37 °C before the suspension was plated on LB-agar plates, substituted with the respective antibiotic (depending on the resistance encoded on the vector and on additional functional plasmids within the bacterial cells). The plates were incubated overnight at 37°C.

5.4.4.7 Colony PCR

The clones grown on the agar plates were verified via colony PCR. 8 to 10 clones of each construct were picked and resuspended in 10 µL of sterile H₂O_{bidest.} The bacterial cells were denatured by heating to 95°C for 5 min. Afterwards a PCR following the steps according to Table 18 was performed and evaluated by agarose gel electrophoresis, to detect colonies containing the insert. The potential positive colonies were picked and incubated overnight in 5 mL liquid LB medium containing the respective antibiotic to ensure the plasmid remains inside the cells.

5.4.4.8 Plasmid isolation

Bacterial cells containing the ligated expression vector (plasmid) were harvested from liquid overnight culture by centrifugation using the *mini-Spin-plus*-centrifuge (Eppendorf). Plasmid isolation was performed by Presto™ Mini Plasmid Kit according to the manufacturer's protocol. For elution 20 µL of H₂O_{bidest} was used.

5.4.4.9 Verification of expression vector and insert by sequencing

After the isolation of the potentially positive plasmid, the sample was prepared for sequencing. 12 µL of the sample were mixed with 3 µL of the respective primers for the insert (to ensure the insert matched the required sequence from IGM-data) or the universal primers of the expression vector (to verify sequence and direction of the insert). To improve the sequencing result a PCR and purification of the PCR-product was performed to get a higher amount of

insert. The samples were sent to *Microsynth SeqLab* GmbH (9436 Balgach, Switzerland), which followed the “chain termination method” by Sanger.

5.4.5 Recombinant enzyme production in *E. coli* Rosetta gami 2 (DE3) and purification

5.4.5.1 Protein overexpression

Overexpression of the His-tagged proteins started with 50 mL overnight precultures in LB-medium (Ampicillin 100 µg/mL, Chloramphenicol 25 µg/mL) at 37 °C, shaking, which were used to inoculate 450 mL of LB-medium (Ampicillin 100 µg/mL, Chloramphenicol 25 µg/mL) to an OD_{600 nm} of about 0.1. After growing to OD_{600 nm} 0.7 at 37 °C, shaking, the expression cultures were induced with isopropyl-β-D-thiogalactopyranoside IPTG (1 mM) and incubated overnight shaking at 22 °C. Cells were harvested by centrifugation (5500 rpm, 8 °C, 20 min, Sorvall® RC 5C PLUS). Pellets were resuspended in 10 mL Lysis Buffer (NaH₂PO₄, 50 mM, NaCl, 300 mM, Imidazol, 10 mM) and transferred to 50 mL reaction tubes. After another centrifugation (5000 rpm, 8 °C, 20 min, Eppendorf centrifuge 5804 R) the supernatant was discarded and the cell pellet was frozen at -20 °C for later use.

5.4.5.2 Protein purification

The cell pellet from protein overexpression was thawed on ice for 15 min and resuspended in 12 mL of Lysis Buffer. Cell disruption was performed on ice by ultrasound (Ultrasonic Processor UP200S, Hielscher, amplitude 70 %, cycle 0.5, 1 min) in six repetitions and breaks of 30 sec before the cell debris was pelleted at 13000 rpm, 30 min (Eppendorf centrifuge 5424 R). The lysates were added to 1.5 mL of 50 % NI-NTA Agarose (Protino®, MACHEREY NAGEL), which was previously washed three times by addition of 3 mL of Lysis Buffer and subsequent centrifugation (Eppendorf centrifuge 5424 R). The lysate/Ni-NTA-Agarose suspension was incubated at 4 °C, rolling, for 1 h and washed four times with 4 mL Washing Buffer (NaH₂PO₄, 50 mM, NaCl, 300 mM, Imidazol, 20 mM). Finally, the proteins were eluted following the principle of competition in 3 mL of Elution Buffer (NaH₂PO₄, 50 mM, NaCl, 300 mM, Imidazol, 250 mM) and dialyzed in 1x PBS at 4 °C overnight. Protein concentration was determined by nanophotometer (Implen, Munich, Germany) measuring absorbance at 280 nm with an extinction coefficient of 43,555 M⁻¹cm⁻¹.

5.4.5.3 Sequence and structural alignments

Structure predictions of the three new enzymes were performed by Robetta (Baek et al., 2021) or AlphaFold (Jumper et al., 2021). Visualization, comparison with related enzymes and depiction of the active site were accomplished by UCSF Chimera 1.16 (Pettersen et al., 2004) or Chimera X (Pettersen et al., 2021). Identification of important domains and characteristic features was performed by InterPro (104.0) (Blum et al., 2025) and UniProt (UniProt, 2025).

5.4.6 RNA extraction for transcriptome establishment

Bacteria from an overnight preculture of *E. anguillarum* were adjusted to OD_{600 nm} 0.05. 165 µL of the prepared bacterial culture were pipetted into each of the inner 24 wells of six 48-well plates (Nunc lon delta surface; Thermo Fisher Scientific, Waltham, MA, USA). 165 µL of test liquid (protein solution of Dlh3, 0.5 mg/mL, control: 1x PBS) were added to the bacterial culture in the inner 24 wells resulting in triplicates for each of the two conditions. The plates were cultivated at 28 °C for 48 h. To obtain the bacterial biofilm, all supernatants were discarded and the wells were washed by pipetting up and down with 1 mL of RNeasy lysis solution (Qiagen, Crawley, UK) for every eight wells, leading to a final 3 mL for each of the six plates. The resulting biofilm suspensions were spun down at 5000 rpm for 30 min (Eppendorf centrifuge 5424 R) and the supernatants were discarded. From the remaining cell pellets, total RNA was isolated using bashing beads (Zymo Research Corporation) on Vortex-Genie[®] 2 (Zymo Research Corporation) for 30 sec. After centrifugation (10,000 x g, 2 min, 4 °C, Eppendorf centrifuge 5415R) the supernatant was transferred into a new 1.5 mL-reaction tube with addition of 1 mL of 99% EtOH and further processed by Direct-zol RNA Miniprep Kit (Zymo Research Corporation) including DNase treatment. The resulting RNA was eluted with 50 µL of diethylpyrocarbonate (DEPC)-treated water. To verify the purity and the absence of DNA in the RNA isolation samples, a PCR of the 16S rRNA gene with 616 V and 1429 R primers was performed and checked on a 0.8 % agarose gel. The concentration and quality of the RNA were measured using Implen nano photometer. The six cDNA pools were sequenced on an Illumina NextSeq 500 system. On average 9.7 million (minimum: 9.53 M) single-end sequence reads of length 75 bp were obtained per each sample (vertis Biotechnologie AG, Freising-Weihenstephan, Germany) (all sequencing results in Supplemental Table S2).

5.4.6.1 Processing and analysis of RNA-seq reads

Sequence reads were processed with fastp (v0.23.2, (S. Chen, Zhou, Y., Chen, Y., Gu, J., 2018)) to remove sequences originating from sequencing adapters and sequences of low quality (Phred quality score below 15) from the 3' end of the sequence reads [FASTP]. The Burrows Wheeler Aligner (BWA v0.7.17, (H. Li & Durbin, 2009)) was used to align the reads to the reference assembly of *E. tarda* EIB202 (ASM2086v1). Counts of reads per gene were obtained using featureCounts (FQ v2.0.3, (Y. Liao, Smyth, & Shi, 2014)). Differential expression was assessed with DESeq2 (v1.34.0, (Love, Huber, & Anders, 2014)). A gene was considered significantly differentially expressed if the corresponding absolute log₂-transformed fold change (log₂FC) was not less than 0.5 and, in addition, the false discovery rate (FDR) did not exceed a value of 0.1. The Pathosystems Resource Integration Center (PATRIC, (Snyder et al., 2007)) was used for circular mapping using the integrated Circular Genome Viewer tool. The volcano plot of the distribution of all DEGs was generated using OriginPro V2021b (OriginLab Corporation, USA, VolcanoPlot. opx, 2016).

5.5 Laboratory approaches to evaluate effects on bacterial growth and biofilm formation

5.5.1 Growth curves of bacterial pathogens incubated with microalgae supernatants

Bacterial precultures were adjusted to OD_{600 nm} 0.05 with LB medium. 200 µL of the bacterial suspension were pipetted in six replicates into non-treated 48-well plates (Thermo Fisher Scientific, flat bottom, Waltham, USA), before 200 µL of test liquids (microalgae supernatant, microalgae growth medium and bacterial growth medium) were added. Microalgae supernatant and growth medium were three times concentrated in a vacufuge concentrator (Eppendorf 5301) and sterile filtered previously. Plates were incubated shaking at 37 °C, while every hour the growth of the cultivated bacteria was determined by measuring OD_{600 nm} in Microplate Reader (Synergy HT, BioTek, Agilent Technologies, Santa Clara, United States).

5.5.2 Static anti-biofilm assay

Biofilm formation was quantified using the crystal violet (CV) method to detect both living and dead bacteria based on staining of extracellular matrix polymers. Bacteria from an overnight preculture were adjusted to OD_{600 nm} 0.05 with the particular bacterial growth medium. 50 µL of the diluted bacterial culture was pipetted in six replicates for each condition into a 96-well plate (Thermo Fisher Scientific, flat bottom, Nunclon Delta surface, Waltham, United States). 50 µL of test liquid was added before the plates were incubated according to the individual bacterial conditions. After incubation, OD_{600 nm} of the supernatants was measured in Microplate Reader (Synergy HT, BioTek, Agilent Technologies, Santa Clara, United States). Previous to staining the supernatant was discarded and all wells were washed three times by 200 µL of H₂O_{bidest.} Subsequently, 125 µL of 0.5% Gram's crystal violet solution (hexamethyl pararosaniline chloride, ethanol, phenol, Merck KGaA, Darmstadt, Germany) was pipetted into each well and the plate was incubated for 10 min at room temperature. After incubation, plates were washed three times in a water bath of tap water and dried at 37 °C for 30 min. 150 µL of 33% acetic acid was added to each well of the dry plates, followed by an incubation of another 10 min at room temperature. Finally, biofilms were quantified at wavelength $\lambda = 595$ nm using the Microplate Reader.

5.5.3 Laser scanning confocal microscopy

Bacteria from an overnight preculture were adjusted to OD_{600 nm} 0.05 with the particular bacterial growth medium. 100 µL of the diluted bacteria culture was pipetted into each well of an eight-well µ-slide (Ibidi USA Inc., Fitchburg, WI). 100 µL of test liquid was added to the bacterial culture (microalgae supernatant or protein solution, for control either microalgae growth medium or 1x PBS was added, depending on assay design the respective bacterial growth medium was additionally added). Incubation took place at the individual bacterial growth conditions. After incubation all supernatants were discarded and 150 µL of staining

solution was added, using the LIVE/DEAD™ BacLight™ bacterial viability kit (Thermo Fisher Scientific, Waltham, United States). 5 ml of dye mix was composed of 10 µL SYTO 9 for living cells and 7,5 µL Propidium iodide for dead cells. The addition of the dye was followed by one hour of incubation in a dark environment to protect the sensitive dye. Visualization of the biofilms was performed with a laser scanning confocal microscope (LSCM) Axio Observer Z1 LSM 800 (Carl Zeiss Microscopy GmbH, Jena, Germany) and a C-Apochromat 63x/1.20W Korr UV VisIR objective. SYTO 9 was imaged at 488 nm, Propidium iodide at 561 nm. For consistency, each well was imaged three times at different positions. The analysis of the LSCM images and three-dimensional reconstructions were done with ZEN software (version 2.3; Carl Zeiss Microscopy GmbH). Living and dead cells within the biofilms were quantified by BiofilmQ70 from drescherlab.org. The segmentation threshold was set manually. For parameter calculation, numbers 5 and 7 (Surface properties and Global biofilm properties) were selected. The data was exported to Microsoft Excel and further processed there. The number of living and dead cells, the biofilm thickness, and the biofilm density were subjected to a paired sample t-test, and the p-value was assigned to determine if the two samples were significantly different from each other.

5.5.4 Observation of biofilm growth in oCelloScope™

Live-cell imaging for observing biofilms while growing was performed with oCelloScope™ automated technology (BioSense Solutions ApS, 3520 Farum, Denmark). A preculture of *E. anguillarum* was diluted to OD_{600 nm} 0.025. 50 µL of the bacterial suspension were pipetted in six replicates into the inner wells of a 96-well plate (Thermo Fisher Scientific, flat bottom, Nunclon Delta surface, Waltham, United States). As test liquids 50 µL of Dlh3 protein solution at 0.5 mg/mL, 1x PBS, and TSB were added. During static incubation inside the device at 28 °C, biofilms were observed by taking photos every second hour over an interval of 20 hours. Data analysis was performed by Uniexplorer (v. 11.0.1.8353 (RL2)), a software provided by BioSense Solutions.

5.5.5 Toxicity assays

5.5.5.1 Tests on *Galleria mellonella* larvae

For a first estimation of the biotoxicity of the novel protein candidates, larvae of *Galleria mellonella* were used as test organisms (Maguire, Duggan, & Kavanagh, 2016). The larvae were obtained from tropic-shop.de and used shortly after arrival. Storage in-between use was done in the dark at 5 °C within the containers, the larvae arrived in. 5 µL of both, protein solution and PBS as control were applied by injection near the last abdominal prolegs with a Microliter syringe from ROTH®. For each protein and PBS, 30 larvae were tested. Another 30 larvae were injected with sterile H₂O and 30 larvae were not injected as wild type control. The incubation of the larvae was done in petri dishes with 10 larvae in each dish. The dishes

were also filled with some filter paper to absorb liquids. Every 24 hours, living larvae were determined by gently pushing them with a blunt pen. If no reactions were observed, the larva was considered deceased. The total incubation time was 48 hours.

5.5.5.2 Tests on fish cell line CHSE-214

The potential toxicity of Dlh3 was also tested on the fish cell line CHSE-214 (*Chinook salmon* embryonic cell line) (McCain, 1970). On day 1, 45,000 cells in 100 μ L medium were transferred to each well of a black, non-coated 96-well plate with optical bottom. On the second day, the medium was removed and replaced with 50 μ L fresh cell medium. 50 μ L of test substance were added; either Dlh3 diluted further in cell medium to a concentration of 0.5 mg/mL (1x), 0.05 mg/mL (0.1x) or 0.005 mg/mL (0.01x), 1x PBS (corresponding to the amount of PBS added with the Dlh3 protein) or pure cell medium. After two days of exposure, the CellTiter-Glo® Luminescent Cell Viability Assay was performed according to the manufacturer's instructions, and the relative luminescence (or survival) was correlated to the control wells containing pure cell medium. Data represent averages and standard deviations from four replicas. The assays with fish cell line CHSE-214 were accomplished by Dr. Gunhild Hageskal.

6 Results and discussion

Approaching the question, how to elucidate and evaluate the potential of microalgae to decrease bacterial biofilm formation, resulted in a workflow from screening of microalgae supernatants to working with promising overexpressed enzymes as displayed in Figure 14. The microalgae cultures of *T. chui*, *I. galbana*, *N. salina*, *I. spec.*, *C. vulgaris* and *S. acuminatus*, which supernatants showed the highest biofilm inhibiting potential in static anti-biofilm assays, were chosen for further investigation. Assays were conducted for the first screenings with the mainly human pathogens *P. aeruginosa* PA14, *B. cenocepacia* K56-2, *S. maltophilia* K279a, *S. maltophilia* SM454 and *K. pneumoniae* WT1617. In order to address the needs of aquaculture, the fish pathogens *E. anguillarum*, *A. salmonicida*, *F. columnare* and *F. psychrophilum* accomplished the pathogenic arsenal for the following assays. Of the initial assays representative results are shown. Complex analyses were performed only on a limited number of pathogens.

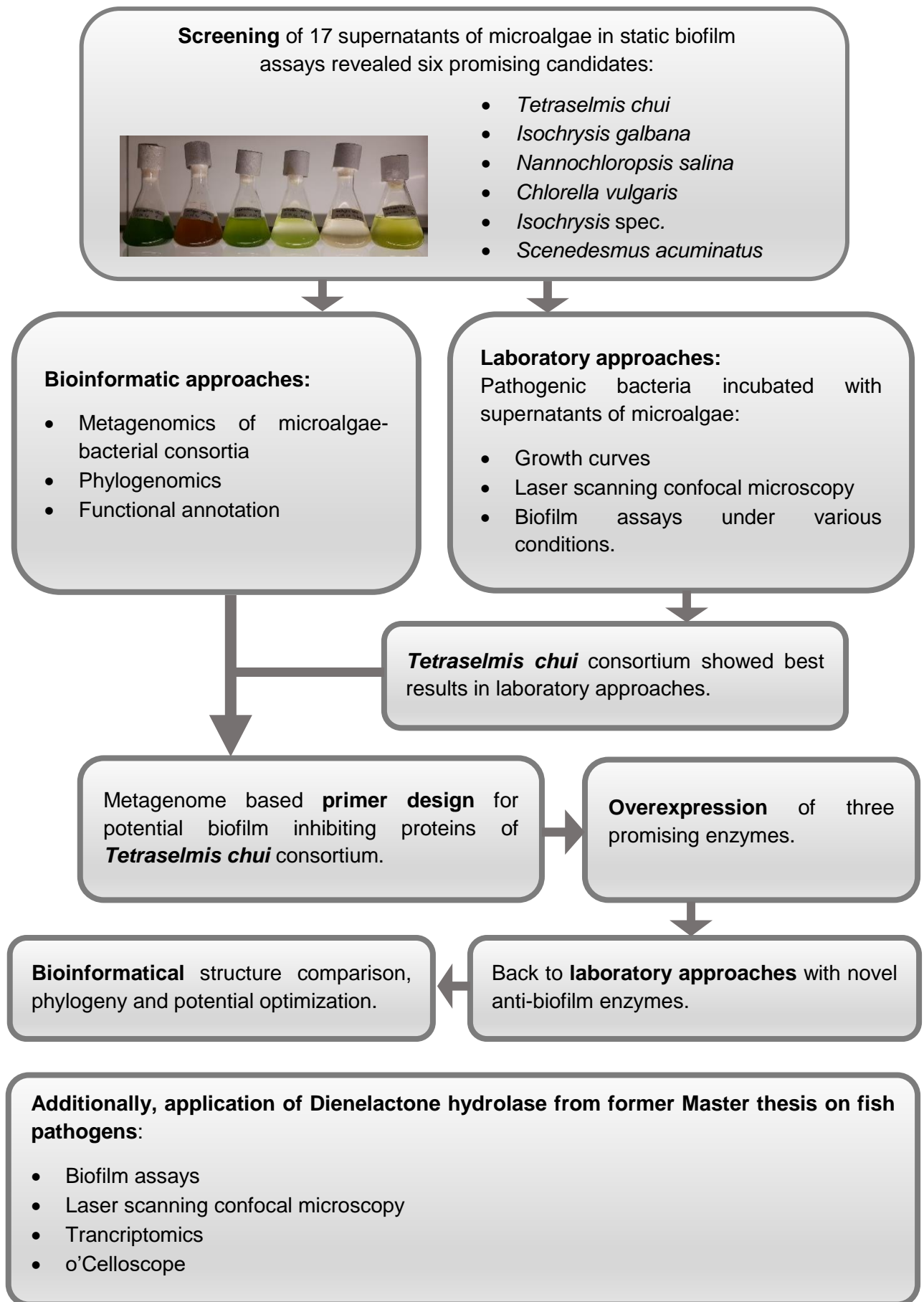


Figure 14: Workflow of laboratory and bioinformatic efforts to find effective anti-biofilm agents.

6.1 Microalgae supernatants

6.1.1 Static anti-biofilm assays

Static anti-biofilm assays were performed with 17 microalgae cultures on five different bacterial pathogens to quantify the effects of microalgae supernatants on bacterial biofilms. For evaluation the absorption values at 595 nm of the biofilms grown under the influence of the microalgae supernatant and the microalgae growth medium as control were compared after crystal violet stain. These static anti-biofilm assays revealed six microalgae cultures that showed the highest biofilm-inhibiting potential and were chosen for further investigations. The six most successful microalgae turned out to be *T. chui*, *N. salina*, *I. galbana*, *I. spec.*, *C. vulgaris* and *S. acuminatus*, as displayed in Figure 15.

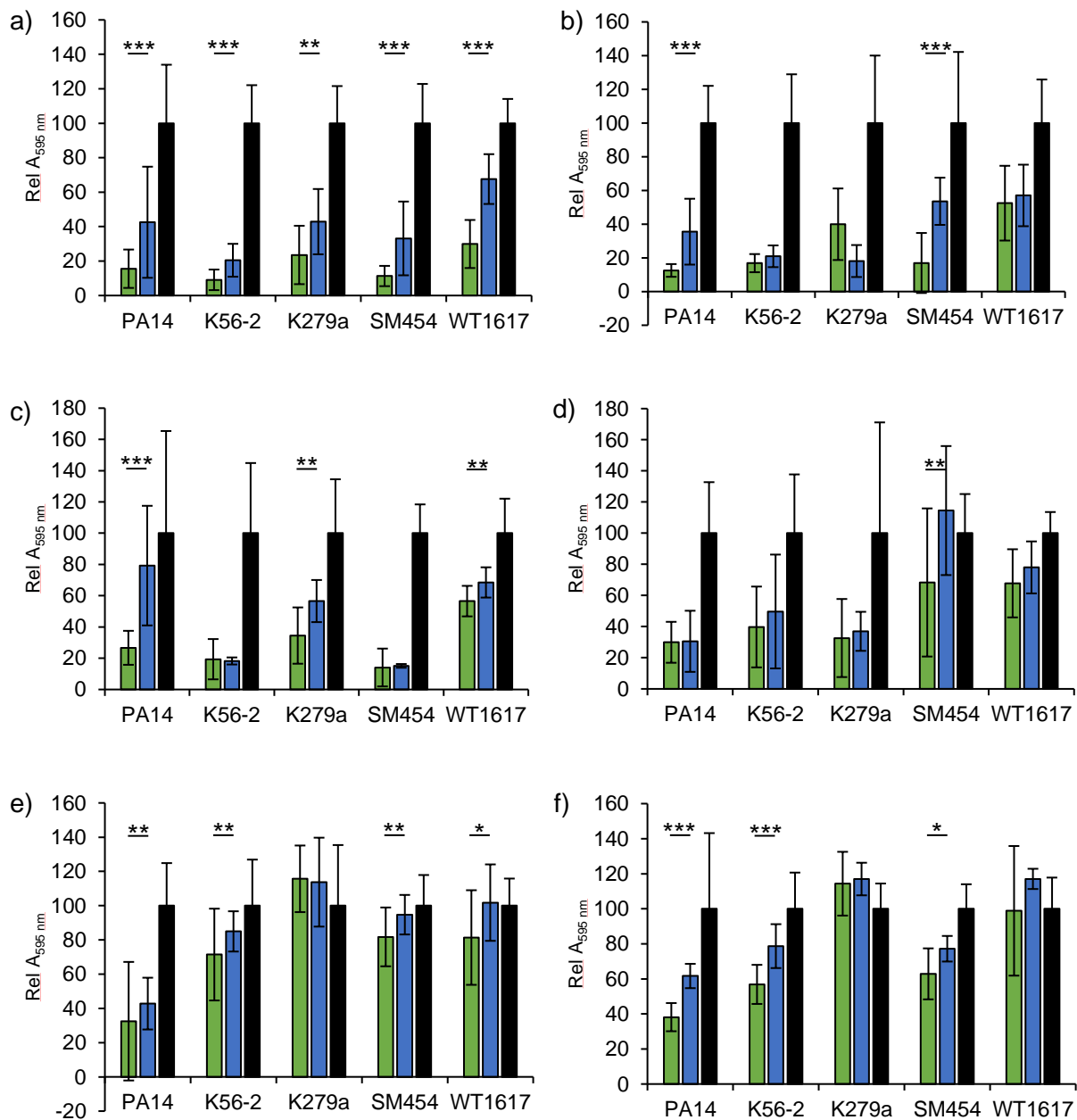


Figure 15: Static biofilm inhibition test with crystal violet staining. Supernatants of microalgae cultures were added to bacterial pathogens as initial testing of biofilm inhibition capacities (50 μ L of pre-cultured bacteria diluted to OD_{600 nm} 0.05 were pipetted into microwell plates, addition of 50 μ L of microalgae cultures and controls, static incubation for 24 h, 37 °C, analysis of biofilm density by crystal violet staining, absorption at 595 nm). The six most successful microalgae cultures of the 17 tested cultures are displayed. a) *T. chui*, b) *I. galbana*, c) *N. salina*, d) *I. spec.*, e) *C. vulgaris*, f) *S. acuminatus*. Bacterial species: PA14: *P. aeruginosa*, K56-2: *B. cenocepacia*, K279a: *S. maltophilia*, SM454: *S. maltophilia*, WT1617: *K. pneumoniae*. *T. chui* showed the most widespread and significant reduction of biofilm formation. Green: Supernatant of microalgae, blue: Growth medium of microalgae, black: Growth medium of bacterial species (LB-medium), supernatant and growth medium three times concentrated and sterile filtered. Significance, based on paired sample *t*-test is indicated by stars, p-value ≤ 0.05 (*), p-value ≤ 0.01 (**), p-value ≤ 0.001 (***).

Overall, the supernatants of the three marine microalgae *T. chui*, *N. salina* and *I. galbana* showed the best results in terms of percentage reduction of biofilm formation and significance. The supernatant of *T. chui* showed a highly significant reduction of biofilm formation observed for all tested bacterial species. The percentage reduction of biofilm formation ranged between 65.9% for *S. maltophilia* SM454 and 45.2% for *S. maltophilia* K279a (remaining results: 63.3% for PA14, 55.6% for K56-2, 55.8% for WT1617). The supernatant of the microalgae *N. salina* was found to reduce biofilm formation in three pathogens. *N. salina* achieved the highest biofilm reduction for *P. aeruginosa* by 66.3% (remaining results: 39% for K279a, 17.4% for WT1617). Of the two freshwater microalgae *C. vulgaris* showed higher biofilm-reducing capabilities compared to *S. acuminatus*. *C. vulgaris* reduced biofilm formation in four pathogens but only to minor degrees and with lower significance than the marine microalgae. The highest effect was achieved by *C. vulgaris* on *K. pneumoniae* WT1617 with biofilm reduction by 20%. Both freshwater microalgae, *C. vulgaris* and *S. acuminatus*, enhanced biofilm formation in *S. maltophilia* K279a, apparently driven by their growth media.

6.1.2 Effect of microalgae supernatants on growth curves of pathogenic bacteria

For a more precise estimation of the physiological impact of microalgae supernatants and microalgae growth media on the bacterial pathogens, growth curves over 30 h were performed with five bacterial pathogens and the six microalgae supernatants. Representatively, growth curves of *P. aeruginosa* PA14, *B. cenocepacia* K56-2 and *S. maltophilia* SM454 incubated with supernatants of *T. chui*, *C. vulgaris* and the respective growth media are shown in Figure 16. The growth curves revealed that the salty medium (F2, provided by BlueBiotech-GmbH, Germany) of the marine algae had the lowest growth retarding effect on *P. aeruginosa*. After 20 h, the growth of *P. aeruginosa* (Figure 16 a)) with F/2 medium equals the growth in LB-medium. The exponential growth phase of *P. aeruginosa* started after two hours in LB-medium compared to four hours in F/2 medium. *S. maltophilia* (Figure 16 c)) was more affected by F/2 medium, starting the exponential growth phase only after 12 h, compared to 3 h with LB-medium. *B. cenocepacia* (Figure 16 b)) showed the highest growth retarding effects caused by F/2 medium, starting a slow-growing phase only after 12 h and an exponential growth phase after 29 h. Interestingly, the supernatant of *T. chui* had a quite different effect on the three bacterial species. *P. aeruginosa* started exponential growth after six hours of incubation, while *S. maltophilia* started growing only after 20 h, not getting into exponential growth during 30 h of observation. *B. cenocepacia* on the other hand needed the longest time to start growing, 27 h, but started exponential growth after 29 h. For *C. vulgaris* supernatant and its Kessler & Czygan (KC) growth medium, no growth retarding effect was measurable for any bacterium. Only a lower OD_{600 nm} was reached in the stationary phase, in particular for *P. aeruginosa* (Figure 16 d)), growing to a final OD_{600 nm} of 1.2 in LB-medium compared to 0.9 in KC medium and 1.0 in *C. vulgaris* supernatant.

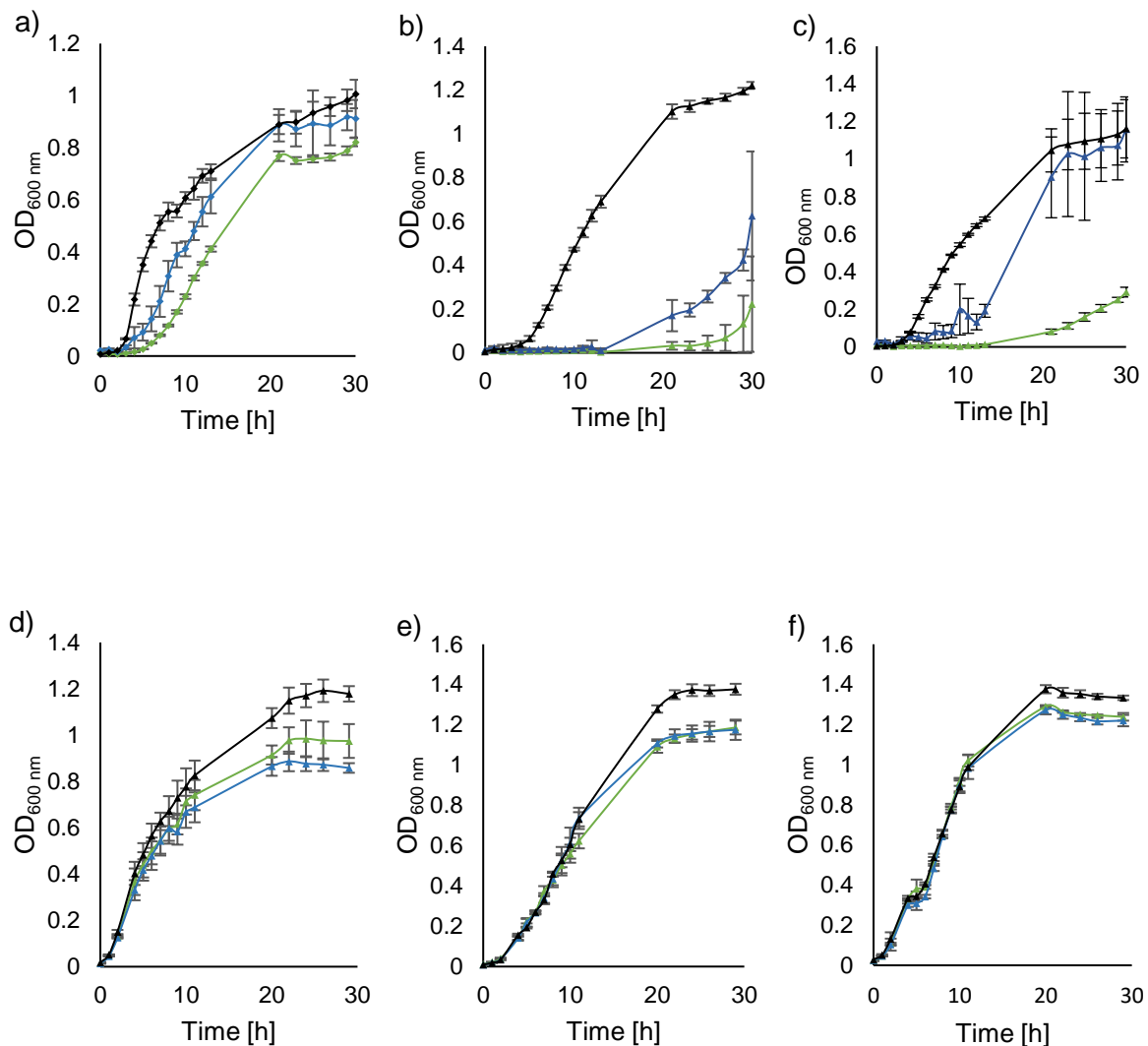


Figure 16: Influence of the supernatants of microalgae cultures and growth media on bacterial growth curves. a) to c) *T. chui* supernatant and the salty marine microalgae medium (F/2 medium), d) to f) *C. vulgaris* supernatant and Kessler & Czygan medium. Bacteria: a) and d) *P. aeruginosa* (PA14), b) and e) *B. cenocepacia* (K56-2), c) and f) *S. maltophilia* (SM454), black: bacterial growth medium, blue: microalgae growth medium, green: supernatant of microalgae. F/2 medium impacts bacterial growth at different intensities. While the growth of *P. aeruginosa* remained almost unaffected by F/2 medium and *T. chui* supernatant, the growth of *B. cenocepacia* and *S. maltophilia* was retarded by F/2 medium and even stronger by *T. chui* supernatant.

6.1.3 Effect of microalgae supernatants on mature biofilms

Classic static anti-biofilm assays focus on impeding biofilm formation from the initial phase on, hence, the anti-biofilm agent is added at the very beginning of the growth phase of a highly diluted bacterial culture and consequently co-cultured. The observed successful reductions of biofilm formation in the classic static anti-biofilm assays, see above, raised the question of the effects of microalgae supernatants on mature biofilms. Biofilms of the pathogens *P. aeruginosa* PA14, *B. cenocepacia* K562 and *S. maltophilia* SM454, matured for 20 h, were covered with

the supernatants of the very successful microalgae cultures *T. chui*, *I. galbana* and *N. salina* and analyzed by crystal violet stain after another 4 h (control), 8 h and 20 h of incubation. The results are presented in Figure 17.

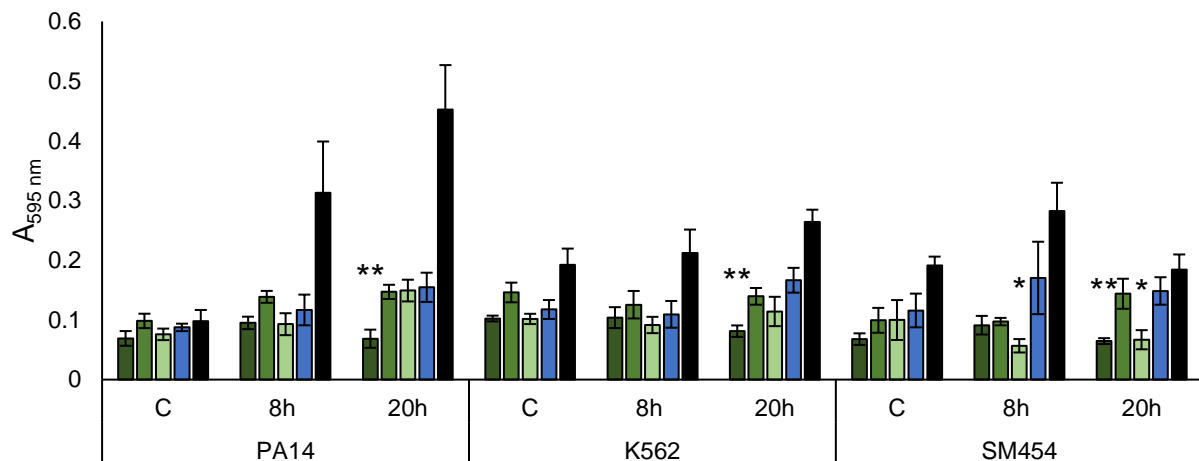


Figure 17: Effect of *T. chui*, *I. galbana* and *N. salina* supernatants on mature biofilms over time. Pre-grown cultures of *P. aeruginosa* PA14, *B. cenocepacia* K562 and *S. maltophilia* SM454 were diluted to OD_{600 nm} 0.05 and grown in microtiter plates for 20 200 μ L, 37 °C, static). Supernatant was carefully removed and 200 μ L of test liquid was added. Dark green: Supernatant of *T. chui*, green: Supernatant of *I. galbana*, light green: Supernatant of *N. salina*, blue: Microalgae growth medium (supernatant and microalgae growth medium three times concentrated and sterile filtered), black: LB-medium. Static incubation was prolonged for another 4 h (Control), 8 h and 20 h. Biofilm formation was analyzed via crystal violet staining. After 8 h of additional incubation significant reduction of the *S. maltophilia* biofilm by 66.7% was observed for incubation with *N. salina* supernatant. After 20 h of additional incubation *T. chui* achieved a reduction of the biofilms of all three pathogens by an average of 54.7%. *N. salina* confirmed the 8 h-result of *S. maltophilia* biofilm with reduction by 55% after 20 h. Significance, based on paired sample *t*-test is indicated by stars, p-value ≤ 0.05 (*), p-value ≤ 0.01 (**).

At first glance, mature biofilms appear not to be strongly affected by microalgae supernatants. By diving deeper into the data, this impression was confirmed for the supernatant of *I. galbana* (green), where no significant reduction of a mature biofilm over time was observable. However, the supernatants of *T. chui* (dark green) and *N. salina* (light green) caused significant reductions in biofilm thickness. While *N. salina* reduced the biofilm of *S. maltophilia* SM454 within eight hours by 66.7% and within 20 hours by 55%, *T. chui* amazingly induced a reduction of the mature biofilm for all tested bacteria. In contrast to *N. salina* which achieved the highest reduction after eight hours compared to the control, *T. chui* reduced the biofilms after the long-term incubation of 20 hours, compared to the eight hours values. The biofilms of *P. aeruginosa* PA14, *B. cenocepacia* K562 and *S. maltophilia* SM454 were significantly reduced by 54.8%, 52.4% and 57%, respectively. These surprising results underlined the outstanding potential of the *T. chui* supernatant.

6.1.4 Effects of microalgae supernatants visualized by LSCM

To confirm a result with a different approach should strengthen the trustworthiness of the result. Would the biofilm diminishing effect of the microalgae supernatants, evidenced in static biofilm assays, also be visible by laser scanning confocal microscopy (LSCM)? The supernatants of *T. chui*, *I. galbana* and *N. salina* were tested for an effect on the biofilm-forming pathogen *P. aeruginosa* PA14 as shown in Figure 18. Of each sample, three positions in the well (upper left, middle and lower right) were visually captured and analyzed. All of the biofilms treated with microalgae supernatants showed an inhomogeneous distribution of biofilm growth with an emphasis on growth in the middle of the well and reduced biofilm growth towards the peripheral regions, while the controls, growth medium of microalgae and bacterium, induced a more uniformly mode of growth. This might be caused by the concave surface meniscus, which is formed by the adhesion of the liquid to the wall of the well and might induce higher levels of the active antibiofilm agent at the periphery of the well, while in the middle the oxygen supply might be favorable. More effort would be necessary to clarify these findings. Optically, a distinct difference was noticeable between the density of the biofilm grown in the bacterial growth medium and all other conditions. Only minor differences appeared between the biofilms treated with microalgae growth medium or any microalgae supernatant. This visual impression was complemented by calculations of absolute numbers of living and dead cells and biofilm density of the scanned areas by BiofilmQ as displayed in Figure 19. The summed number of living and dead cells declined by 28.1% from 22569 cells to 16226 cells, when comparing the *P. aeruginosa* biofilm grown in bacterial or microalgae growth medium. The higher number of dead cells visible in the bacterial growth medium might have been caused by the faster beginning of the exponential growth phase of *P. aeruginosa* cells in bacterial growth broth compared to growth with microalgae growth medium or supernatant as depicted in Figure 16, above. Cultures that start their exponential growth phase later are supposedly more viable at a certain time point. Differences between treatment with microalgae growth medium or supernatants were far less obvious than observed with crystal violet staining. Cell numbers decreased by 25% from 16226 to 12112 taking living and dead cells together when comparing the biofilm treated with microalgae growth medium or supernatant of *T. chui*. Due to the uneven distribution of biofilm growth and the small sample size, no statistics had been calculable. On the other hand, diving deeper into the provided data of BiofilmQ a remarkable effect was observed. The height of the biofilms treated with bacterial or microalgae growth medium versus supernatant of *T. chui* increased from 4.0 μm to 5.2 μm and 6.0 μm , respectively. Correlating this increasing volume of the biofilms to the cell numbers within the respective volumes, a lower cell density within the treated biofilms was revealed with the supernatant of *T. chui*. A very flat and dense biofilm of *P. aeruginosa* turned into a more uneven, loosened biofilm

architecture exhibiting a lower cell density. Possibly, this leads to increased accessibility and susceptibility of inhabiting cells for antibiotic agents.

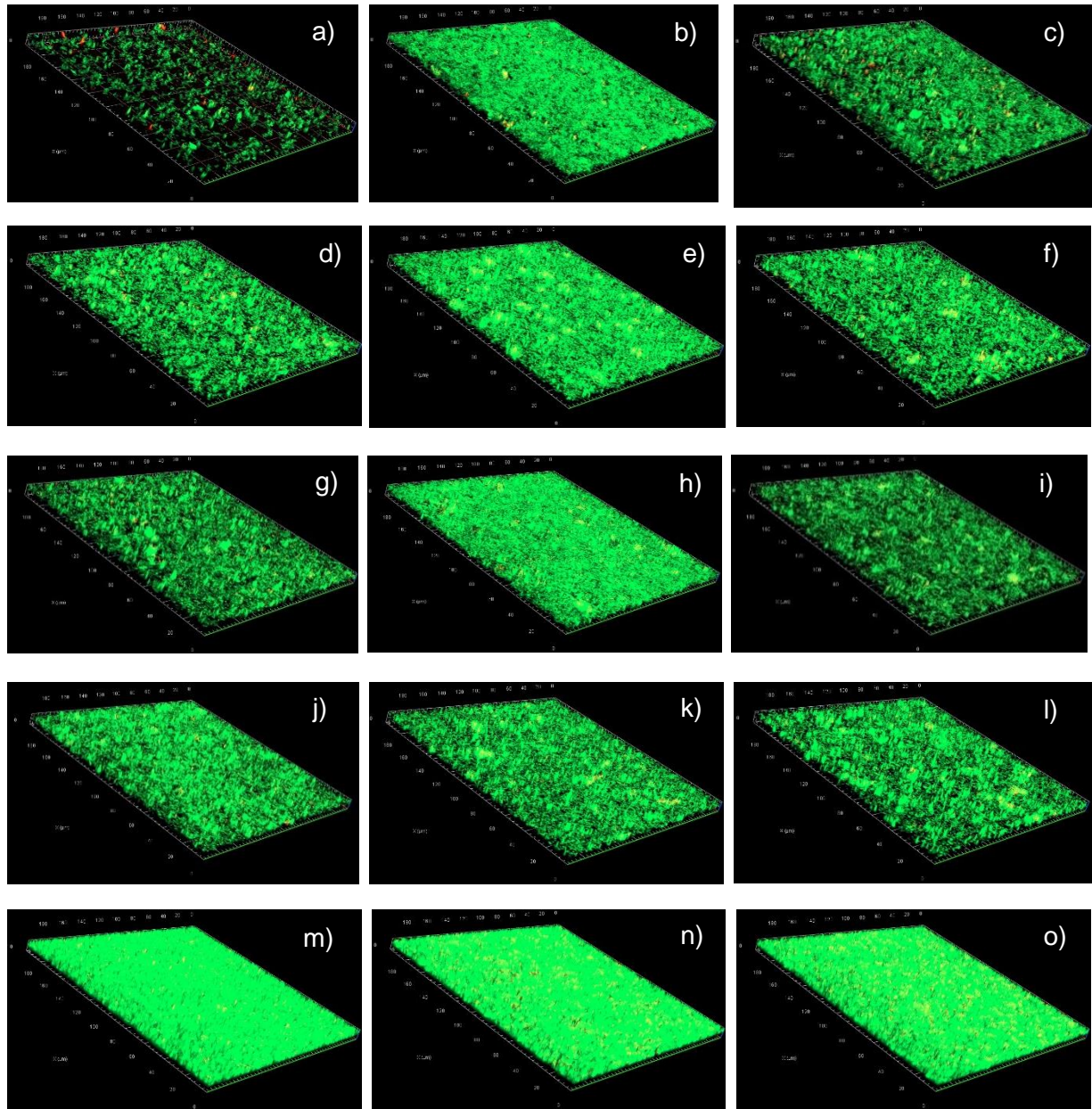


Figure 18: Confocal microscopy to visualize the effects of microalgae supernatants on bacterial biofilm producer *P. aeruginosa* PA14. Supernatants of *T. chui* a) to c), *I. galbana* d) to f) and *N. salina* g) to i) were tested for an effect on *P. aeruginosa* PA14 biofilm formation. j) to l) control microalgae growth medium, m) to o) control bacterial growth medium. 100 μ L of pre-grown bacterial culture diluted to OD_{600 nm} 0.05, addition of 100 μ L of test-liquid (microalgae supernatants and growth medium three times concentrated and sterile filtered), static incubation in eight-well μ -slide (Ibidi USA Inc., Fitchburg, WI), 37 $^{\circ}$ C, 24 h, after incubation removal of 100 μ L of supernatants and addition of 100 μ L of staining solution LIVE/DEAD BacLight bacterial viability kit (Thermo Fisher Scientific, Waltham, MA), static incubation for 1 h in the dark at room temperature, visualization of biofilms by CLSM Axio Observer Z1/7 LSM 800 (Carl Zeiss Microscopy GmbH, Jena, Germany) and C-Apochromat 63 \times /1.20W Korr UV VisIR objective, analysis and three-dimensional reconstructions by ZEN software (version 2.3; Carl Zeiss Microscopy GmbH). Images represent an area of 200 μ m by 200 μ m, Z-stack: Interval: 0,44 μ m, 21 slices, range 9.10 μ m. Stronger biofilm growth for *P. aeruginosa* PA14 in bacterial growth medium supported the findings of crystal violet stained biofilms, the differences between treatment with microalgae growth medium or microalgae supernatant remained less distinct than observed by crystal violet stain.

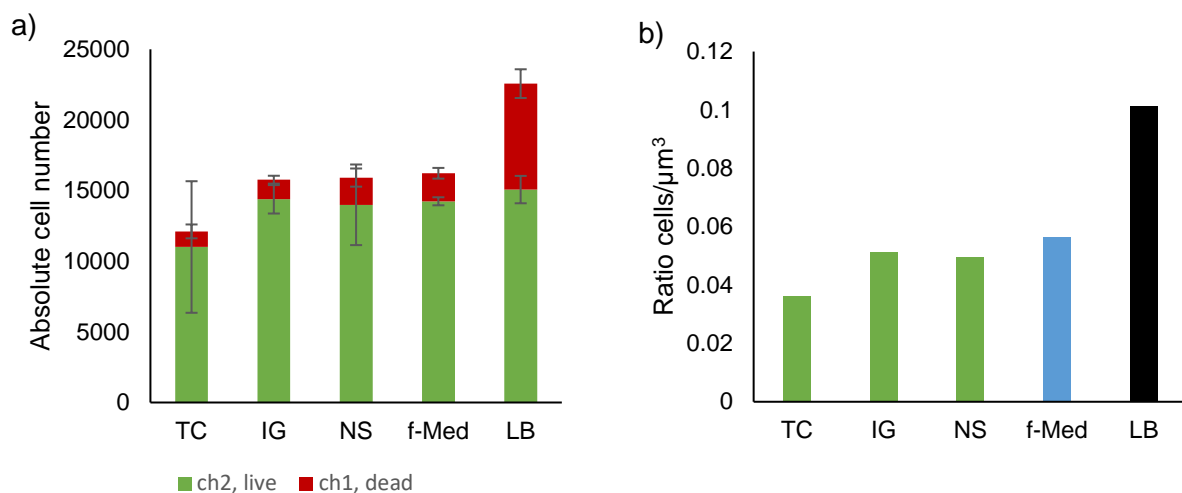


Figure 19: Analysis of LSCM data. a) absolute cell numbers, b) cell densities of *P. aeruginosa* PA14 biofilms treated with microalgae supernatants, analyzed by BiofilmQ (Hartmann et al., 2021). TC: *T. chui*, IG: *I. galbana*, NS: *N. salina*, f-Med: microalgae growth medium, LB: bacterial growth medium. Incubation with *T. chui* supernatant resulted in decrease by 25% of absolute cells numbers within a *P. aeruginosa* PA14 biofilm compared to the control of microalgae growth medium. Supernatants of *I. galbana* and *N. salina* had no effect on absolute cell numbers. The *T. chui*-treated biofilm of *P. aeruginosa* exhibited a lower cell density when the absolute cell numbers were related to the biofilm volume. Possibly, accessibility of biofilm inhabitants by anti-microbial agents is facilitated by loosened architectural structure. Huge deviations within the analyzed areas and few sample sizes made statistical significance incalculable.

As mentioned above, these findings only gave a hint and are not meant to be scientifically proven. However, this attempt helped to improve the assay for further trials. The lower discriminability of the different conditions in LSCM compared to the very reproducible results of the crystal violet stained static biofilms could be reasoned by huge differences during the procedure. While the wells of 96-well-plates for static anti-biofilm assay were rigorously emptied of bacterial supernatant and washed with ddH₂O (double deionized water) before staining, only 100 μL of the grown bacterial culture in ibidi slides for LSCM were discarded and replaced by 100 μL of staining solution. What was stained with this procedure? Alongside the biofilm cells, presumably, remaining planktonic cells or simply sedimented cells were stained. Washing the ibidi wells turned out to be too harsh for biofilms grown in ibidi slides and parts of the biofilms broke off, but carefully taking off the entire bacterial supernatant and replacing it with 150 μL of staining solution should be proposed for the future, underlining, that growing and staining conditions should be optimized for the individual bacterium.

To the author's knowledge, this is one of the most comprehensive studies evaluating the potential of microalgae supernatants. Former studies worked with extracts of total cell-lysates of microalgae which were tested on biofilms of human pathogenic bacteria (Cepas et al., 2019; Lopez & Soto, 2019). The use of solvents with different properties regarding their polarity for extraction only gave a rough estimation of the extracted agents and therefore, missed a

concept for practical applicability and host tolerance. Unfortunately, the total supernatants of microalgae cultures, used in this study, are black-boxes of ingredients as well. The fact that the molecules within the aqueous supernatant must have been secreted narrows the potential candidates to metabolites, signaling molecules or enzymatic compounds.

6.1.5 Composition of the microalgae supernatants

To test whether the observed effects on bacterial growth and biofilm formation could be attributed to protein-based enzymes, static biofilm assays were performed using native and heat-treated microalgae supernatants by comparison (heat-treated supernatants were heated to 95 °C for 10 min, all supernatants and microalgae growth medium were three times concentrated and sterile filtered). Due to denaturation, enzymes are supposed to alter or lose their function after heat treatment. This assay was performed for all six successful microalgae supernatants (see above) on the pathogens *P. aeruginosa* PA14, *B. cenocepacia* K562 and *S. maltophilia* SM454. For reasons of clarity, the presentation was reduced to the results of *T. chui*. The diminishing effect of *T. chui* supernatant on biofilm formation was distinctly impaired after heat treatment as presented in Figure 20.

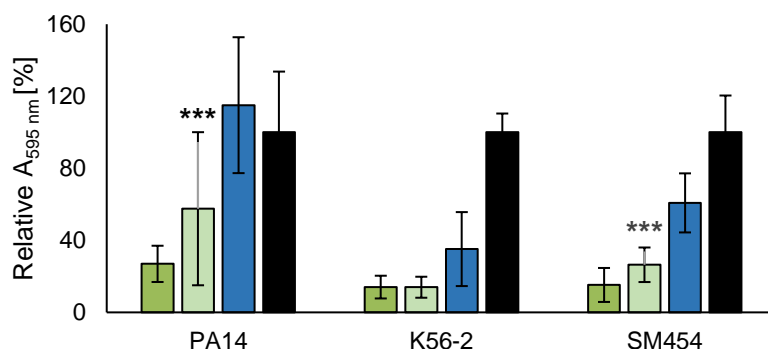


Figure 20: Comparison of biofilm-forming capacity. *P. aeruginosa* (PA14), *B. cenocepacia* (K56-2) and *S. maltophilia* (SM454) were treated with native or heat-treated supernatant of the microalgae *T. chui*. Green: Native supernatant, light green: Heat-treated supernatant (95 °C, 10 min), blue: Microalgae growth medium, black: Bacterial growth medium. All test liquids (apart from bacterial growth medium), three times concentrated and sterile filtered, were administered 1:1 to pre-grown bacterial cultures at OD_{600 nm} 0.5. The heat-treated supernatant of *T. chui* resulted in an increase in biofilm formation of 113.5% and 73.6% for *P. aeruginosa* (PA14), and *S. maltophilia* (SM454), respectively. The impaired effectivity of heated supernatant possibly points to a presence of proteins. Significance, based on paired sample *t*-test is indicated by stars, p-value ≤ 0.05 (*), p-value ≤ 0.01(**), p-value ≤ 0.001 (***).

In particular for *P. aeruginosa* PA14 the relative absorption maximum at 595 nm ($A_{595 \text{ nm}}$) increased by 113.5% when heat-treated supernatant was used. Hence, the heat-treated supernatant of *T. chui* allowed *P. aeruginosa* PA14 to double its biofilm-forming ability compared to the native supernatant. While the biofilm formation remained weak for *B. cenocepacia* K562, if treated with native or heated supernatant, *S. maltophilia* SM454 increased its biofilm forming capacity by 73.6% when treated with heated *T. chui* supernatant.

Comparable results were achieved by the heated supernatant of *N. salina* for *P. aeruginosa*, which showed an increase in biofilm formation of 123%. For *S. maltophilia* biofilm formation increased only by 28.4% when heat-treated supernatant of *N. salina* was used. The heated supernatant of *C. vulgaris* caused an increase in biofilm formation by 58% only for *P. aeruginosa* PA14 and no alterations in biofilm formation for any other bacteria. None of the other microalgae supernatants (*I. galbana*, *I. spec.* and *S. acuminatus*) showed comparable losses of biofilm inhibition to *T. chui* after their heat-treatment.

The impaired inhibitory effect of the heat-treated *T. chui* and *N. salina* supernatants on the biofilm formation of *P. aeruginosa* and *S. maltophilia* indicated a presence of proteins within the composition of the supernatants. Efforts to identify the bioactive proteins relied on massive up-concentration of the supernatants. Neither silver staining of SDS-electrophoresis gels, nor FPLC-approaches or professional proteome analysis rendered reasonable results. The identity of the putative anti-biofilm enzyme(s) remained undiscovered hitherto. However, further attempts to discover the powerful agents might be rewarding.

6.1.6 Current use of microalgae in fish farming

The addition of complete microalgae cultures alongside the corresponding bacteria to aquacultures was practiced up to date predominantly with the intention of wastewater



Figure 21: Project of NAFi - Verwertung der Nährstoffe aus Prozesswasser und Schlamm von Fischkulturanlagen ((<https://blaue-biooekonomie.de/de/projekte/nafi>, 21.03.2025)

treatment, oxygen production, or nutrition of the farmed fishes and is, to the author's knowledge, still under investigation (Han, 2019). One model aquaculture is located in Gönnebek (24610 Schleswig-Holstein, Germany) (see Figure 21). The project NAFi - Verwertung der Nährstoffe aus Prozesswasser und Schlamm von Fischkulturanlagen (Utilization of nutrients from process water and sludge from fish farming facilities) aims to establish a closed circle economy wherein the production of microalgal biomass for healthy fish nutrition

is fueled by the process water of the aquaculture (<https://blaue-biooekonomie.de/de/projekte/nafi> 21.03.2025). Microalgae directly convert ammonia and phosphate, raise the pH value by photosynthesis and release oxygen, which ameliorates the water quality, reduces the water exchange rate and has a positive effect on the general health of the farmed fish. Additional benefits, contributing to the cycle economy come from the aquaculture sludge, which is digested by earthworms, producing high-quality fertilizer. Moreover, the resulting warmth from the microalgae bioreactors can be utilized for species-

dependent heating of fish ponds. Auxiliary advancement of the closed-cycle aquaculture is the co-cultivation of higher plants like salads or herbs, referred to as aquaponic a hybrid of aquaculture and hydroponic (cultivation of crop plants in water), as shown in Figure 22.



Figure 22: Aquaponic system. photo D. Ausserhofer, IGB – Leibnitz-Institut für Gewässerökologie und Binnenfischerei (<https://www.aquakulturinfo.de>, 21.03.2025)

Still, the beneficial accomplishments face corresponding challenges. Closed-cycle aquaculture and aquaponic are cost-intensive in construction, operation and maintenance, while the yield is still lower compared to classic aquaculture. The choice of convenient aquatic animals for farming as well as suitable crop plants was under investigation for a long period. Cultivation of unpretentious fish like *Tilapia*, *Rainbow sprout* or *Pike* is successfully established, while plants beyond salads and herbs turned out to react more sensitively to changes in pH values and nutrition composition (<https://www.aquakulturinfo.de/aquaponik>). Biomass production of microalgae in particular in economically favorable open raceway pond systems is threatened by contamination risks through bacteria or other microbes and potentially limited by adverse conditions, such as temperature fluctuation and light deficiency (Han, 2019). Specific attention must be paid to the choice of the microalgae. Summarizing the above, microalgae strains, in particular for co-cultivation, need to fulfill certain requirements, such as high nutritional value in terms of protein and fatty acid content, fast reproduction rates, tolerance to variable water conditions like salinity, temperature and pH value, resilience to ammonium, low risk of forming harmful biofilms or blooms.

Considering the results of this part of the study, which made use of the supernatants of whole microalgae cultures, could strengthen the assumption of the suitability of the investigated microalgae for plain culture use. The potential of the microalgae for feed and water improvement should be explored in further studies.

However, the focus of this study lies in the possible development of target-specific enzymes derived from microalgae-bacterial consortia. To address that question, a better understanding of the communities on a genetic level is inevitable.

6.2 Metagenomic exploration of microalgae-bacterial consortia

6.2.1 Phylogenetic composition of microalgae-bacterial consortia

Metagenomes of the six microalgae that exhibited biofilm-decreasing properties were sequenced to gain insight into the composition of the surrounding bacterial community and the potential of biofilm inhibitory enzymes (sequencing details in supplemental Table S1). The phylogenetic compositions of the microalgae-bacterial consortia were analyzed on genus level, based on IMG gene count (Integrated Microbial Genomes and Microbiomes (Chen Min, 2021)) and displayed by pie charts in Figure 23. A cutoff of gene counts which were included in the analysis was set for each metagenome according to the overall number of gene counts. Due to processing, gene counts that could be assigned to organisms varied from 64,890 for *I. galbana* to 2,097 for *S. acuminatus*. The most abundant bacteria within all six metagenome data was found to be the class of Alphaproteobacteria (Woese et al., 1984). The gram-negative Alphaproteobacteria form one of the largest groups within bacteria. Due to a huge diversity in morphology and metabolism they are abundant in various marine and terrestrial environments (Giovannoni et al., 2005). The metagenomes of *T. chui*, *I. galbana* and *C. vulgaris* were dominated by Alphaproteobacteria accounting for 94%, 81% and 75% of gene counts, respectively. The microalgae metagenomes of *N. salina*, *I. spec.* and *S. acuminatus* still had pronounced proportions of Alphaproteobacteria (30%, 20% and 46%) but they showed exceptions like 40% of Bacteroidia (Krieg, 2011) for *N. salina* and 25% of Gammaproteobacteria (Garrrity, 2005) for *I. spec.*, while *S. acuminatus* showed a high proportion of 54% of Chlorophyta (Pascher, 1914). On genus level, the six metagenomes presented only some accordance. No genus was present in all of the six metagenomes but the marine bacteria *Roseovarius* (Labrenz et al., 1999), *Muricauda* (Bruns, Rohde, & Berthe-Corti, 2001) and *Marinobacter* (Gauthier et al., 1992) each appeared within three metagenomes. The rod-shaped, aerobic *Roseovarius* was found in *T. chui*, *I. galbana* and *I. spec.*, the facultatively anaerobic, appendaged *Muricauda* appeared in *N. salina*, *I. galbana* and *I. spec.* as did the aerobic *Marinobacter*, a genus that includes several motile species known as important hydrocarbon degraders. The greatest similarities were found between the metagenomes of *T. chui* and *I. galbana*, which shared the four genera *Parasphingorhabdus* (Feng et al., 2020), *Sulfitobacter* (Sorokin, 1995), *Roseobacter* (Shiba, 1991) and *Roseovarius* as well as *N. salina* and *I. galbana*, which shared *Hoeflea* (Peix et al., 2005), *Dinoroseobacter* (Biebl et al., 2005), *Marinobacter* and *Muricauda* as shown in Figure 24, illustrated by VennPainter (Lin et al., 2016).

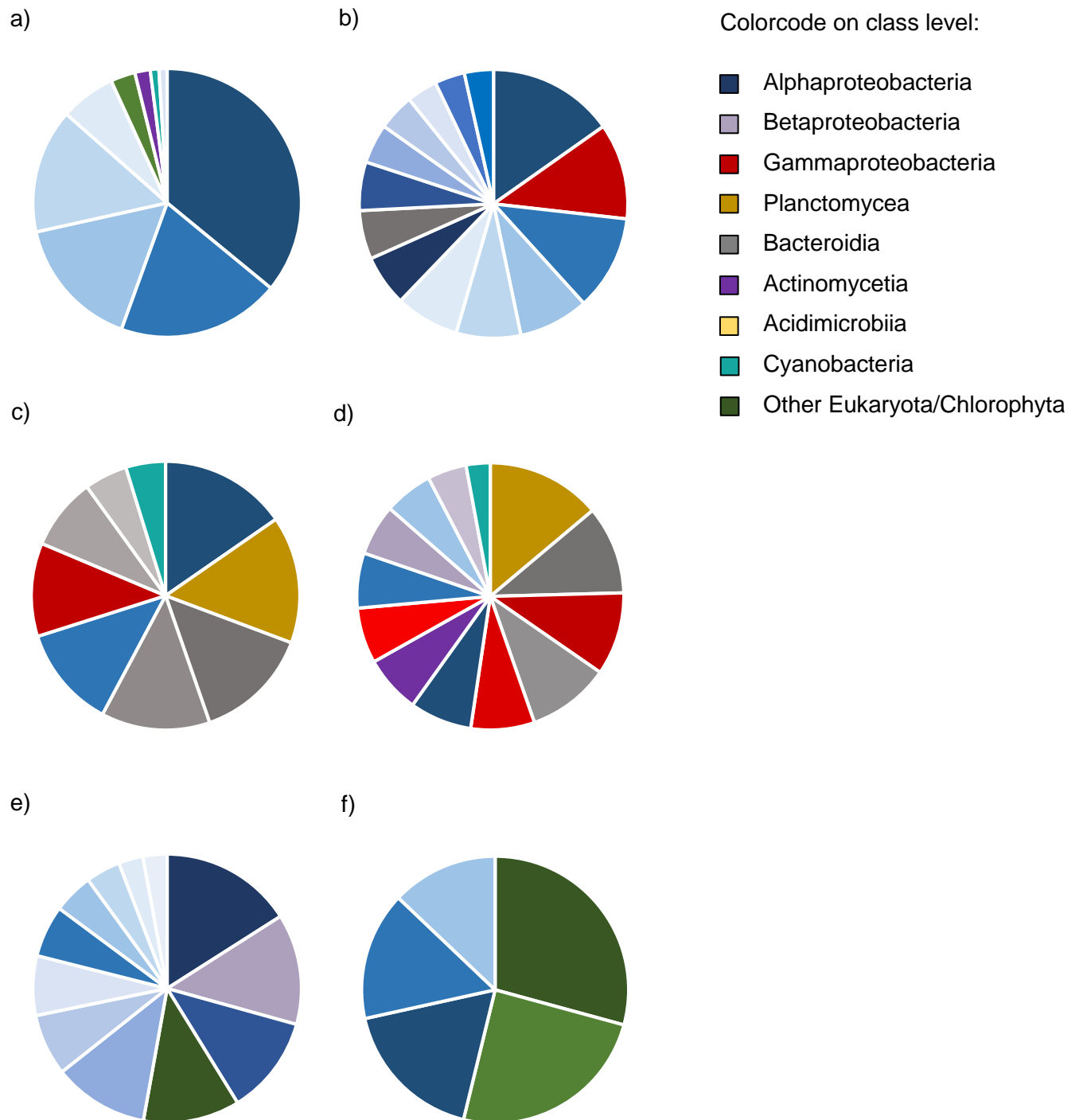


Figure 23: Metagenomic analyses of the phylogeny of the microalgae-bacterial consortia. Phylogenetic compositions of the microalgae metagenomes on genus level, based on IMG gene count. Organisms are displayed clockwise, colors refer to the superordinate class level. A cutoff of gene counts was set for each metagenome according to the overall number of gene counts which defined the minimal number of gene counts for a genus to be included the diagrams.

- a) ***Tetraselmis chui*** (cutoff 100 gene counts): *Sulfitobacter*, *Parasphingorhabdus*, *Roseobacter*, *Roseovarius*, *Paracoccus*, *Chlorophyta*, *Serinicoccus*, *Lyngbya*, *Puniceibacterium*
- b) ***Isocrysis galbana*** (cutoff 1000 gene counts): *Roseovarius*, *Marinobacter*, *Marivita*, *Dinoroseobacter*, *Stappia*, *Roseobacter*, *Muricauda*, *Erythrobacter*, *Nioella*, *Labrenzia*, *Sulfitobacter*, *Hoeflea*, *Parasphingorhabdus*

- c) ***Nannochloropsis salina*** (cutoff 1000 gene counts): *Hoeflea*, *Rhodopirellula*, *Algoriphagus*, *Muricauda*, *Dinoroseobacter*, *Marinobacter*, *Phaeodactylibacter*, *Marivirga*, *Aphanocapsa*, other Alphaproteobacteria
- d) ***Isochrysis spec.*** (cutoff 1000 gene counts): *Gimesia*, *Muricauda*, *Marinobacter*, *Arenibacter*, *Alcanivorax*, *Jannaschia*, *Nocardioides*, *Haliea*, *Roseovarius*, *Pusillimona*, *Marivita*, *Limnobacter*, *Moorea*
- e) ***Chlorella vulgaris*** (cutoff 1000 gene counts): *Methylobacterium*, *Variovorax*, *Mesorhizobium*, *Chlorella*, *Phyllobacterium*, *Tardiphaga*, *Blastomonas*, *Sphingomona*, *Sphingopyxis*, *Afipia*, *Phreatobacter*, *Bradyrhizobium*
- f) ***Scenedesmus acuminatus*** (cutoff 100 gene counts): *Chlamydomonas*, *Volvox*, *Reyranella*, *Enhydrobacter*, other Alphaproteobacteria

The most abundant class of bacteria within the microalgae metagenome data is the class of Alphaproteobacteria, illustrated in blueish colors. The metagenomes of *T. chui*, *I. galbana* and *C. vulgaris* were dominated by Alphaproteobacteria counting for 94%, 81% and 75% of gene counts, respectively. The microalgae metagenomes of *N. salina*, *I. spec.* and *S. acuminatus* still had pronounced proportions of Alphaproteobacteria (30%, 20% and 46%) but they showed exceptions like 40% of Bacteroidia for *N. salina* and 25% of Gammaproteobacteria for *I. spec.* *S. acuminatus* is the only metagenome showing a huge part of Chlorophyta (54%). On genus level the six metagenomes present only little accordance. No genus is present in all of the six metagenomes but the marine bacteria *Roseovarius*, *Muricauda* and *Marinobacter* each appear within three metagenomes.

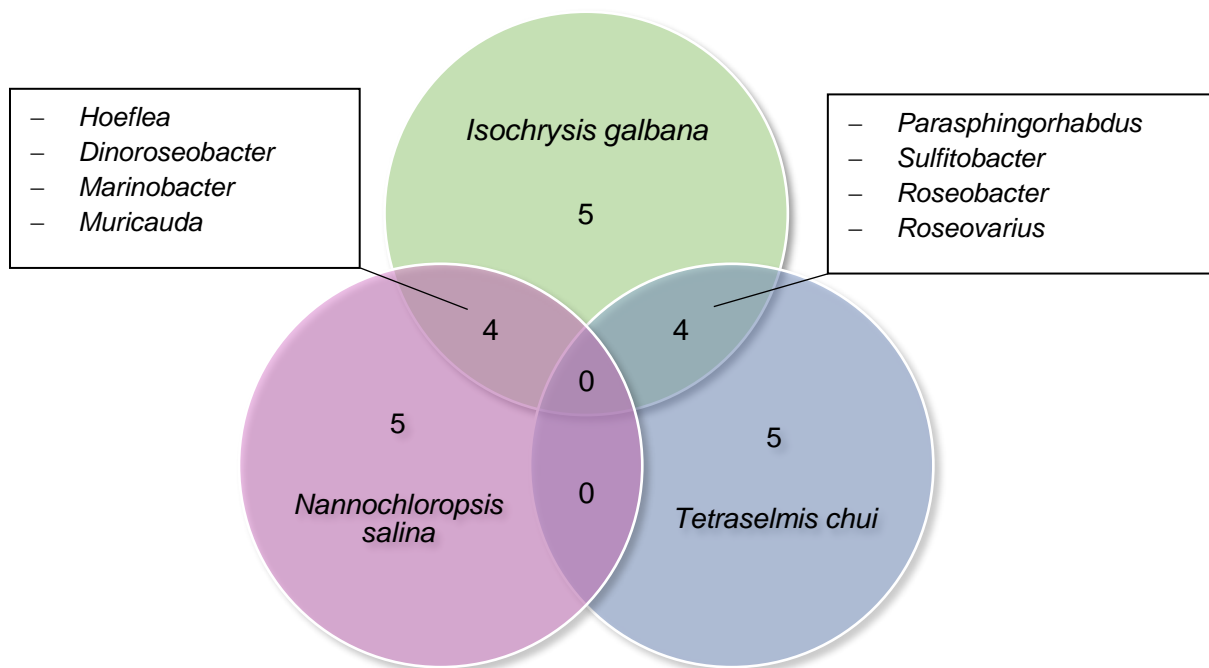


Figure 24: Venn diagram of shared organisms between the three marine microalgae *I. galbana*, *T. chui* and *N. salina* on genus level. Analysis of sequencing data by IMG. *I. galbana* and *T. chui* shared the genera *Parasphingorhabdus*, *Sulfitobacter*, *Roseobacter* and *Roseovarius*. *I. galbana* and *N. salina* shared *Hoeflea*, *Dinoroseobacter*, *Marinobacter* and *Muricauda*. These three microalgae cultures turned out to have the greatest similarities, which appeared to be consistent with their equal habitat and shared growth medium.

Similarities between these three microalgae were to be expected due to consistencies in natural habitat and usage of the same growth medium in laboratory conditions. Taking these circumstances into account, the similarities on genus level are surprisingly small as is the complete missing of similarities between the remaining microalgae cultures.

6.2.2 General key features of microalgae-bacterial consortia

To gain insight into the metabolic potential of the six microalgae-bacterial consortia KEGG analysis (Kyoto Encyclopedia of Genes and Genomes (Kanehisa, Furumichi, Sato, Matsuura, & Ishiguro-Watanabe, 2025) of the metagenomic data was performed via IMG (Table 21).

Table 21: General key features of microalgae-bacterial consortia.

	<i>Tetraselmis chui</i>	<i>Nannochloropsis salina</i>	<i>Isochrysis galbana</i>	<i>Isochrysis spec.</i>	<i>Chlorella vulgaris</i>	<i>Scenedesmus acuminatus</i>
Trait	Percent of all hits					
Aging, cell growth and death	2.2	1.5	1.3	1.2	1.7	2.1
Biosynthesis of secondary metabolites	1.1	1.4	1.3	1.4	1.2	1.1
Carbohydrate and glycan metabolism	9.4	10.5	10.2	10.4	9.7	9.3
Cell motility	0.8	1.5	1.6	1.4	1.7	0.3
Circulation, excretion, substance dependence	1.5	0.4	0.2	0.3	0.6	1.9
Endocrine and immune system	2.3	0.9	0.7	0.9	1.4	2.8
Energy metabolism	5.9	6.1	6.5	6.6	6.1	5.9
Folding, degradation, transport and catabolism	4.9	2.9	2.3	2.7	3.3	6.5
Global and overview maps	25.8	28.5	28.5	29.0	26.8	25.3
Lipid and nucleotide metabolism	6.9	7.2	6.9	7.2	6.9	7.2
Membrane transport	4.6	5.0	6.6	5.1	6.6	3.2
Metabolism of amino acids, cofactors and vitamins	16.5	18.6	19.2	18.6	17.7	15.1
Metabolism of terpenoids, polyketides, xenobiotics	3.7	4.6	4.8	4.8	4.8	3.7
Nervous and sensory system, environmental adaptation	1.5	0.5	0.4	0.5	0.7	1.8
Replication and repair	2.3	2.2	2.0	2.2	1.8	2.0
Signal transduction, signaling molecules and interaction	4.2	3.9	4.0	3.8	4.3	3.7
Transcription and translation	6.6	4.2	3.4	4.0	4.6	8.1
Total	100	100	100	100	100	100

Percent of gene counts, KEGG analysis of IMG metagenome annotation

All six microalgae-bacterial consortia showed comparable distribution patterns of key features with a strong emphasis on the metabolism of amino acids, carbohydrates, lipids and nucleotides, counting together for 34.6% of all activities, considering the respective means overall metagenomes. Energy metabolism accounted for additional 6.2%, while metabolism of terpenoids, polyketides and xenobiotics represented 4.4%. Genes of interest were expected to be included in membrane transport, signaling and interaction which were represented by 9.2%. Another 2.1% counted for replication and repair, 1.3% for biosynthesis of secondary metabolites and 0.9% for sensory systems and environmental adaptation, all of them features, that might harbor important functions for biofilm inhibition. No outliers were observed for any data set.

6.2.3 Potential of highly interesting enzyme candidates for antibiofilm and quorum quenching agents in microalgae metagenomes

Possible strategies for combating biofilms include either degradation of extracellular polymeric substances (EPS) performed by e.g. proteases, restriction endonucleases, deaminases and amylases or disturbing quorum sensing via degradation of signaling molecules by e.g. lactonases, oxidoreductases or further enzymes of the large family of hydrolases. It may also be relevant to synthesize antimicrobial agents like polyketides or to impair bacterial enzyme function by chelating ions like magnesium or iron. The COG-based (Clusters of Orthologous Genes (Tatusov, Koonin, & Lipman, 1997)) function search via IMG revealed a promising number of interesting biomolecules for today or future affords to combat bacteria and their sheltering surroundings within the microalgae metagenomes (Table 22).

Table 22: COG-based function search for potential molecules affecting either biofilm architecture or bacterial signaling within microalgae metagenomes

	<i>Tetraselmis chui</i>	<i>Isochrysis galbana</i>	<i>Nannochloropsis salina</i>	<i>Isochrysis spec.</i>	<i>Chlorella vulgaris.</i>	<i>Scenedesmus acuminatus</i>
Antibiofilm/antimicrobial agents						
Polyketide synthases	2	11	5	6	7	18
Restriction endonucleases	8	40	39	38	30	11
Amylases	13	12	23	23	15	34
Chelataes	33	237	163	132	130	75
Deaminases	67	430	291	330	274	97
Decarboxylases	62	371	312	371	260	143
Lyases	130	850	638	621	540	220
Proteases	246	1231	1056	1106	810	449
Quorum quenching agents						
Lactonases	15	132	112	107	85	28
Acylases	20	133	116	130	70	34
Oxidoreductases	177	1075	789	1005	742	380
Other Hydrolases	335	2055	1783	1798	1378	576
IMG Gene counts per 100 Mb						

Gene counts were normalized to 100 Mb for each metagenome. The unequal sequencing outcome was reflected by huge deviations in gene counts. In particular, the metagenomes of *T. chui* and *S. acuminatus* generated considerably fewer gene counts than the remaining metagenomes, while *I. galbana* showed the largest number of annotated genes within the majority of categories. In total, proteases appeared to be the most abundant enzyme class within all metagenomes, followed by oxidoreductases and lyases with a maximum of 1231, 1075 and 850 related genes, respectively in *I. galbana*. The category of other hydrolases included promising enzymes like glycosyl hydrolases that contribute to biofilm dispersal (Rumbaugh & Sauer, 2020) or diene lactone hydrolases and amidohydrolases to interfere with quorum sensing (Bergmann et al., 2024; Fetzner, 2015). Lowest abundance was revealed for

polyketide synthases, restriction endonucleases as well as amylases in a comparable distribution for all six metagenomes.

6.3 Novel dienelactone hydrolase (Dlh3) from *Scenedesmus communis* metagenome

As proof of principle, a novel dienelactone hydrolase (Dlh3), provided by Lena Preuß and derived from *Erythrobacter colymbi* (synonymous *Porphyrobacter colymbi* (Furuhata, Edagawa, Miyamoto, Kawakami, & Fukuyama, 2013)) from the previously sequenced metagenome of the microalgae *Scenedesmus communis* (synonymous *Scenedesmus quadricauda* (Brébisson, 1835)) (*S. communis* associated microbial communities, available at IMG), was tested for its biofilm inhibiting capacity (Bergmann et al., 2024) during the time-consuming process of sequencing and data analysis of the six new microalgae metagenomes. The *dlh3* gene was amplified by PCR from the metagenomic DNA of *S. communis* culture and cloned into the vector pET21a+. After overexpression in *E. coli* Rosetta-gami™ 2(DE3), a 32-kDa His-tagged Dlh3 protein could be purified.

According to Ngai et al., the enzyme dienelactone hydrolase (EC 3.1.1.45) catalyzes the conversion of *cis*- or *trans*-4-carboxymethylenebut-2-en-4-olide (dienelactone) to maleylacetate (Ngai, Schlomann, Knackmuss, & Ornston, 1987) as depicted in Figure 25.

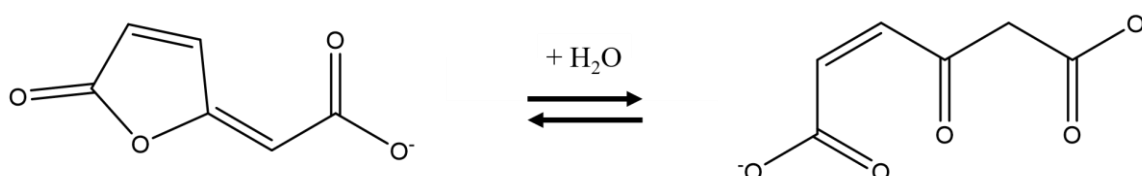


Figure 25: Catalyzed reaction by dienelactone hydrolase. Left: substrate dienelactone, right: product maleylacetate, reaction mechanism according to (Ngai et al., 1987)

The reaction mechanism of cleaving the lactone ring of dienelactone makes the dienelactone hydrolase a promising candidate for cleaving the lactone ring of *N*-acyl-L-homoserine lactones, the ubiquitously used signaling molecules for bacterial quorum sensing (see above). Degradation of signaling molecules silences quorum sensing, referred to as quorum quenching.

6.3.1 Quorum quenching

Interrupting the cell-cell communication at any point is called quorum quenching, presumably deployed by a given species of bacteria to outcompete another quorum-sensing species or by eukaryotes to fend off an invader (Bassler & Losick, 2006). The first description of an enzyme that could inactivate autoinducer molecules was published by Dong et al. in 2000. The authors found a strong ability to eliminate AHL activity of *Erwinia carotovora* (Jones, 1901) in the total protein extract from a *Bacillus* sp. (Cohn, 1872) strain. A 250 amino acid (aa) long product of

the *aiiA* gene was identified as an effective enzyme acting on autoinducer molecules. Due to its 'HXHXDH' domain, it was classified as metalloprotease, though the exact reaction mechanism on the AHL remained initially unclear (Dong, Xu, Li, & Zhang, 2000). AiiA turned out to act as lactonase and in a nonspecific way on acyl side chains, thus, it was believed to inactivate various AHLs. Isolated from *Bacillus* species made AiiA noteworthy because *Bacillus* as a Gram-positive bacterium uses peptide autoinducer for its own communication. Thus, *Bacillus* silences the Gram-negative community while keeping its own conversations uninterrupted (Bassler & Losick, 2006).

6.3.1.1 Halogenated furanones

Anti-quorum-sensing activity in eukaryotes was first discovered in the marine macroalga *Delisea pulchra* which produces halogenated furanones. As structural analogs to AHLs these molecules were proposed to bind competitively to LuxR-type proteins, the regulator proteins, which detect AHLs and act as transcription factors for further AHL-synthesis and virulence. Binding of furanones by LuxR causes conformational changes of LuxR, followed by proteolytic degradation of the furanone-LuxR complex. Moreover, the authors attributed an extended function to native AHLs as they were supposed not only to initiate transcription once bound to LuxR but also to maintain the steady-state concentration of LuxR by shielding the regulator from proteolysis (Manefield et al., 2002).

6.3.1.2 Modulation of host immune system by AHLs

Further activities of AHL became obvious in *in vitro* assays with *P. aeruginosa*, which uses AHLs of different chain lengths. In particular *N*-(3-oxododecanoyl)-L-homoserine lactone (3-oxo-C12 AHL) with a longer side chain and AHLs with shorter side chains like *N*-(3-oxohexanoyl)-L-homoserine lactone (3-oxo-C6 AHL) and *N*-butyryl-L-homoserine lactone (C4 AHL) became molecules of interest. Due to their lipophilic carbohydrate side chain AHLs appeared to readily diffuse across cell membranes and hence, were suspected to influence the outcome of an infection by modulating the host immune response per se (Telford et al., 1998). Telford et al. demonstrated for 3-oxo-C12 AHL a dose-dependent influence on antibody production in mice spleen cells and suppression of TNF- α and Interleukin-12 (IL-12) production in macrophages, possibly a downregulation of the host immune response. None of these effects was observed for the shorter 3-oxo-C6 AHL. Later, 3-oxo-C12 AHL revealed even more activity. After previous hints for induction of IL-8, cyclooxygenase 2 and prostaglandin E₂ production, suggesting a pivotal role for 3-oxo-C12 AHL in inflammation, Tateda et al. demonstrated a loss of viability and an induction of apoptotic factors (caspase 3 and 8), accelerating apoptosis in macrophages and neutrophils after incubation with 3-oxo-C12 AHL. Again, treatment with a shorter AHL, in this study C4 AHL, had no such effects (Tateda et al., 2003). Conversely, 3-oxo-C12 AHL inhibited lipopolysaccharide (LPS) induction of proinflammatory mediators by repressing nuclear factor κ -light chain enhancer of activated B-

cell (NF- κ B) signaling (Kravchenko et al., 2008), the host response to bacterial invasion. The effects of 3-oxo-C12 AHL appeared to be multifaceted and depended upon the cell type and dose. In conclusion, it seemed to be advantageous for *P. aeruginosa* to suppress the host immune response against bacterial invasion and thereby become invisible while simultaneously enhancing cell stress and apoptosis in mammalian immune cells like macrophages and neutrophils.

6.3.1.3 Paraoxonase family

Human defense against AHL-dependent quorum sensing was discovered in the well-conserved paraoxonase (PON) family which has three members PON1, PON2 and PON3, all of them identified as lactonases (Draganov et al., 2005). Examining the enzymatic activities of the three PONs on a wide range of compounds, Draganov et al. revealed that all of the tested AHLs were preferably hydrolyzed by PON2. PON2 is expressed intracellularly, is widely found in mammalian tissues, hosted in mitochondria and endoplasmic reticulum of various cell types and efficiently hydrolyzes 3-oxo-C12 AHL to 3-oxo-C12 acid (Horke et al., 2015). Horke et al. identified a unique mechanism by which PON2 can mediate the biological effects of 3-oxo-C12 AHL. The authors demonstrated that the hydrolyzed product 3-oxo-C12 acid accumulated in the cell and rapidly acidified the cytosol. Enhanced acidity triggers Ca^{2+} liberation and phosphorylation of p38 and eIF2 α , promoters of autophagy and apoptosis. Hence, PON2 activity has a dual outcome. It interferes with bacterial QS by hydrolyzing 3-oxo-C12 AHL and attenuating 3-oxo-C12-mediated effects on host cells, a beneficial effect. Conversely, the accumulation of 3-oxoC12 acid lowers the intracellular pH and triggers a series of biological effects, finally stimulating apoptosis (Horke et al., 2015; Tao et al., 2016). Since many effects of AHLs were observed to be dose-dependent, the levels of AHL that cells are exposed to *in vivo* are to be investigated.

The proposed reaction mechanism of DIh on AHL, the cleavage of the lactone ring of AHL, yielding acylhomoserine is presented in Figure 26 (Kusada, Zhang, Tamaki, Kimura, & Kamagata, 2019).

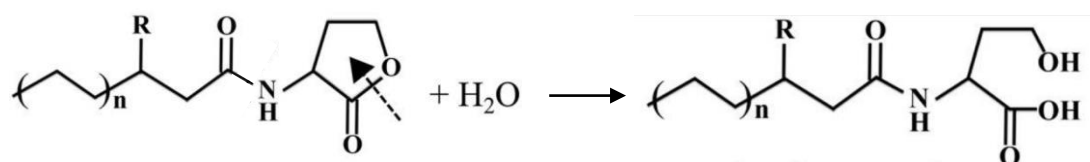


Figure 26: Proposed reaction mechanism of DIh on AHLs. The cleavage of the lactone ring of AHL (left) yields acylhomoserine (right), (Kusada et al., 2019).

Facing the numerous activities of AHL molecules beyond signaling underlines the urgency of degrading these signaling molecules.

6.3.2 Characterization of the novel Dlh3

6.3.2.1 Phylogenetic tree of different types of dienelactone hydrolases (Dlhs)

The Dlh family can be divided into three types according to their substrate specificities (Schlömann, Schmidt, & Knackmuss, 1990). Type I Dlhs possess *trans*-dienelactone hydrolyzing activity (e.g., Dlh from *Saccharolobus solfataricus* (Park, Yoon, & Lee, 2010)), Type II Dlhs only *cis*-dienelactone hydrolyzing activity (e.g., Dlh from *Pseudomonas cepacia* (Schlömann, Ngai, Ornston, & Knackmuss, 1993)), while Type III Dlhs are active against both *cis*- and *trans*-dienelactones (e.g., 2 Dlhs from *Cupriavidus necator* (A. Kumar, Pillay, & Olaniran, 2014)). The phylogenetic tree shown in Figure 27 implies that Type III Dlhs are clustered into two sub-groups, i.e., group A Dlhs exhibit higher catalytic rate to *trans*-dienelactone, such as Dlh from *Pseudomonas knackmussii* (Pathak & Ollis, 1990) and TfDEI from *C. necator* (A. Kumar et al., 2014), while group B Dlhs show higher rate of *cis*-dienelactone conversion, e.g., TfDEII from *C. necator* (A. Kumar et al., 2014). The phylogenetic tree also shows that Type III Dlhs from group B have a closer evolutionary relationship to Type II Dlhs and group A Dlhs are closer to Type I Dlhs.

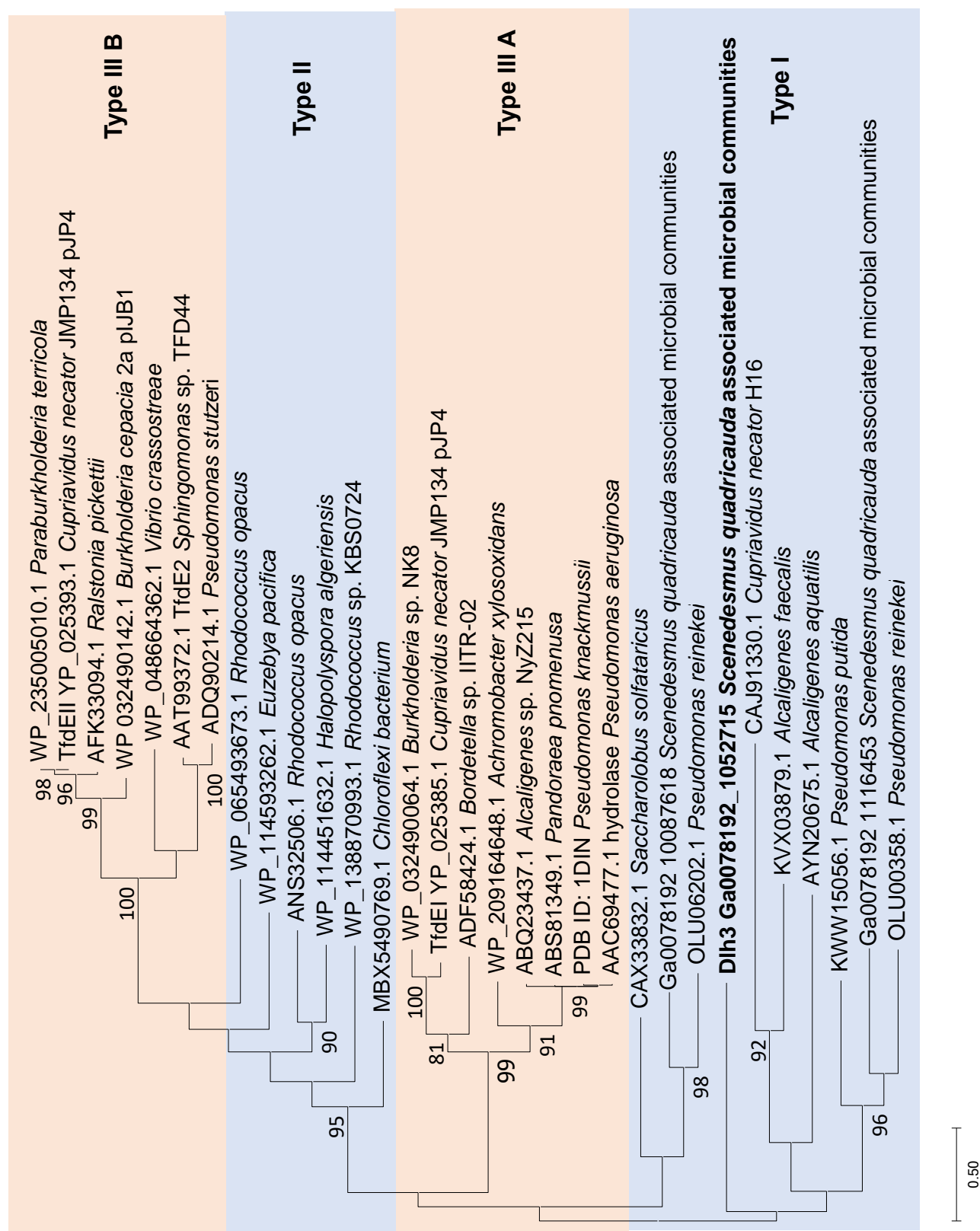


Figure 27: Phylogenetic tree of different types of diene lactone hydrolases (DIhs)

Phylogenetic relationships of DIh sequences. The sequences of DIhs were compared with the non-redundant protein database of NCBI by using BLASTP. The phylogenetic tree was constructed with MEGA-X (S. Kumar, Stecher, Li, Knyaz, & Tamura, 2018) based on the Maximum-likelihood method

and JTT matrix-based model (Jones, Taylor, & Thornton, 1992) with 1000 bootstrap replications after multiple alignments with T-Coffee (Notredame, Higgins, & Heringa, 2000). The percentage of bootstrap resamplings ≥ 70 is indicated on the branches. The scale bar represents the expected number of changes per amino acid position. The types of DIhs are classified according to (Schlömann et al., 1990). Type I DIhs possess *trans*-dienelactone hydrolyzing activity, type II DIhs are only active on *cis*-dienelactone, while type III DIhs are active on both, *cis*- and *trans*-dienelactones. The phylogenetic tree implies that Type III DIhs are clustered into two sub-groups, i.e., group A DIhs exhibit a higher catalytic rate to *trans*-dienelactone, while group B DIhs show a higher rate of *cis*-dienelactone conversion. The phylogenetic tree also shows that type III DIhs from group B have a closer evolutionary relationship to Type II DIhs and group A DIhs are closer to type I DIhs. DIh3 found from *Scenedesmus quadricauda* associated microbial communities (IMG) is phylogenetically clustered within type I DIhs, indicating that it might only be active on *trans*-dienelactone. The phylogenetic tree was provided by Dr. Yuchen Han (Bergmann et al., 2024).

The DIh3 identified from *S. communis* associated microbial communities is phylogenetically clustered within Type I DIhs, indicating that it may only be active on *trans*-dienelactone.

6.3.2.2 DIh3 active site and structure comparison

The identified DIh3 protein comprises a DIh domain as revealed by Pfam (Mistry et al., 2021) (E-value: $4.3e-33$). According to NCBI (<https://www.ncbi.nlm.nih.gov/>) DIh3 has 73% identity to a DIh from Alphaproteobacteria *Erythrobacter colymbi* (WP_086738354.1, E-value: $5e-104$). Its predicted 3-D structure by AlphaFold (Jumper et al., 2021) shows that DIh3 resembles a typical α/β -hydrolase with 8 α -helices and 8 β -sheets (Figure 28 a)). According to the sequence and structure alignments, DIh3 contains the typical catalytic triad Cys-His-Asp (C176, H262 and D231 of DIh3) in the active site (Figure 28 b)).

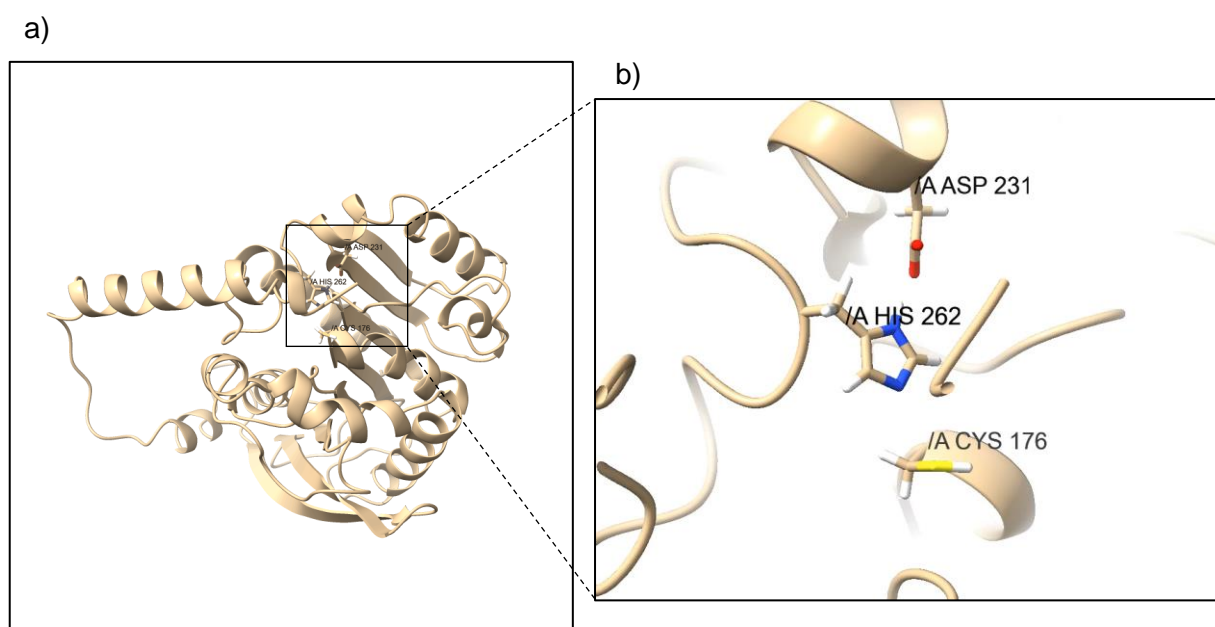


Figure 28: Predicted DIh3 structure by AlphaFold (Jumper et al., 2021) a) DIh3 resembles a typical α/β -hydrolase with 8 α -helices and 8 β -sheets. b) Active site of DIh3. The three critical amino acids (C176, D231 and H262) at the active site are highlighted. Images provided by Dr. Yuchen Han (Bergmann et al., 2024).

When compared to the Dlh crystal structure from *Pseudomonas knackmussii* (Pathak & Ollis, 1990), the Dlh domain of Dlh3 fits well with this reference structure (Figure 29). Dlh3 exhibits an additional N-terminal sequence of about 40 aa. SignalP prediction identified the additional sequence as a twin arginine translocation pathway (TAT) signal peptide (Tat/SPI, likelihood 0.948). A possible cleavage site is located between position 40 and 41.



Figure 29: Structure comparison of predicted Dlh3 structure (gold) with dienelactone hydrolase from *Pseudomonas knackmussii* (sky blue). The structure match was derived with UCSF Chimera (Pettersen et al., 2004). Except additional N-terminal sequence from Dlh3, the other parts including hydrolytic domain fit quite well with each other. From SignalP prediction (Nielsen, Tsirigos, Brunak, & von Heijne, 2019), the N-terminus of Dlh3 is a twin arginine translocation pathway (TAT) signal peptide (Tat/SPI, likelihood 0.948), possible cleavage site between pos. 40 and 41. Image provided by Dr. Yuchen Han (Bergmann et al., 2024).

6.3.2.3 Activity of Dlh3

The hydrolase activity of Dlh3 was analyzed with 4-Nitrophenyl octanoate (*p*NP-C₈) as substrate under different conditions (structure depicted in Figure 30). At 37 °C and 55 °C Dlh3 exhibited its highest activity in a buffer at pH 8.0. The activity was strongly reduced at 65 °C. The enzyme also hydrolyzed *p*NP-C₈ at moderate temperatures of 22–42 °C. The activity assay was performed by Dr. Yuchen Han.

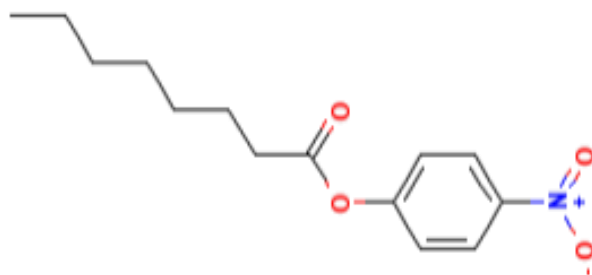


Figure 30: CID 97416, 4-Nitrophenyl octanoate, NCBI (2025), PubChem, Retrieved March 28, 2025 <https://pubchem.ncbi.nlm.nih.gov/compound/4-Nitrophenyl-caprylate> (synonymous for 4-Nitrophenyl octanoate). The colorless substrate releases chromogenic para-nitrophenol (yellow) when the ester bond is hydrolyzed, which can then be detected photometric at a wavelength of 405 nm. The concentration of Dlh3 was 0.825 mg/mL and 5 μ L protein was added to each assay. Each reaction was performed with 2 mM pNP-C₈ as substrate in 100 mM potassium phosphate buffer with different pH. The reactions were incubated for 1 hour and stopped by adding Na₂CO₃ with final concentration of 200 mM. The best condition for Dlh3 activity turned out to be at 55 °C and pH 8.0 The results indicated that Dlh3 is a thermostable enzyme and exhibits carboxylesterase activity. The activity assay was performed by Dr. Yuchen Han (Bergmann et al., 2024).

These results indicated that Dlh3 is a thermostable enzyme and exhibits carboxylesterase activity (Bergmann et al., 2024).

6.3.3 Effect of Dlh3 on biofilm formation of various fish pathogens

With respect to the applicability of the novel enzymes in aquaculture, all following assays were performed on the highly pathogenic bacteria for fish and potentially humans *E. anguillarum* ALM26, *A. salmonicida* A1 and *P. aeruginosa* PA14. Moreover, Dlh3 was tested on *F. columnare* B185R and *F. psychrophilum* NCIMB 13384. For associated diseases see Introduction – ‘Bacterial infections of farmed aquatic animals’.

6.3.3.1 Static anti-biofilm assays with Dlh3

For its mode of action in hydrolyzing lactone rings, Dlh3 is assumed to act as a quorum quenching agent. The effects of Dlh3 on various fish pathogens were evaluated by performing static biofilm assays with crystal violet (CV) staining for detecting all attached bacteria and extracellular matrix. A statistically significant reduction in biofilm formation, compared to the PBS control, was detected for *A. salmonicida* (44.2%±6.2%), *E. anguillarum* (41.5%±3.1%) and *F. psychrophilum* (21.4%±4.0%) after treatment with the highest concentration of 0.5 mg/mL of Dlh3 (based on a p-value ≤ 0.05). The addition of lower concentrated Dlh3 of 0.05 mg/mL, achieved a reduction in biofilm formation for *A. salmonicida* (35.9%±3.3%), *E. anguillarum* (54.5%±6.5%) and *P. aeruginosa* (19.1%±2.4%), all statistically significant. Treatment with a one hundred times diluted protein solution of 0.005 mg/mL of Dlh3 only showed an effect in reducing *P. aeruginosa* biofilm. Bacterial growth was not affected by Dlh3 (Figure 31).

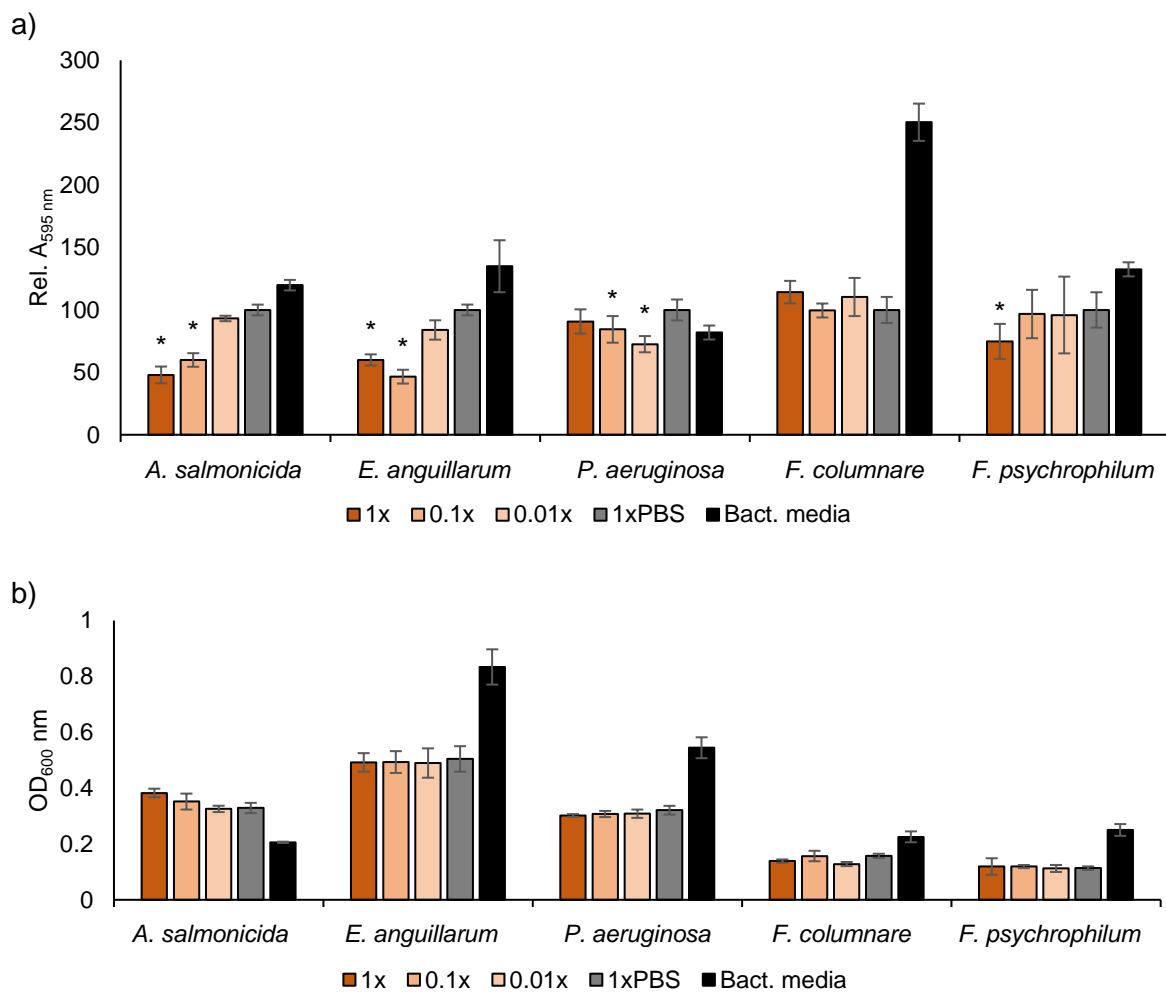


Figure 31: Effects of Dlh3 on various fish pathogens. a) static anti-biofilm assay, 48 h of static incubation at 28 °C, stained with cristal violet 0.5%, biofilm producer: *A. salmonicida*, *E. anguillarum*, *P. aeruginosa*, *F. columnare/psychrophilum*, protein: Dienelactone hydrolase (Dlh3), overexpressed in *Rosetta gami 2* DE3, concentrations: brown: 0.5 mg/mL, orange: 0.05 mg/mL, apricot: 0.005 mg/mL, grey: 1x PBS control, black: bacterial media control. Significance, based on paired sample *t*-test is indicated by stars, p -value ≤ 0.05 (*). b) Measurement of optical density (OD_{600 nm}) after 48 h of incubation at 28 °C.

The most constant results could be achieved with the highest enzyme concentration of 0.5 mg/mL, which was the selected concentration for the following assays.

Based on the promising results of up to 54.5% *E. anguillarum* biofilm inhibition by Dlh3, the following analyses focused on *E. anguillarum* to uncover the underlying mechanisms and possible pathways.

6.3.3.2 Reduced cell numbers in LSCM analysis

LSCM analysis was performed to evaluate biofilm characteristics beyond the quantitative biofilm assays and to obtain absolute cell numbers in observed biofilms as well as portions of living and dead cells. The results from the CV-based biofilm assays were confirmed by LSCM imaging of *E. anguillarum* biofilm treated with Dlh3 (Figure 32).

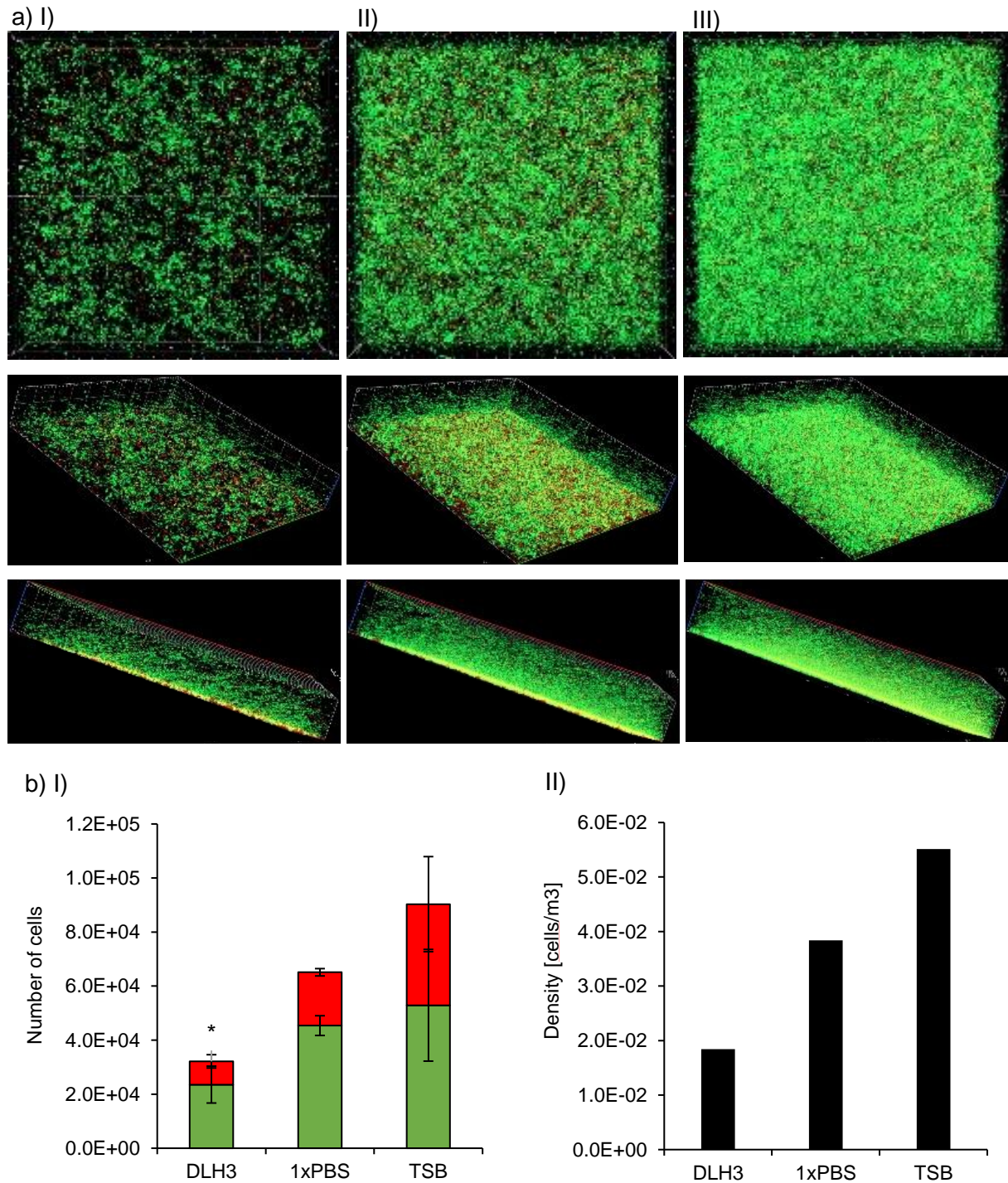


Figure 32: LSCM analysis of static biofilms. a) LSCM, biofilm producer: *E. anguillarum* ALM26. Static incubation with test liquids, 0.5 mg/mL Dlh3, 1x PBS at 28 °C for 48 h. Staining: SYTO 9 (green fluorescence) for living cells, propidium iodide (red fluorescence) for dead cells, x-axis 200 μ m, y-axis 200 μ m, z-axis 20 μ m, z-stacks of 80 slides. I) Dienelactone hydrolase (Dlh3), II) control: 1x PBS, III) control: bacterial growth medium TSB (Tryptic soy broth). Shown is surface of z-stack (first row), top-position (second row) and side-position (third row). b) Calculation of cell numbers I) and density II) of the biofilm, performed by MatLab/BiofilmQ (<https://drescherlab.org/data/biofilmQ/docs/>). Significance, based on paired sample *t*-test is indicated by stars, *p*-value ≤ 0.05 (*).

A reduction of 51% in total cell number was observed compared to the PBS control. The number of living cells was reduced by 48%, while the number of dead cells was 56% lower

when treated with 0.5 mg/mL Dlh3. The biofilm structure changed significantly by appearing more porous and pitted. In contrast to the homogenous character of the untreated biofilm, the Dlh3-treated biofilm showed patches of higher and lower density up to areas free from attached bacteria. A calculated reduction of the biofilm density by 52% compared to the control confirmed the visual impression and confirmed the disturbing effect of Dlh3 on the organization of the unicellular bacteria in the biofilm.

6.3.4 Transcriptome analysis of *E. anguillarum* in the presence of Dlh3

To unravel the potential inhibitory mechanism of Dlh3 on biofilm formation, the transcriptomes of *E. anguillarum* in the presence of Dlh3 and PBS as control were compared. These data elucidated the gene expression of *E. anguillarum* in response to Dlh3, with potential implications for biofilm formation. Sequencing of the mRNA resulted in a minimum of 9.53 million sequences with an average length of 75 bp and a GC content of 55% (supplemental Table S2). Overall, a total of 3297 expressed genes were identified from the dataset as documented in the supplemental of (Bergmann et al., 2024). The circular genome mapping of the datasets was generated to the reference genome of *E. tarda* EIB202 (NC_013508.1) and visualized in supplemental Figure S1. To quantify the differential gene expression of *E. anguillarum* under the influence of Dlh3 log₂ (Fold change) values were calculated for all identified genes indicating up- or down-regulation of respective functions. Their significances were plotted in a Volcano plot and a functional profile analysis (Figure 33). In addition to the generally regulated metabolic genes, e.g., for transport and metabolism of amino acids, carbohydrates, lipids and nucleotides, transcription and translation, as well as signaling transduction mechanisms, genes linked to secretion systems, biofilm formation, quorum quenching and quorum sensing mechanisms could be identified. The analysis shows high expression levels for transporter and channel proteins. The most significantly up-regulated genes were affiliated with transport mechanisms and membrane proteins, including antiporter membrane proteins (e.g., CysZ, EamA family, chloride channel protein). The highest upregulation of gene expression was discovered for the copper-exporting P-type ATPase CopA (Gourdon et al., 2011). Copper as a cofactor in proteins is involved in electron transport and iron trafficking and thus has a high importance in the cellular metabolism of bacteria (Comolli & Donohue, 2004; Huston, Jennings, & McEwan, 2002). Proper regulation of intracellular copper levels is vital, as high levels of copper can induce cell damage or death (Teitzel et al., 2006). As a reaction to host- or environmental-mediated copper intoxication, bacteria can express a wide range of efflux systems to maintain metal ion homeostasis, e.g., further members of the P-type ATPase family. CopA is regulated by the MerR-family regulator CueR which is activated by quorum sensing signaling via AHL autoinducer molecule (Thaden, Lory, & Gardner, 2010). Furthermore, CopA is known to modulate oxidative stress resistance,

potentially contributing to increased tolerance to toxic metal species in biofilms induced by quorum sensing pathways (Alquethamy et al., 2019).

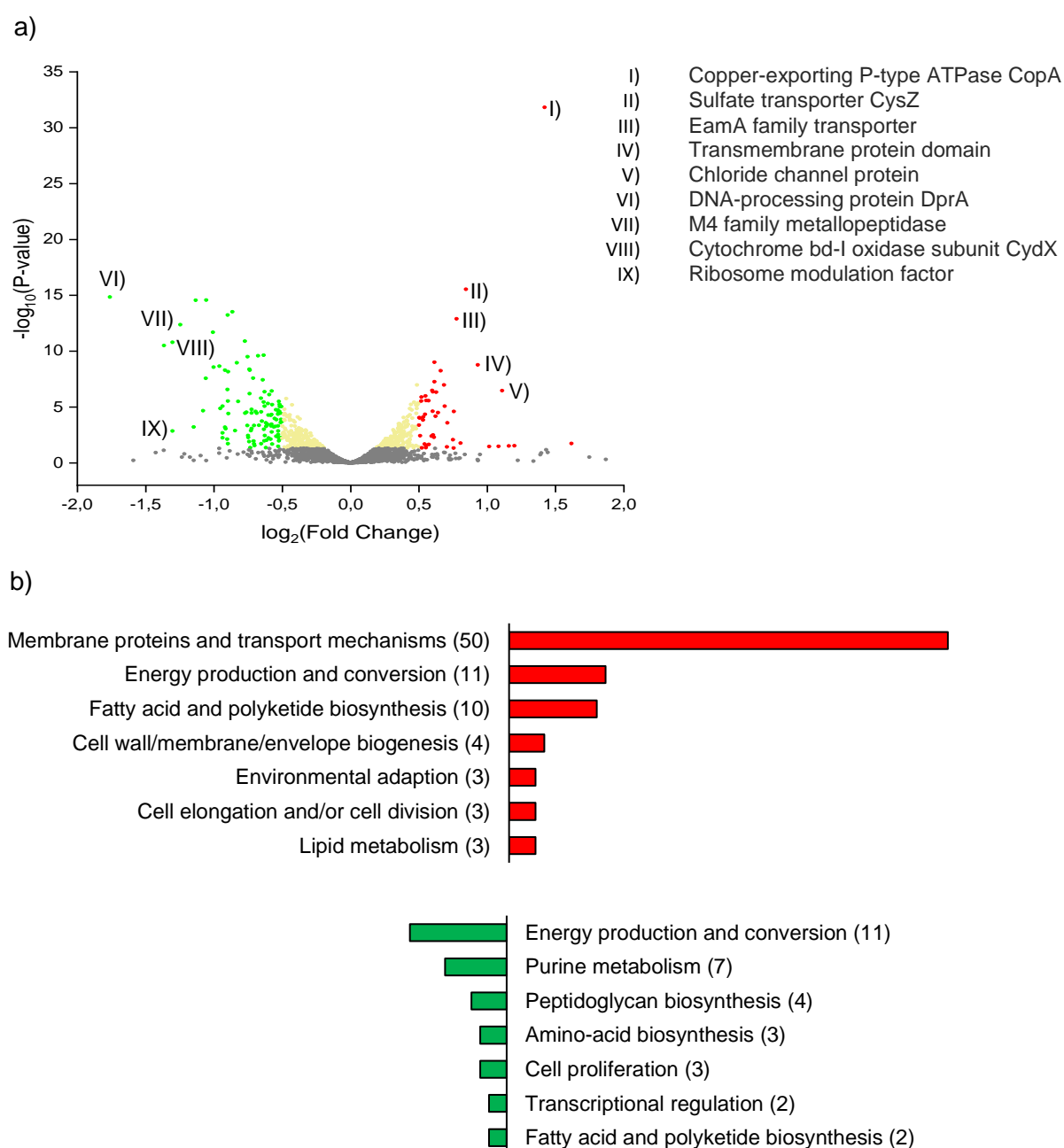


Figure 33. Differentially expressed genes (DEGs). DEGs in *E. anguillarum* ALM26 cultured in the presence of 0.5 mg/mL Dlh3 compared with 1x PBS control dataset. a) Volcano plot build with OriginLab (<https://www.originlab.com/>) of transcriptome data highlights up- and down-regulated genes in *E. anguillarum* encoding the following proteins: I) copper-exporting P-type ATPase CopA, II) sulfate transporter CysZ, III) EamA family transporter, IV) transmembrane protein domain, V) chloride channel protein, VI) DNA-processing protein DprA, VII) M4 family metalloproteinase, VIII) cytochrome bd-I oxidase subunit CydX, XI) ribosome modulation factor. Color key: red: up-regulated genes ($\log_2(\text{FoldChange}) > 0.5$, $p\text{-value} < 0.05$), green: down-regulated genes ($\log_2(\text{FoldChange}) < -0.5$, $p\text{-value} < 0.05$), yellow: $\log_2(\text{FoldChange})$ between $-0.5 - 0.5$, $p\text{-value} < 0.05$, grey: $p\text{-value} > 0.05$. b) The function profile of differentially expressed genes in *E. anguillarum* presents the groups of most active genes. Total number of genes are shown in brackets. Data of Figure 33 b) provided by Dr. Yekaterina Astafyeva (Bergmann et al., 2024).

These findings suggest that comparable mechanisms exist for further molecules or elements since the majority of the significantly upregulated genes were involved in transport mechanisms or membrane proteins (50 genes) e.g., chloride channel protein and sulfate transporter *cysZ*. Down-regulated genes were mainly found to encode for energy production and conversion mechanisms (11 genes), purine metabolism (7 genes), fatty acid and polyketide biosynthesis (2 genes), amino-acid biosynthesis (3 genes), cell wall biogenesis (3 genes), and peptidoglycan biosynthesis (4 genes). Of high relevance appeared to be the DNA-processing protein DprA, M4 family metallopeptidases, cytochrome bd-I oxidase subunit *CydX*, and ribosome modulation factors.

6.3.5 Inhomogeneous cell layers of *E. anguillarum* in the presence of Dlh3

oCelloScope™ offers the opportunity of an automated microbial live-cell imaging technology (BioSense Solutions ApS, 3520 Farum, Denmark). By taking photos according to an individual interval, microorganisms can be observed and compared while growing under varying conditions in flat bottom 96-well microtiter plates. *E. anguillarum* at start OD_{600 nm} 0.025 was grown in the presence of Dlh3 (0.5 mg/mL) and PBS as well as the bacterial growth medium TSB (Tryptic soy broth) as controls for 16 h at 28 °C, taking photos every two hours (Figure 34, last 4 h not shown). From 6 h on, differences in cell density became obvious. *E. anguillarum* cells grew the fastest in TSB medium, as predictable. PBS attenuated the bacterial growth, while in the presence of Dlh3 growth rates appeared to be at an intermediate level according to the light transmittance of the bacterial layers in the wells. At the timepoint of 8 h of incubation, uncharacteristic darker spots of about 100 to 150 µm in length and about 10 to 50 µm in width with irregular, often curved formations appeared in the wells of *E. anguillarum* incubated with Dlh3 (Figure 34 I)). These formations occurred in all of the six replicates of *E. anguillarum* grown with Dlh3 but not in any of the wells of *E. anguillarum* grown with PBS or TSB, at any timepoint. Moreover, the same experiment with *A. salmonicida* grown with Dlh3, PBS and bacterial growth medium NB (Nutrient broth) rendered only smooth bacterial layers with well-distributed cells over the entire time of incubation. One can only speculate, if mechanisms of defense (see upregulation of transport mechanisms in transcriptome), impaired coordination due to the loss of the signaling AHL molecules, or a yet unknown reaction induced the uncharacteristic dark spots. Most likely, the observed structures refer to bacterial auto-aggregation. Interbacterial adhesion, promoted by proteins, appendages such as fimbriae and pili or secreted macromolecules like extracellular DNA (eDNA) and exopolysaccharides is assumed as the third bacterial lifestyle (Nwoko & Okeke, 2021) beyond planktonic and surface attached existence as described in section 'Lifecycle of biofilms' above. Hitherto, bacterial aggregates are mainly recognized and investigated in liquid environments such as marine gel particles (MGP), aggregates in sea surface multilayer (SML), ocean mixed layer (ML), or in freshwater surroundings forming 'river snow' as documented in Elbe river in Germany

(Böckelmann, Manza, Neub, & Szewzyka, 2000; Cai, 2020). Bacterial flocs are subjects in wastewater treatment and they are of concern in medical context, forming biofilm-like aggregates in the mucus of cystic fibrosis patients and chronic wounds (Alhede et al., 2011; Bay et al., 2018; Flemming et al., 2024). Studies on biofilm formation of *Edwardsiella tarda* focused on the type of appendages required for auto-aggregation as physiologic initiation of biofilm formation and proposed, that filamentous appendages induced by type III secretion system *eseB* were crucial in early stages of biofilm formation (Z. Gao et al., 2015). If auto-aggregation was regarded as a prerequisite for biofilm formation, the data of this study would contradict this suggestion, since biofilm formation was reduced while auto-aggregates were formed. Within this experiment, growing of *E. anguillarum* was observed in three different conditions by oCelloScope. Even though growth was more impaired in the condition with PBS, *E. anguillarum* only formed the potential auto-aggregates in the presence of Dlh3. Little is published about signaling involved in auto-aggregation. Either irritation due to missing signaling molecules, hyper-protection, or dysregulation of one of the additional functions found for AHL molecules, understanding which stimuli drove the cells to aggregate and which signaling pathways were used by the cells would accomplish our understanding of biofilm formation and virulence. According to Nwoko & Okeke, 2021 and Gao et al., 2015, filamentous appendages are necessary for auto-aggregation and therefore, presumably will be up-regulated in the timeframe of 8 h after incubation of *E. anguillarum* with Dlh3. The transcriptome of *E. anguillarum* in the presence of Dlh3, see above, pointed towards upregulation of genes involved in transport but genes involved in flagellar synthesis and export were not significantly altered. A transcriptome is a comprehensive description of an organism's physiology at a given time point. Due to cost-intensiveness and time-consuming data analysis, transcriptomes cannot be prepared repeatedly. For a better understanding of the physiological changes and the underlying genetic reprogramming after incubation of *E. anguillarum* with Dlh3, more cost-effective and repeatable assays would be worthwhile. Focusing on a certain set of genes of interest a qPCR (quantitative polymerase chain reaction) could be performed at different time points and display the genetic changes over time. If critical genes were identified, oCelloScope could be repeated with genetically modified *E. anguillarum*, showing the relation of the respective gene to auto-aggregation.

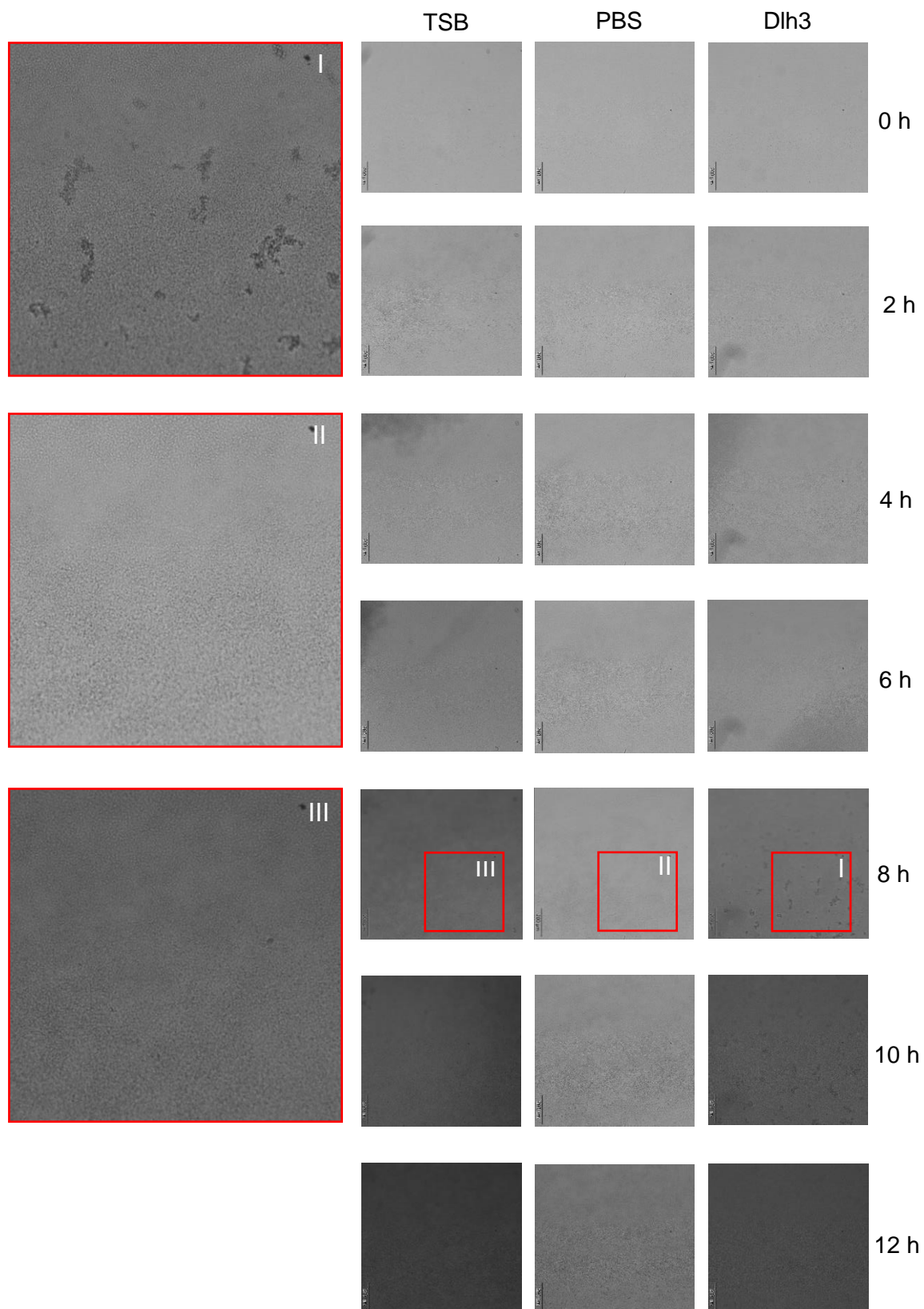


Figure 34: Comparison of cell layer formation by oCelloScope. *E. anguillarum* was incubated at OD_{600 nm} 0.025, 1:2 with DIH3 at 0.5 mg/mL, static growth at 28 °C in 96-well plates with nunclon delta surface, photos were taken every second hour, scale bar 200 μm. I – III detail enlargements of oCelloScope scans after 8 h of incubation. Inhomogeneous spots of cell growth were detectable for *E. anguillarum* in growing conditions under DIH3.

6.3.6 Cell toxicity assays show no influence on fish cell line CHSE-214

In order to consider a possible biotechnological application of the enzyme Dlh3 in the aquaculture sector, compatibility with living cells had to be confirmed. For this, *in vitro* cytotoxicity of Dlh3 was studied in CHSE-214 cells (Chinook Salmon Embryo). At all tested concentrations (0.5, 0.05 and 0.005 mg/mL), Dlh3 did not markedly affect cell viability relative to cells exposed to PBS (Figure 35). It could be proven, that in a fish cell model, the viability was not impaired by Dlh3.

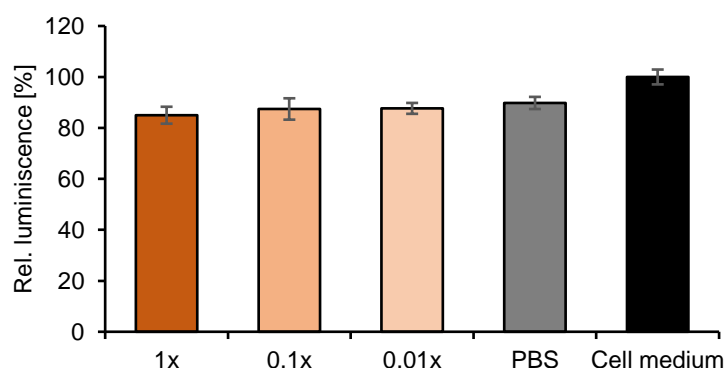


Figure 35: Effect of different concentrations of Dlh3 on growth of fish cell line CHSE-214. On day 1, 45,000 cells in 100 μ L medium were transferred to each well of a black, non-coated 96-well plate with optical bottom. On the second day, the medium was removed and replaced with 50 μ L fresh cell medium. 50 μ L of test substance were added; either Dlh3 diluted further in cell medium to a concentration of 0.5 mg/mL (1x), 0.05 mg/mL (0.1x) or 0.005 mg/mL (0.01x), 1x PBS (corresponding to the amount of PBS added with the Dlh3 protein) or pure cell medium. After two days of exposure, the CellTiter-Glo® Luminescent Cell Viability Assay was performed according to the manufacturer's instructions and the relative luminescence (or survival) was correlated to the control wells containing pure cell medium. Data represent averages and standard deviations from four replicas. Data was provided by Dr. Gunhild Hageskal (Bergmann et al., 2024).

One of the first steps of the biofilm-forming pathway of an individual bacterium is the secretion of autoinducer molecules, most often types of acetyl homoserine lactones (AHL), into the bacteria's environment. Once the production of these molecules by numerous individuals passes a certain threshold, they bind to bacterial transmembrane receptors and activate a DNA-binding element to differentiate gene expression in order to attach to surfaces and induce virulence (Juhas, Eberl, & Tummli, 2005). Homologues of autoinducer synthases, receptors and DNA-binding elements were identified in a wide range of bacterial species. This part of the study focused mainly on disrupting this first communication signal between planktonic, unicellular bacteria by adding a novel diene lactone hydrolase to growing bacteria. The successful reduction of biofilm formation of *A. salmonicida* and *E. anguillarum* by 44.2% and 54.5%, respectively could be explained by the use of LuxRI homologs for quorum sensing in both bacteria. Genes encoding a quorum sensing signal generator and a response regulator named *asaRI* as well as the AHL homolog N-butanoyl-L-homoserine lactone (also known as N-butyryl-L-homoserine lactone (C4-HSL)) were found for *A. salmonicida* (Swift et al., 1997).

Comparable findings were made for *E. tarda*, a closely related species to *E. anguillarum*. Homologs of the quorum sensing genes *luxI* and *luxR* could be proved in *E. tarda*, named *edwI* and *edwR*, respectively, as well as two kinds of AHLs produced by *E. tarda*, which seemed to be N-hexanoyl-L-homoserine lactone (C6-HSL) and N-heptanoyl-L-homoserine lactone (C7-HSL) (Morohoshi, Inaba, Kato, Kanai, & Ikeda, 2004). Biofilm formation and virulence factors therefore seem to be under the regulation of a lactone ring-based AHL autoinducer, which makes them susceptible to the cleavage mechanism of diene lactone hydrolases. Surprisingly, *P. aeruginosa* showed a minor reduction in biofilm formation, compared to *E. anguillarum* and *A. salmonicida*, although it belongs to the most extensively studied cell-to-cell communication systems with known AHL-dependent regulatory circuits. However, according to current knowledge, *P. aeruginosa* uses at least three different autoinducer molecules. Besides AHL it synthesizes cyclic dipeptides and quinolone, which may replace each other and lead to lower susceptibility towards a specific anti-AHL agent (Lade, Paul, & Kweon, 2014). Unexpectedly, the transcriptomic data revealed mainly altered regulation of transport systems in the presence of Dlh3. No significant changes in expression of the virulence-associated type III, IV, V secretion systems or genes associated with biofilm forming, like genes for flagella or pili were observed. However, transcriptomic data represent the “one moment in time”. The timepoint for cell collection was chosen according to the timepoint used for former experiments, which was after 48 h of incubation. As revealed by oCelloScope, the greatest visible changes occurred at about 8 h of incubation. Given, that the number of cells collected at earlier stages would be sufficient for transcriptomic protocols, a glance into earlier alterations of gene expression could surely be enlightening. Overall, the results of this part of the study gave a detailed insight into the effects of the metagenome-derived diene lactone hydrolase Dlh3, to have measurable reductive effects on biofilm formation of fish pathogens. The anti-biofilm activity of Dlh3 proven on five bacterial strains highlights the potential for interventions targeting specific metabolic pathways or physiological processes critical for biofilm formation and maintenance. Understanding these characteristics can pave the way for the development of more precise and effective strategies for combating biofilm-related issues and controlling the growth and persistence of pathogenic bacterial populations e.g., in aquaculture settings. In addition, the absence of toxic effects on the growth of fish cell line CHSE-214 opens up a putative biotechnological application of Dlh3.

6.4 Putative anti-biofilm enzymes from *T. chui* metagenome

Based on the metagenome data of *T. chui*, 31 primer pairs were designed for the synthesis of putative anti-biofilm enzymes. The enzyme classes comprised polyketide synthases (PksN), 5-methylcytosine-specific restriction endonucleases (McrA), acyl-homoserine-lactone acylases, alpha-amylases, beta-amylases, glycosidases, ferro-chelataes, magnesium chelataes, 1-aminocyclopropane-1-carboxylate deaminases, 8-oxoguanine deaminases

(OxoD) and dienelactone hydrolases (Dlh). Of these, the 28-84 McrA, 28-08 OxoD and 28-50 Dlh could be successfully overexpressed by *E. coli* Rosetta gami 2 (DE3) and introduced into anti-biofilm assays. Both, the McrA enzyme as well as the OxoD enzyme are supposed to act on DNA either by cleavage (28-84 McrA) or by modification (28-08 OxoD). Characterization and first results of these enzymes in anti-biofilm assays are presented in the following. All LSCM experiments were performed by MSc. student Johannes Amann.

6.4.1 5-methylcytosine-specific restriction endonuclease 28-84 McrA

The enzyme 5-methylcytosine-specific restriction endonuclease (McrA), also called modification dependent or methyl-directed restriction endonuclease (EC:3.1.21.) belongs to the Type IV restriction enzymes which are characterized by recognizing modified DNA, in particular methylated DNA, contrary to Type I-III restriction endonucleases which target unmethylated DNA (Loenen & Raleigh, 2014). Restriction enzymes are part of the bacterial defense mechanism that provides a barrier for incoming DNA. McrA exhibits its endonuclease activity explicitly at 5-methylated cytosines in specific contexts, such as C5mCGG sequence or methylated CpG sites (Czapinska et al., 2018). According to InterPro (104.0) (Blum et al., 2025) the active site of the 172 aa long 28-84 McrA from *T. chui* metagenome is represented by an HNH domain which is characterized by conserved Histidine residues for coordinating a divalent cation, Mg^{2+} or Mn^{2+} , and a H_2O molecule for the nucleophilic attack on the phosphorus atom of the DNA backbone phosphodiester bond as well as conserved Cysteine residues to complex a Zn^{2+} as ligand. InterPro predicted several conserved residues within the DNA binding active site, located between residue 84 and 121 as visualized by ChimeraX (Pettersen et al., 2021) in Figure 36, though along with the current literature, the mechanism of DNA cleavage by McrA is not exactly characterized. Structure comparison with the closest related McrA of *Roseitalea porphyridii* (Hyeon, Jeong, Baek, & Jeon, 2017) strain MA7-20 predicted by NCBI blastP (Altschul, Gish, Miller, Myers, & Lipman, 1990) revealed high similarity between both enzymes, in particular at the active site when matched by Chimera (Pettersen et al., 2004). Chimera sequence alignment calculated a 90.7% identity.

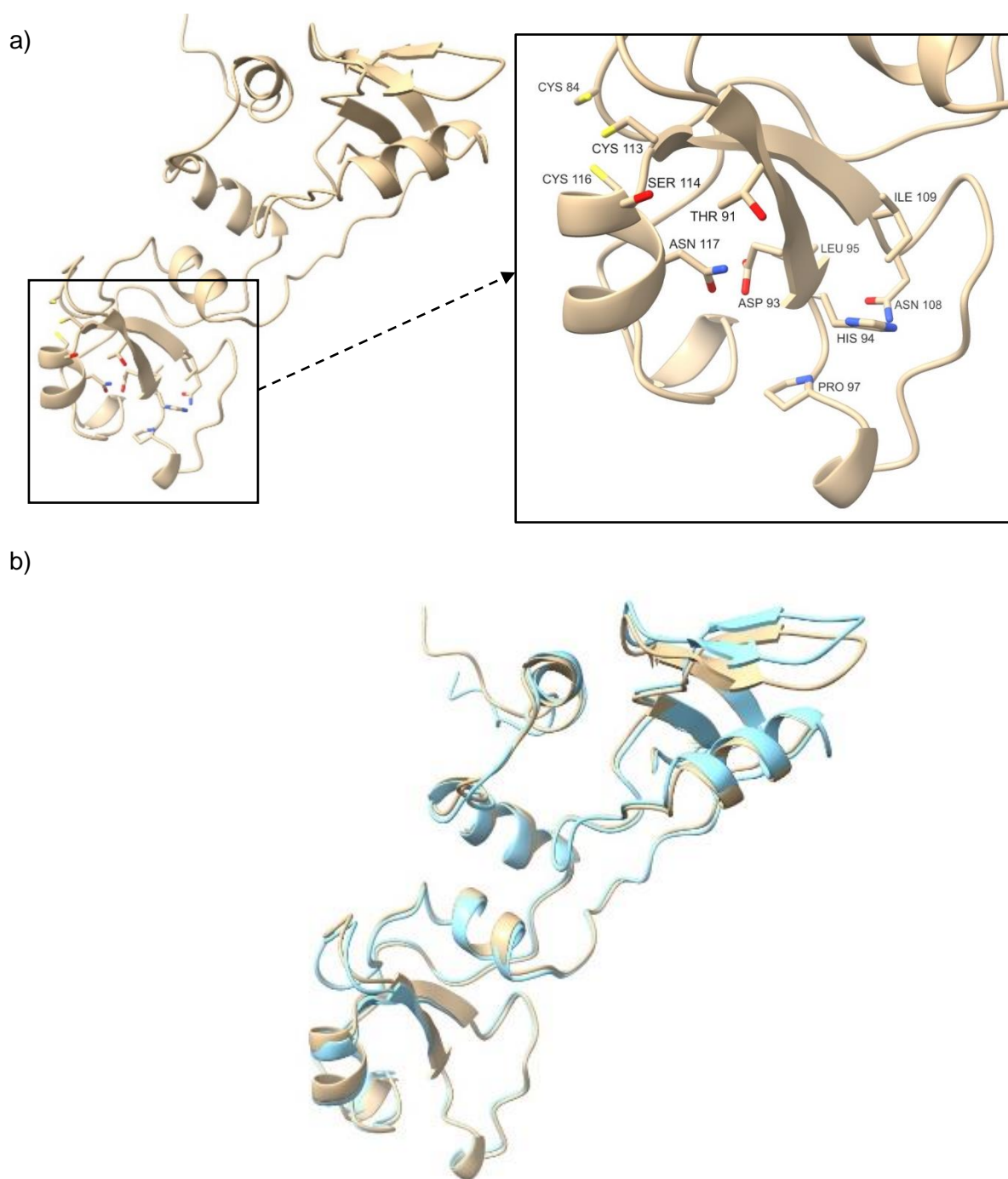
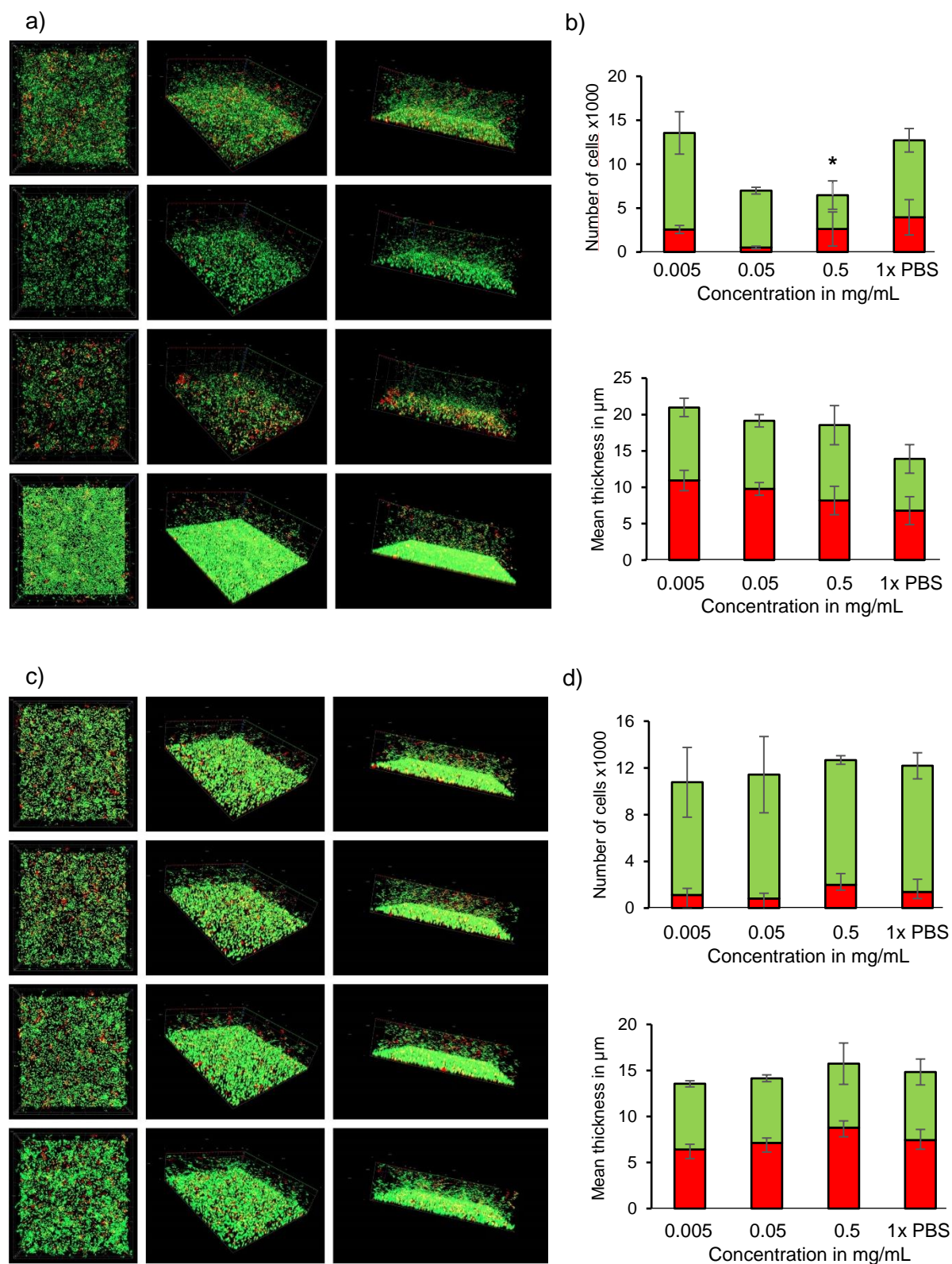


Figure 36: Predicted structure of 28-84 McrA from *T. chui* metagenome. a) Typical structure of Type IV restriction endonuclease, predicted by AlphaFold Server (Jumper et al., 2021) and visualized by ChimeraX (Pettersen et al., 2021). Conserved residues of the DNA binding HNH domain, as predicted by InterPro (104.0) analysis (Blum et al., 2025) are highlighted, b) structure comparison of 28-84 McrA (gold) with closest relative McrA from *Roseitaea porphyridii* strain MA7-20 Sequence ID: CP036532.1 (sky blue) based on NCBI blastP (Altschul et al., 1990), visualized by Chimera X, sequence identity of 90.7%.

The overexpressed enzyme 28-84 McrA was tested for its anti-biofilm effectivity against *E. anguillarum*, *A. salmonicida* and *P. aeruginosa* in LSCM by MSc. student Johannes Amann. His results gave a first hint for the effectiveness of DNA-restricting enzymes in strategies against biofilms, but must clearly be validated and investigated more deeply (Figure 37).



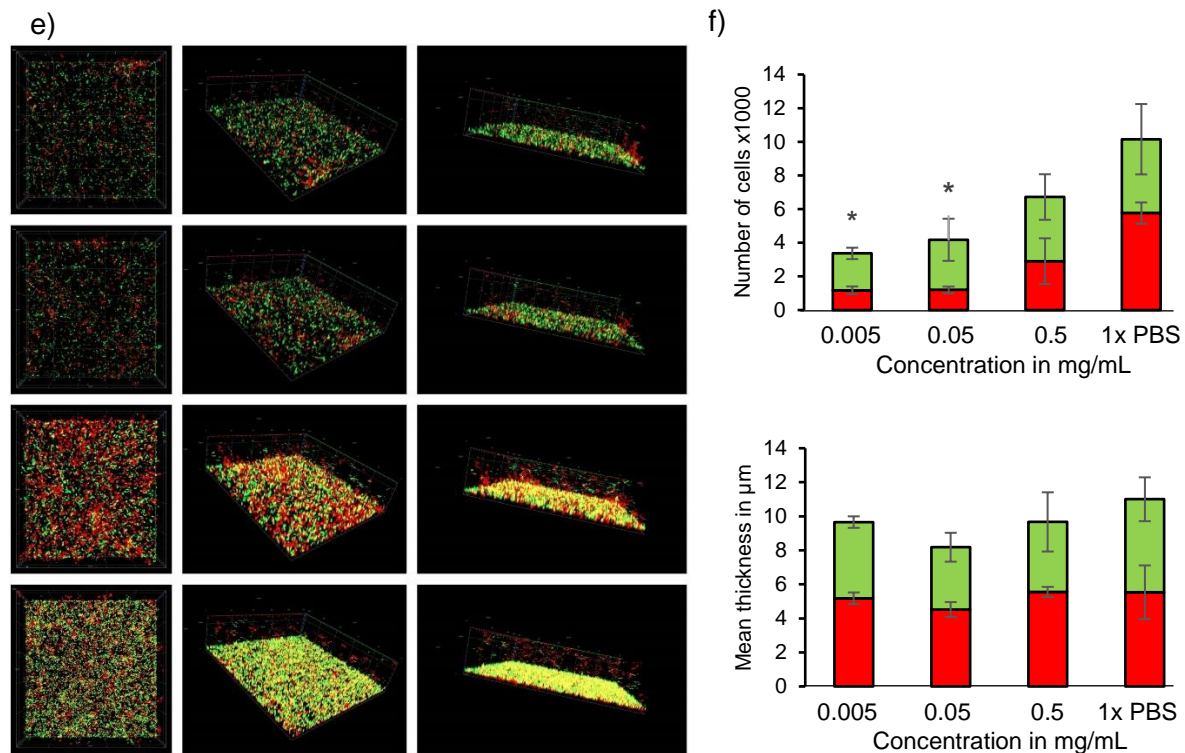


Figure 37: Laser scanning confocal microscopy of bacterial pathogens incubated with 28-84 McrA. a) *E. anguillarum*, c) *A. salmonicida*, e) *P. aeruginosa*, incubation with test liquids at 28 °C (*E. anguillarum*, *A. salmonicida*) and 37 °C (*P. aeruginosa*) for 24 h, static. Staining: SYTO 9 for living cells, Propidium iodide for dead cells, x-axis 200 μm, y-axis 200 μm, z-axis 34 μm, z-stacks of 80 slides, from left to right: Surface, top position, side position. b), d), f) respective calculations of absolute numbers of living (green) and dead (red) cells and mean thickness of the biofilms by BiofilmQ/MATLAB. Three different concentrations were tested, top row 0.005 mg/mL, second row 0.05 mg/mL, third row 0.5 mg/mL, bottom row control 1x PBS. Decreased cell numbers were observed for *E. anguillarum* (for the highest concentration of 0.5 mg/mL) and *P. aeruginosa* (for the lowest concentration of 0.005 mg/mL). No cell reduction was observed for *A. salmonicida* with McrA. The biofilm thicknesses didn't change significantly for all pathogens in any condition. Significance, based on paired sample *t*-test is indicated by stars, *p*-value ≤ 0.05 (*).

Optical impression and calculated cell numbers revealed decreased cell numbers with varying proportions of living and dead cells for *E. anguillarum* and *P. aeruginosa* after incubation with the restriction endonuclease 28-84 McrA if compared to the control of PBS. *E. anguillarum* showed significantly reduced total cell numbers by 49% after treatment with the highest concentration of 0.5 mg/mL, while *P. aeruginosa* showed the fewest total cell numbers, a reduction of 66.8%, after incubation with the lowest concentration of 0.005 mg/mL. Neither the cell numbers of *A. salmonicida* nor the mean biofilm thickness of any condition changed significantly.

6.4.2 8-oxoguanine deaminase 28-08 OxoD

The 8-oxoguanine deaminase belongs to the Amidohydrolase superfamily (AHS) which contains many enzymes known to catalyze the deamination of aromatic bases. 8-oxoguanine deaminase catalyzes the deamination of 8-oxoguanine (8-oxoG) to uric acid but is also active on guanine and isocytosine (Hall et al., 2010). 8-oxoG is formed by oxidation of guanine within

DNA by reactive oxygen species (ROS) including superoxide ($O_2^{\cdot-}$), hydroxyl radicals ($OH\cdot$) or hydrogen peroxide (H_2O_2). ROS are continuously produced as byproducts of aerobic metabolism and are balanced actively. Pathophysiological conditions can induce increased ROS production, leading to oxidative stress and damage (Hahm, Park, Jang, & Chi, 2022; Holmström & Finkel, 2014). The nucleobase guanine is highly susceptible to being oxidized to 8-oxoguanine, thus it has been widely used as a ROS biomarker (Ock et al., 2012). Since 8-oxoguanine can mismatch with adenine it behaves as a potent oncogenic mutagen, producing the transcriptional mutations (G>T) and (C>A), which underlines the importance of immediate repair (Hahm et al., 2022). After excision from DNA 8-oxoguanine is supposedly converted to uric acid and ammoniac as depicted in Figure 38.

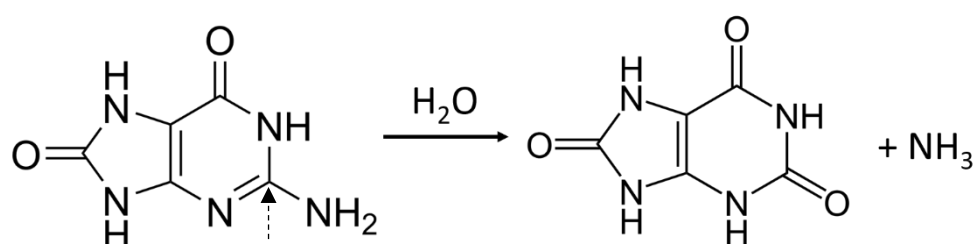


Figure 38: Conversion of 8-oxoguanine to uric acid and ammoniac (Hall et al., 2010). Left: substrate 8-oxoguanine, right: products uric acid and ammoniac.

In general, 8-oxoguanine deaminase forms as $(\beta/\alpha)_8$ -barrel with a single Zn^{2+} in the active site. InterPro (104.0) confirmed the Amidohydrolase domain within the 452 aa large 28-08 OxoD from *T. chui* metagenome. The active site is formed by four histamines in positions 68, 70, 236 and 273, alongside with glutamine, glutamic acid and aspartic acid in positions 73, 239 and 324, respectively. In particular, the histamines in positions 68 and 70 are complexing a Zn^{2+} ion, which polarizes a water molecule for the nucleophilic attack on the C2 carbon, forming a carbonyl group and releasing the exocyclic amino group. The proposed structure of 28-08 OxoD, predicted by Robetta (Baek et al., 2021) and visualized by UCSF Chimera 1.16 is presented in Figure 39. The active site is highlighted. Furthermore, the structure of 28-08 OxoD is compared to the nearest neighbor (NP 248832.1 8-oxoGDA PA0142 from *P. aeruginosa* PAO1) within the phylogenetic tree of the Amidohydrolase family (Supplemental Figure S2), which was friendly provided by Dr. Yuchen Han. According to UCSF Chimera sequence alignment, 28-08 OxoD revealed 61.7% identity to NP 248832.1

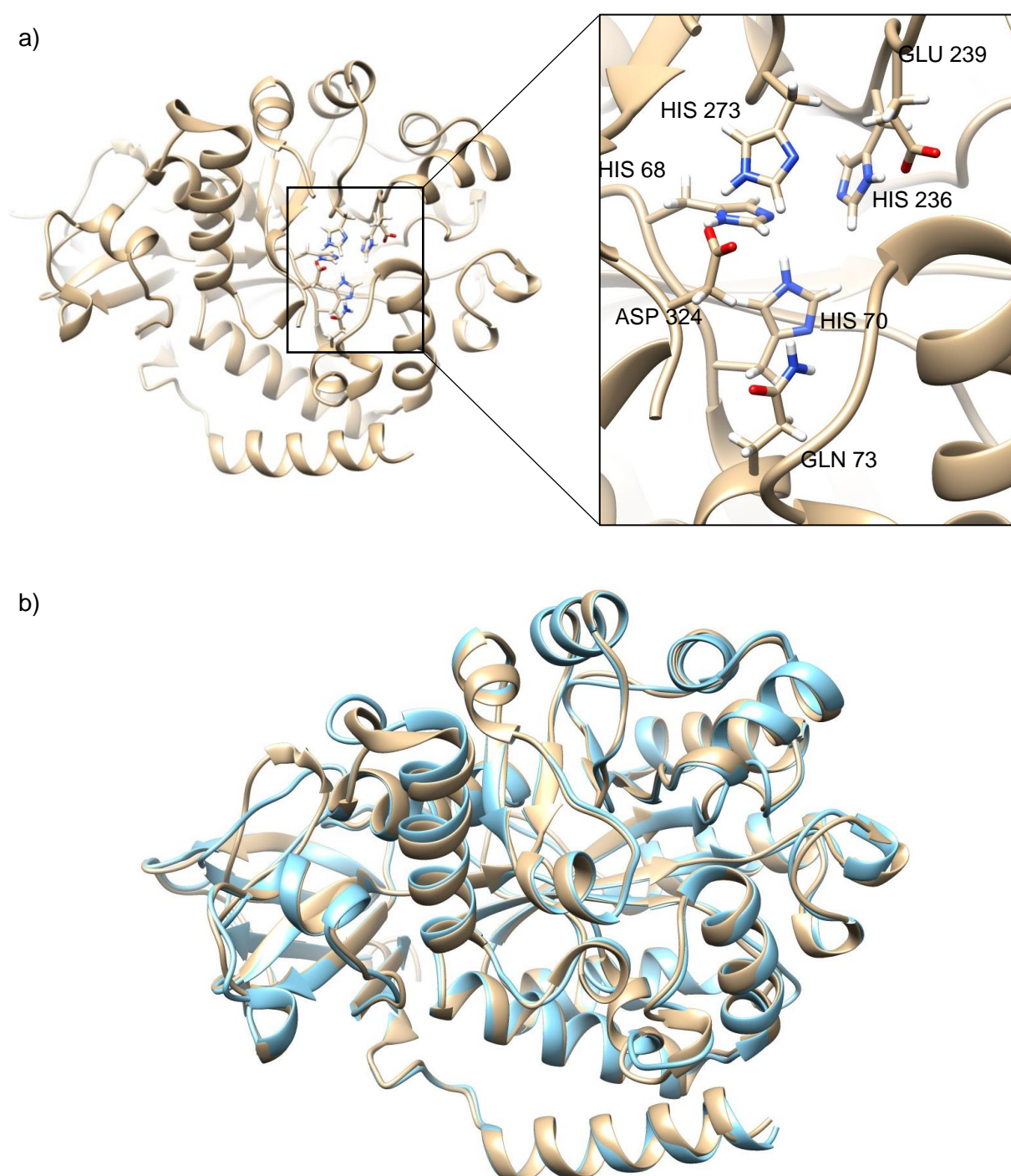
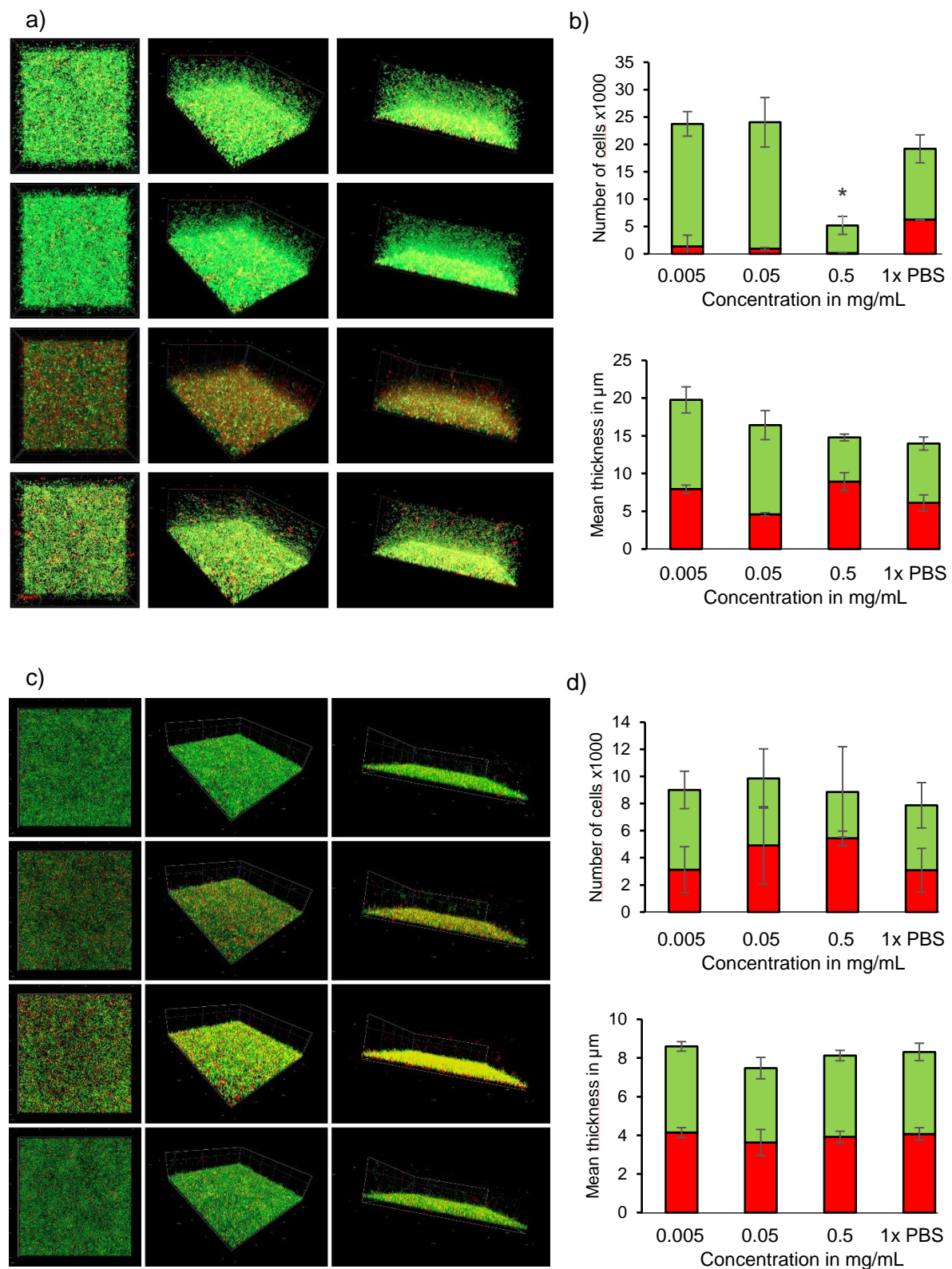


Figure 39: Predicted structure of 28-08 OxoD from *T. chui* metagenome. a) Typical structure of Amidohydrolase family protein, predicted by Robetta (Baek et al., 2021) and visualized by UCSF Chimera 1.16. (Pettersen et al., 2004). Conserved residues of the active site, as predicted by InterPro (104.0) analysis (Blum et al., 2025) are highlighted, b) structure comparison of 28-08 OxoD (gold) with closest relative 8-oxoguanine deaminase from *P. aeruginosa* PAO1, NP 248832.1 8-oxoGDA PA0142, (sky blue) based on phylogenetic tree in Supplemental (Figure S2), visualized by Chimera, sequence identity of 61.7%.

The overexpressed enzyme 28-08 OxoD was tested for its anti-biofilm effectivity against *E. anguillarum*, *A. salmonicida* and *P. aeruginosa* in LSCM by MSc. student Johannes Amann. His results gave a first hint for the effectiveness of DNA-restricting enzymes in strategies against biofilms, but must clearly be validated and investigated more deeply (Figure 40).



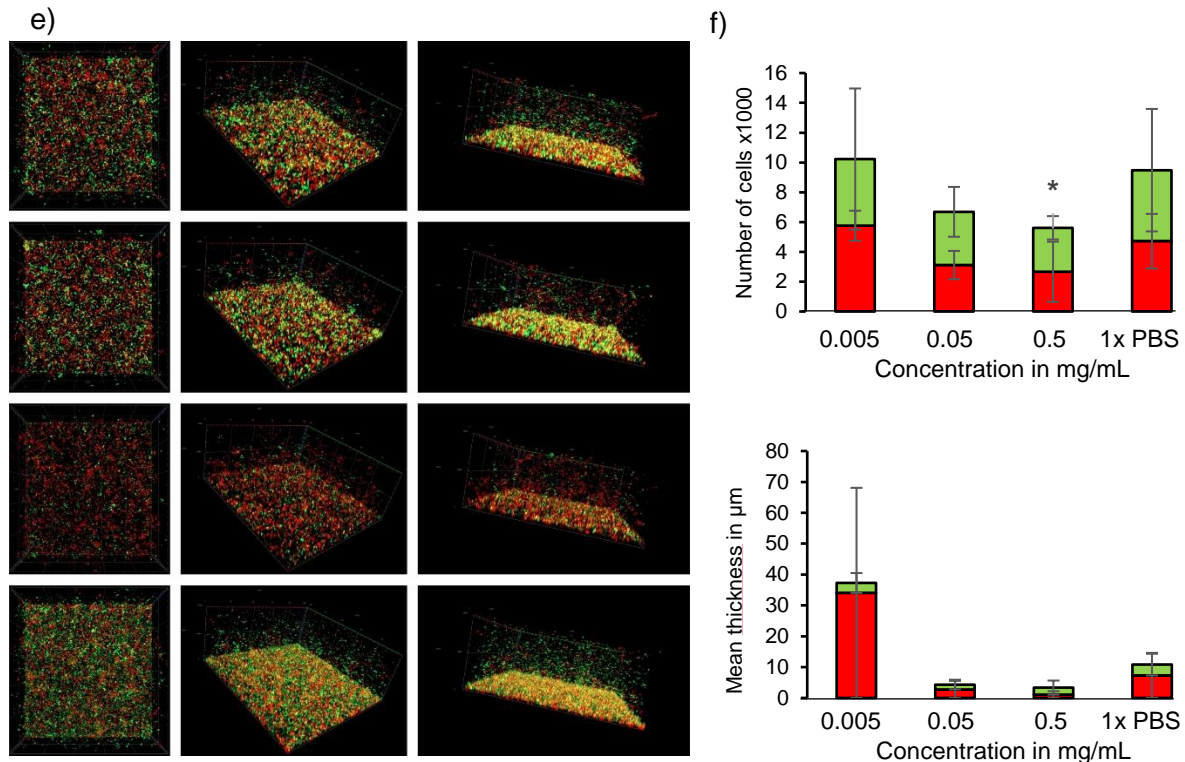


Figure 40: Laser scanning confocal microscopy of bacterial pathogens incubated with 28-08 OxoD. a) *E. anguillarum*, c) *A. salmonicida*, e) *P. aeruginosa*, incubation with test liquids at 28 °C (*E. anguillarum*, *A. salmonicida*) and 37 °C (*P. aeruginosa*) for 24 h, static. Staining: SYTO 9 for living cells, Propidium iodide for dead cells, x-axis 200 µm, y-axis 200 µm, z-axis 34 µm, z-stacks of 80 slides, from left to right: Surface, top position, side position. b), d), f) respective calculations of absolute numbers of living (green) and dead (red) cells and mean thickness of the biofilms by BiofilmQ/MATLAB. Three different concentrations were tested, top row 0.005 mg/mL, second row 0.05 mg/mL, third row 0.5 mg/mL, bottom row control 1x PBS. Decreased cell numbers were observed for *E. anguillarum* and *P. aeruginosa* (for the highest concentration of 0.5 mg/mL). No cell reduction was observed for *A. salmonicida* with 28-08 OxoD. The biofilm thicknesses didn't change significantly for all pathogens in any condition. Significance, based on paired sample *t*-test is indicated by stars, $p\text{-value} \leq 0.05$ (*).

Interestingly, also 28-08 OxoD had an effect on both, *E. anguillarum* and *P. aeruginosa*. Total cell numbers decreased significantly after incubation with the highest concentration of 0.5 mg/mL by 73.8% and 40.8%, respectively. The optical impression of high proportions of dead cells in this condition was not reflected by the calculations of living and dead cells. Contrary to 28-84 McrA, 28-08 OxoD had effects on *A. salmonicida* as well. From the lowest to the highest concentration, the biofilm color changed from green to increasing yellow, indicating growing numbers of dead cells. The calculated cell numbers confirmed the higher proportion of dead cells, in particular for the 0.5 mg/mL concentration, but the overall cell numbers rather increased if compared to the control of PBS. Again, the mean biofilm thickness did not change significantly in any condition. The optical results, in particular for *P. aeruginosa*, suggest, that the incubation time was too long, showing numerous dead cells also in the control. The protocol therefore should be adjusted.

Both enzymes, 28-84 McrA and 28-08 OxoD interfere with DNA, either by restriction or modification of the DNA molecule, which is likely to be an essential target for a multidirectional attack on biofilm formation or integrity.

6.4.2.1 Extracellular DNA

Whitchurch et al., discovered in 2002 that the vast majority of a *P. aeruginosa* biofilm was found not to be polysaccharide or proteins, but DNA and was actively released within small vesicles from the outer membrane (OMV) of living bacteria instead of deriving only from lysed cells (Whitchurch, Tolker-Nielsen, Ragas, & Mattick, 2002). The hypothesized importance of extracellular DNA (eDNA) for the sheltering character of biofilms was supported by findings, that the highly negatively charged DNA molecule acts as a cation chelator. Chelation of essential cations such as Mg^{2+} , Ca^{2+} or Mn^{2+} by the addition of DNA to planktonic growth cultures of *P. aeruginosa* resulted in cell damage and immediate cell death, presumably due to a loss of membrane integrity (D. D. Lee et al., 2019; Mulcahy, Charron-Mazenod, & Lewenza, 2008; Zaharik & Finlay, 2004). On the other hand, eDNA was shown to chelate positively charged antibiotics such as vancomycin (Doroshenko et al., 2014). As it was found out, that *P. aeruginosa* developed defense ways against disruption of its own cell membrane (Lesley & Waldburger, 2001; McPhee, Lewenza, & Hancock, 2003; Moskowitz, Ernst, & Miller, 2004) eDNA was suspected to act as shield against certain antibiotics in biofilms. Penetration studies finally demonstrated that the positively charged antibiotic tobramycin became sequestered near the surface and did not fully penetrate the biofilm, while the negatively charged antibiotic ciprofloxacin penetrated readily (Chiang et al., 2013; Tseng et al., 2013).

Today the EPS matrix is considered hydrophilic and negatively charged owing to the presence of molecules such as anionic polysaccharides, teichoic acids and extracellular DNA (eDNA), which can all bind to cationic substances, including toxic metals and antibiotics such as vancomycin and tobramycin (Flemming et al., 2024; Harrison, Turner, & Ceri, 2005).

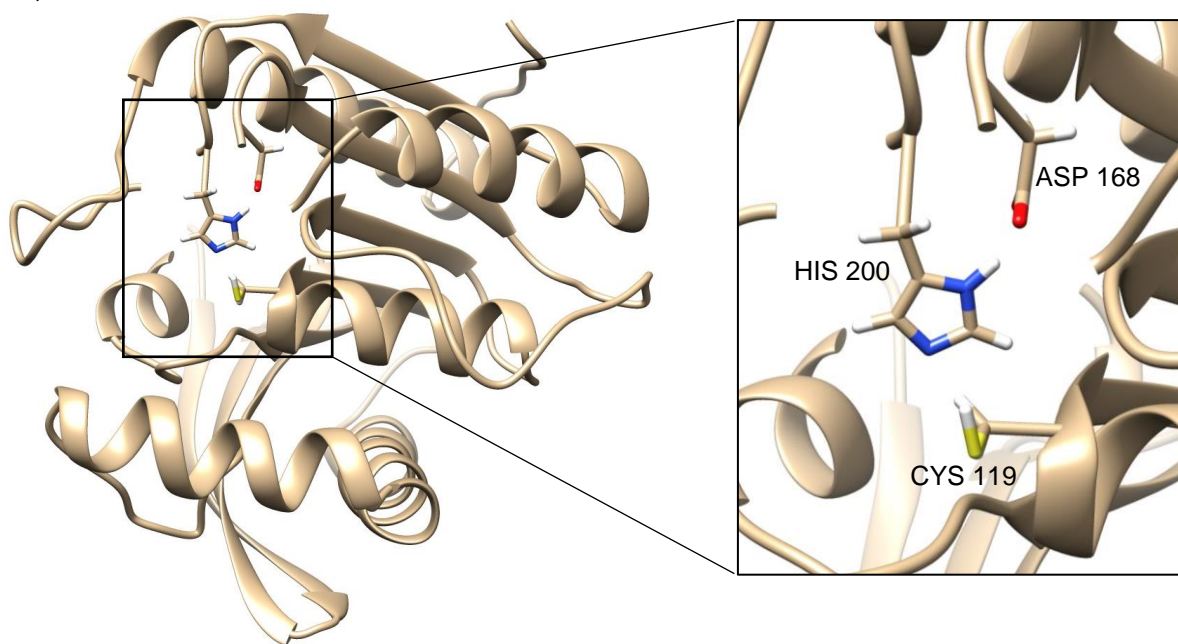
Facing all these diverse, specified and highly evolved mechanisms performed by components of the biofilm matrix to shield resident bacterial cells makes it worthwhile to investigate finding breakpoints, disrupting the protection and consequently impairing growth and virulence of harming pathogens as was intended by the enzymes 28-84 McrA and 28-08 OxoD and should be accomplished by a growing number of active enzymes.

6.4.3 Dienelactone hydrolase 28-50 DIh

Successfully, a second dienelactone hydrolase could be overexpressed from *T. chui* metagenome. Structure prediction by Robetta and visualization by Chimera revealed the typical core of α/β -hydrolases consisting of 8 β -sheets in consistency to the DIh3 characterized above (see Figure 41). Deviating from DIh3, the 8 β -sheets of the 246 aa long 28-50 DIh were only flanked by 6 α -helices. Two α -helices were replaced by loops. Structure comparison of

28-50 DIh and DIh3 by Chimera showed the distinct differences between these two enzymes. 28-50 DIh not only missed α -helices but also the prolonged N-terminal (TAT) signal peptide. The hypothesized cleavage site at position 40 or 41 was confirmed by this structure comparison, with the sequence of 28-50 DIh starting at position 41 of DIh3 within the aligned sequences. Though Chimera calculated only 21.1% identity between 28-50 DIh and DIh3, the functionally important residues matched perfectly. InterPro identified the catalytic triad of 28-50 DIh consisting of Cys-His-Asp at the positions C119, H200 and D168, which appeared in perfect overlay with C176, H262 and D231 of DIh3 when both proteins were matched (Figure 41 c)). According to the phylogenetic tree for 28-50 DIh, which was provided by Dr. Yuchen Han, 28-50 DIh clustered within the Type I DIhs thus, *trans*-dienelactone hydrolyzing activity for 28-50 DIh should be expected. 28-50 DIh was also compared to the nearest neighbor of the phylogenetic tree, which was a DIh (DIh2) from *S. communis* metagenome. Sequence alignment calculated 41.8% identity between 28-50 DIh and DIh2. The results of the first anti-biofilm assays documented by LSCM are presented in the following.

a)



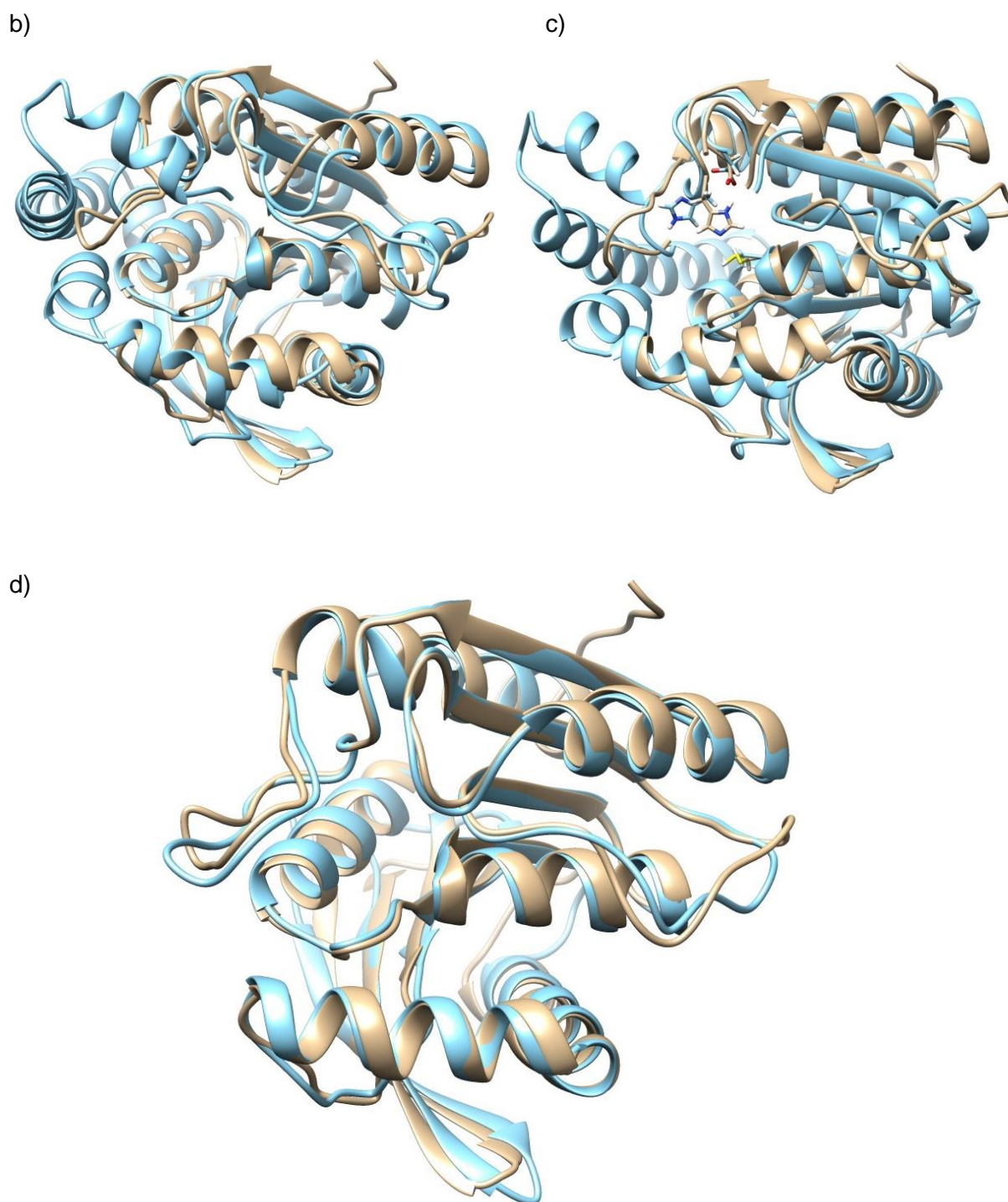
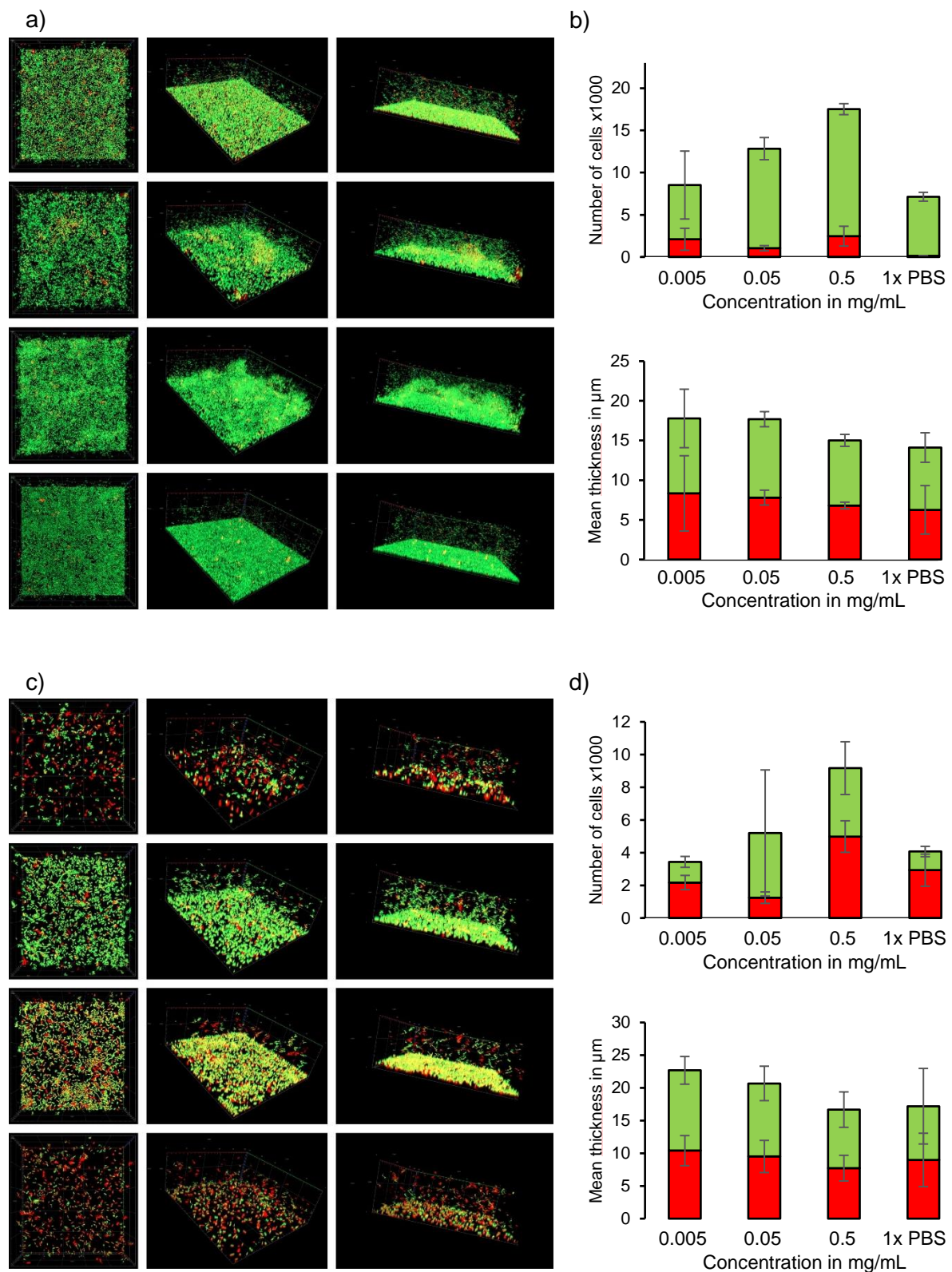


Figure 41: Predicted structure of 28-05 DIh from *T. chui* metagenome. a) Typical structure of Dienelactone hydrolase family protein with a core of 8 β -sheets, predicted by Robetta (Baek et al., 2021) and visualized by UCSF Chimera 1.16. (Pettersen et al., 2004). Deviating from DIh3 the 8 β -sheets are flanked by only 6 α -helices Conserved residues of the active site, as predicted by InterPro (104.0) analysis (Blum et al., 2025) are highlighted, b) structure comparison of 28-05 DIh (gold) DIh3 (sky blue) with the identity of 21.1%. c) perfect match of the residues Cys, His and Asp of the active site of aligned enzymes 28-50 DIh and DIh3. d) Structure comparison of 28-50 DIh (gold) with the closest related DIh from the phylogenetic tree in Supplemental (Figure S3) DIh2 from *S. communis* metagenome (sky blue) visualized by Chimera, sequence identity of 41.8%.

The overexpressed enzyme 28-50 DIh was tested for its anti-biofilm effectivity against *E. anguillarum*, *A. salmonicida* and *P. aeruginosa* in LSCM by MSc. student Johannes Amann. His results confirmed the findings for DIh3 (see above), but must clearly be validated and investigated more deeply (Figure 42).



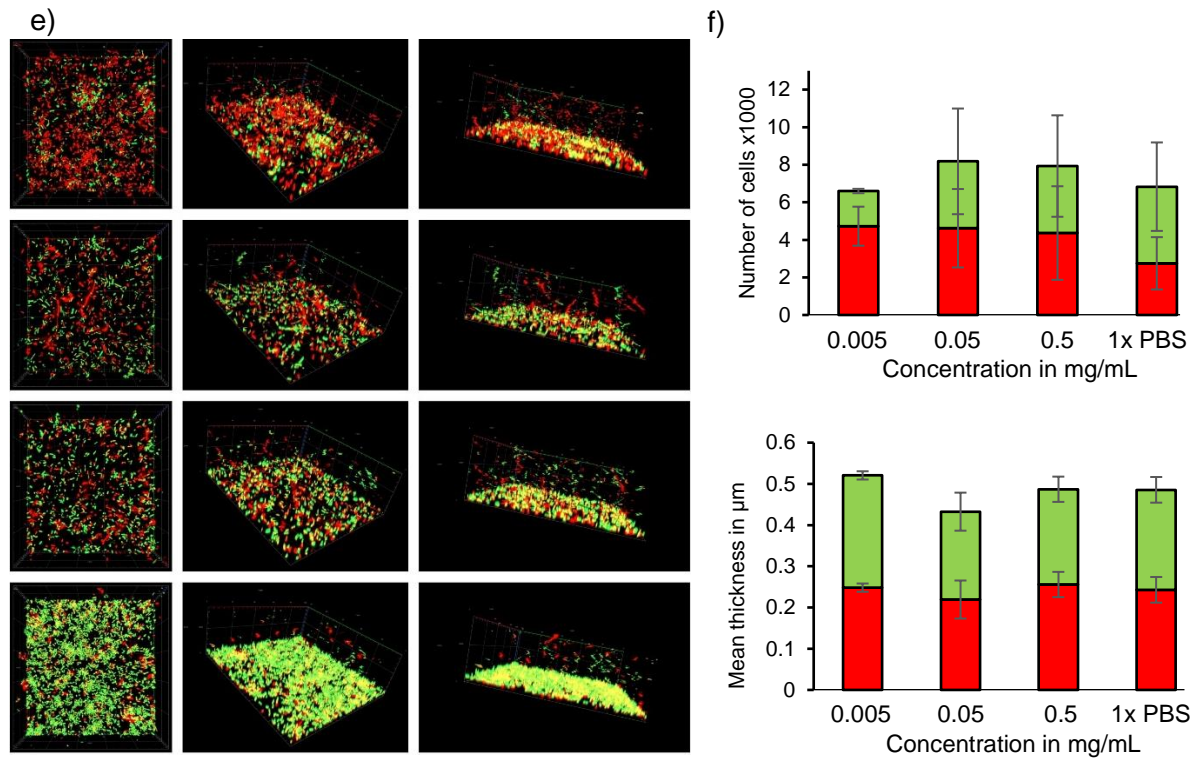


Figure 42: Laser scanning confocal microscopy of bacterial pathogens incubated with 28-50 DIh. a) *E. anguillarum*, c) *A. salmonicida*, e) *P. aeruginosa*, incubation with test liquids at 28 °C (*E. anguillarum*, *A. salmonicida*) and 37 °C (*P. aeruginosa*) for 24 h, static. Staining: SYTO 9 for living cells, Propidium iodide for dead cells, x-axis 200 μm, y-axis 200 μm, z-axis 34 μm, z-stacks of 80 slides, from left to right: Surface, top position, side position. b), d), f) respective calculations of absolute numbers of living (green) and dead (red) cells and mean thickness of the biofilms by BiofilmQ/MATLAB. Three different concentrations were tested, top row 0.005 mg/mL, second row 0.05 mg/mL, third row 0.5 mg/mL, bottom row control 1x PBS. Alterations in biofilm architecture became obvious for *E. anguillarum* in particular for the highest concentration of 0.5 mg/mL. Inhomogeneous structures appeared, resembling the observations made in oCelloScope with DIh3. *A. salmonicida* showed dose-dependent optical cell density and viability with the fewest and deadest cells for the lowest concentration of 0.005 mg/mL, which equaled the control of 1x PBS. The cells of *P. aeruginosa* appeared mainly dead after incubation with the lowest concentration of 0.005 mg/mL. The difference in the viability of treated cells compared to the control appeared to be significant, but could not be verified by calculated cell numbers. The biofilm thicknesses didn't change significantly for all pathogens in any condition.

After incubation with 28-50 DIh no cell reduction was measured for any pathogen at any condition, if compared to the PBS control. However, biofilm morphology altered remarkably. In particular, *E. anguillarum* reacted to increasing concentrations of 28-50 DIh with a growing inhomogeneity of the biofilm architecture. The highest concentration of 0.5 mg/mL of 28-50 DIh provoked putative auto-aggregation in a highly comparable way to the findings in oCelloScope for *E. anguillarum* incubated with DIh3, see above. Based on the length of the x- and y-axis of 200 μm, the size of the aggregates of about 100 μm in length was consistent with the presumed auto-aggregates in oCelloScope. Seeing the same reaction of *E. anguillarum* in two different settings with two different enzymes of the same type enhances the curiosity of enlightening the detailed mechanism beyond this behavior. *A. salmonicida* showed a vastly varying biofilm morphology with decreasing cell numbers and viability referred to decreasing

concentrations of 28-50 DIh. The unusual appearance of the PBS control, with few numbers of mainly dead cells put the trustworthiness of these conditions in question. *P. aeruginosa* reacted to 28-50 DIh treatment with a shift to lesser viability with decreasing concentration.

6.4.4 Toxicity assay with *Galleria mellonella*

Finally, the toxicity of the enzymes 28-50 DIh and 28-08 OxoD on the test animal model *Galleria mellonella*, the greater wax moth, was evaluated (Figure 43), while 28-84 McrA was not tested yet. *Galleria mellonella* was chosen as a suitable test organism, as immune responses between insects and the immune systems of higher organisms share a number of structural and functional similarities (Browne & Kavanagh, 2013; Kavanagh & Reeves, 2004). 28-50 DIh and 28-08 OxoD showed a similar development with at least nine larvae alive after 24 hours, and a decreasing survivability rate after 48 hours. 28-08 OxoD showed the best results, with at least eight surviving larvae after 48 hours, while 28-50 DIh kept at least seven larvae alive after 48 hours. The PBS controls remained fairly constant with only one larva being deceased after 48 hours. Whether dying of larvae was influenced by the test liquids or the injection itself could not finally be determined.

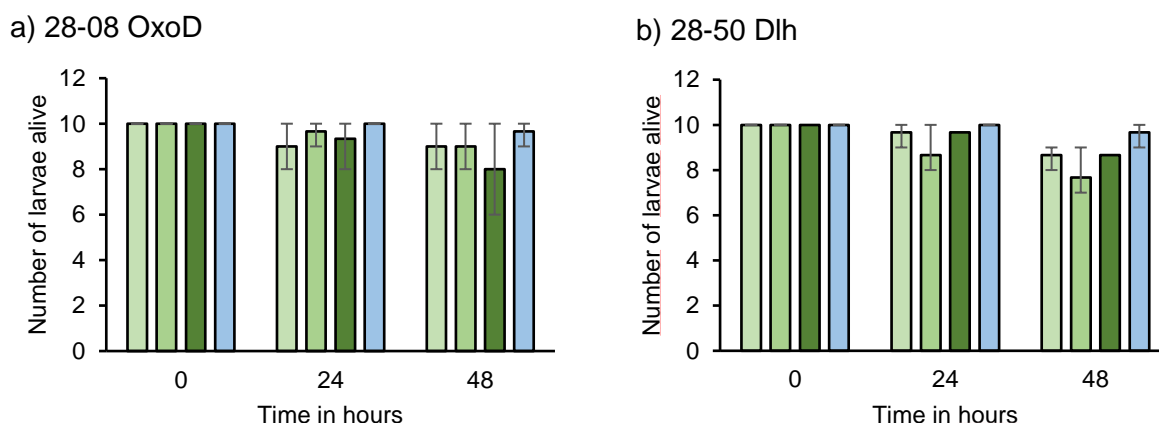


Figure 43: Toxicity assay for the anti-biofilm enzymes performed with larvae of *Galleria mellonella*. a) 28-08 OxoD, b) 28-50 DIh, 5 μ L of sterile enzyme solution were used in triplets of 10 larvae with 30 larvae in total for each concentration. Larvae were kept at 28°C. The error bars show the minimum and maximum number of larvae alive at each sample point, the bars represent the mean value. Light green: 0,005 mg/mL, green: 0,05 mg/mL, dark green: 0,5 mg/mL, blue: 1x PBS.

Overall, this assay showed, that the tested enzymes might affect higher organisms, though the extent of that appeared to be minor. To further solidify these results, it is suggested, to use a cellular test model which offers easier and more reproducible experimental conditions.

6.5 Outlook

The first results with the newly overexpressed enzymes showed a distinct influence on biofilm formation of the pathogens *E. anguillarum*, *A. salmonicida* and *P. aeruginosa*. Though cell numbers did not change significantly, the architecture of the biofilm structure and the optical impression of viability did change. Technically, results seemed to be impaired by prolonged incubation time or processing time during microscopy. Rather than preparing numerous samples at once, smaller sample sizes should be analyzed within one session. Optimization of the enzyme's efficiency could be performed by bioengineering of the active site. Docking studies with putative ligands could develop the active sites to a more balanced ratio of flexibility and stability in order to improve catalytic activity and enhance resistance to changing environmental conditions, respectively. Furthermore, the addition of the corresponding metal ion during enzyme preparation could increase the catalytic activity.

Sustainability is a major goal in aquaculture farming with animal health and welfare being a high priority and need. In addition to vaccination, new strategies to treat bacterial infectious diseases and biofilms with agents other than antibiotics or chemotherapeutics are of great interest. This study focused on the fish pathogens *E. anguillarum*, *A. salmonicida* and *P. aeruginosa*, all important causatives of severe infections like edwardsiellosis, furunculosis and hemorrhagic septicemia, respectively (Algammal et al., 2020; Charette, 2021; Katharios et al., 2019). In summary, the results underlined the remarkable potential of microalgae as additives in aquaculture by demonstrating impaired biofilm formation due to treatment with microalgae supernatants. Moreover, the genetic resources of microalgae-bacterial consortia and their biological antimicrobial properties were investigated, exemplified by the reduction or altering of biofilm formation of *E. anguillarum*, *A. salmonicida* and *P. aeruginosa*. Nevertheless, the potential for application of the explored enzymes in aquaculture settings needs further studies, concerning both fish welfare and possible ways for product utilization. Beyond the investigated single-species biofilms, multi-species biofilms, commonly found in aquaculture systems, present a complex interplay of dynamic interactions among different microbial species, which needs attention and specified answers. Future work should address further bioactive molecules to target a broader spectrum of fish pathogens, face the usage of different autoinducer molecules and answer local demands. Several novel enzymes could be applied in a concerted way (e.g., use for pre-treatment and cleaning of fish or surface preparation of tanks), each of them low-dosed and neutral to farmed animals and environment, but in the way of targeting various aspects of biofilm formation and avoiding quick adaptation and resistance in the pathogenic bacteria.

7 References

- Abate, R., Oon, Y. S., Oon, Y. L., & Bi, Y. (2024). Microalgae-bacteria nexus for environmental remediation and renewable energy resources: Advances, mechanisms and biotechnological applications. *Heliyon*, 10(10), e31170. doi:10.1016/j.heliyon.2024.e31170
- Abd-El-Aziz, A., Elnagdy, S. M., Han, J., Mihelic, R., Wang, X., Agathos, S. N., & Li, J. (2025). Bacteria-microalgae interactions from an evolutionary perspective and their biotechnological significance. *Biotechnol Adv*, 82, 108591. doi:10.1016/j.biotechadv.2025.108591
- Ahmed, N., Thompson, S., & Glaser, M. (2019). Global Aquaculture Productivity, Environmental Sustainability, and Climate Change Adaptability. *Environ Manage*, 63(2), 159–172. doi:10.1007/s00267-018-1117-3
- Alday-Sanz, V., Corsin, F., Irde, E., Bondad-Reantaso, M.G. (2012). *Survey on the use of veterinary medicines in aquaculture*. Retrieved from 00153 Rome, Italy:
- Algammal, A. M., Mabrok, M., Sivaramasamy, E., Youssef, F. M., Atwa, M. H., El-Kholy, A. W., . . . Hozzein, W. N. (2020). Emerging MDR-*Pseudomonas aeruginosa* in fish commonly harbor oprL and toxA virulence genes and bla(TEM), bla(CTX-M), and tetA antibiotic-resistance genes. *Sci Rep*, 10(1), 15961. doi:10.1038/s41598-020-72264-4
- Alhede, M., Kragh, K. N., Qvortrup, K., Allesen-Holm, M., van Gennip, M., Christensen, L. D., . . . Bjarnsholt, T. (2011). Phenotypes of non-attached *Pseudomonas aeruginosa* aggregates resemble surface attached biofilm. *PLoS One*, 6(11), e27943. doi:10.1371/journal.pone.0027943
- Alquethamy, S. F., Khorvash, M., Pederick, V. G., Whittall, J. J., Paton, J. C., Paulsen, I. T., . . . Eijkelkamp, B. A. (2019). The Role of the CopA Copper Efflux System in *Acinetobacter baumannii* Virulence. *Int J Mol Sci*, 20(3). doi:10.3390/ijms20030575
- Altschul, S. F., Gish, W., Miller, W., Myers, E. W., & Lipman, D. J. (1990). Basic local alignment search tool. *J Mol Biol*, 215(3), 403–410. doi:10.1016/S0022-2836(05)80360-2
- Armwood, A. R., Camus, A. C., Lopez-Porras, A., Ware, C., Griffin, M. J., & Soto, E. (2019). Pathologic changes in cultured Nile tilapia (*Oreochromis niloticus*) associated with an outbreak of *Edwardsiella anguillarum*. *J Fish Dis*, 42(10), 1463–1469. doi:10.1111/jfd.13058
- Arsene, M. M. J., Davares, A. K. L., Viktorovna, P. I., Andreevna, S. L., Sarra, S., Khelifi, I., & Sergueievna, D. M. (2022). The public health issue of antibiotic residues in food and feed: Causes, consequences, and potential solutions. *Vet World*, 15(3), 662–671. doi:10.14202/vetworld.2022.662-671
- Austin, B. (2011). Taxonomy of bacterial fish pathogens. *Vet Res*, 42(1), 20. doi:10.1186/1297-9716-42-20
- Baek, M., DiMaio, F., Anishchenko, I., Dauparas, J., Ovchinnikov, S., Lee, G. R., . . . Baker, D. (2021). Accurate prediction of protein structures and interactions using a three-track neural network. *Science*, 373(6557), 871–876. doi:10.1126/science.abj8754
- Baloch, A., Zhang, X., Schade, R. (2015). IgY Technology in aquaculture – a review. *Reviews in Aquaculture*, 7(3), 153–160 doi:10.1111/raq.12059
- Barnard, A. M., Bowden, S. D., Burr, T., Coulthurst, S. J., Monson, R. E., & Salmond, G. P. (2007). Quorum sensing, virulence and secondary metabolite production in plant soft-rotting bacteria. *Philos Trans R Soc Lond B Biol Sci*, 362(1483), 1165–1183. doi:10.1098/rstb.2007.2042
- Bassler, B. L., & Losick, R. (2006). Bacterially speaking. *Cell*, 125(2), 237–246. doi:10.1016/j.cell.2006.04.001
- Bassler, B. L., Wright, M., & Silverman, M. R. (1994). Multiple signalling systems controlling expression of luminescence in *Vibrio harveyi*: sequence and function of genes encoding a second sensory pathway. *Mol Microbiol*, 13(2), 273–286. doi:10.1111/j.1365-2958.1994.tb00422.x
- Bauer, M., Knebel, J., Lechner, M., Pickl, P., & Frey, E. (2017). Ecological feedback in quorum-sensing microbial populations can induce heterogeneous production of autoinducers. *Elife*, 6. doi:10.7554/eLife.25773

- Bay, L., Kragh, K. N., Eickhardt, S. R., Poulsen, S. S., Gjerdrum, L. M. R., Ghathian, K., . . . Bjarnsholt, T. (2018). Bacterial Aggregates Establish at the Edges of Acute Epidermal Wounds. *Adv Wound Care (New Rochelle)*, 7(4), 105–113. doi:10.1089/wound.2017.0770
- Beijerinck, M. W. (1890). Culturversuche mit Zoochlorellen, Lichenengonidien und anderen niederen Algen. *Botanische Zeitung*, 47, 725–739, 741–754, 757–768, 781–785.
- Beloin, C., & Ghigo, J. M. (2005). Finding gene-expression patterns in bacterial biofilms. *Trends Microbiol*, 13(1), 16–19. doi:10.1016/j.tim.2004.11.008
- Bergmann, L., Balzer Le, S., Hageskal, G., Preuss, L., Han, Y., Astafyeva, Y., . . . Krohn, I. (2024). New dienelactone hydrolase from microalgae bacterial community-Antibiofilm activity against fish pathogens and potential applications for aquaculture. *Sci Rep*, 14(1), 377. doi:10.1038/s41598-023-50734-9
- Bernardet, J.-F., Grimont, Patrick. (1986). Deoxyribonucleic Acid Relatedness and Phenotypic Characterization of *Flexibacter columnaris* sp. nov., nom. rev., *Flexibacter psychrophilus* sp. nov., nom. rev., and *Flexibacter maritimus* Wakabayashi, Hikida, and Masumura. *International Journal of Systematic and Evolutionary Microbiology*, 39(3). doi:10.1099/00207713-39-3-346
- Bertani, G. (1951). Studies on lysogenesis. I. The mode of phage liberation by lysogenic *Escherichia coli*. *J Bacteriol*, 62(3), 293–300. doi:10.1128/jb.62.3.293-300.1951
- Bettenworth, V., Steinfeld, B., Duin, H., Petersen, K., Streit, W. R., Bischofs, I., & Becker, A. (2019). Phenotypic Heterogeneity in Bacterial Quorum Sensing Systems. *J Mol Biol*, 431(23), 4530–4546. doi:10.1016/j.jmb.2019.04.036
- Bhagirath, A. Y., Pydi, S. P., Li, Y., Lin, C., Kong, W., Chelikani, P., & Duan, K. (2017). Characterization of the Direct Interaction between Hybrid Sensor Kinases PA1611 and RetS That Controls Biofilm Formation and the Type III Secretion System in *Pseudomonas aeruginosa*. *ACS Infect Dis*, 3(2), 162–175. doi:10.1021/acsinfecdis.6b00153
- Biebl, H., Allgaier, M., Tindall, B. J., Koblizek, M., Lunsdorf, H., Pukall, R., & Wagner-Dobler, I. (2005). *Dinoroseobacter shibae* gen. nov., sp. nov., a new aerobic phototrophic bacterium isolated from dinoflagellates. *Int J Syst Evol Microbiol*, 55(Pt 3), 1089–1096. doi:10.1099/ijs.0.63511-0
- Blum, M., Andreeva, A., Florentino, L. C., Chuguransky, S. R., Grego, T., Hobbs, E., . . . Bateman, A. (2025). InterPro: the protein sequence classification resource in 2025. *Nucleic Acids Res*, 53(D1), D444–D456. doi:10.1093/nar/gkae1082
- Böckelmann, U., Manza, W., Neub, T. R., & Szewzyka, U. (2000). Characterization of the microbial community of lotic organic aggregates ('river snow') in the Elbe River of Germany by cultivation and molecular methods. *FEMS Microbiol Ecol*, 33(2), 157–170. doi:10.1111/j.1574-6941.2000.tb00738.x
- Bondad-Reantaso, M., MacKinnon, Brett, Karunasaga, Iddya, Fridman, Sophie, Alday-Sanz, Victoria, Brun, Edgar, Caputo, Andrea. (2023). Review of alternatives to antibiotic use in aquaculture. *Reviews in Aquaculture*, 15(4), 1421–1451. doi:10.1111/raq.12786
- Brencic, A., & Lory, S. (2009). Determination of the regulon and identification of novel mRNA targets of *Pseudomonas aeruginosa* RsmA. *Mol Microbiol*, 72(3), 612–632. doi:10.1111/j.1365-2958.2009.06670.x
- Bronesky, D., Wu, Z., Marzi, S., Walter, P., Geissmann, T., Moreau, K., . . . Romby, P. (2016). *Staphylococcus aureus* RNAIII and Its Regulon Link Quorum Sensing, Stress Responses, Metabolic Adaptation, and Regulation of Virulence Gene Expression. *Annu Rev Microbiol*, 70, 299–316. doi:10.1146/annurev-micro-102215-095708
- Browne, N., & Kavanagh, K. (2013). Developing the potential of using *Galleria mellonella* larvae as models for studying brain infection by *Listeria monocytogenes*. *Virulence*, 4(4), 271–272. doi:10.4161/viru.24174
- Bruns, A., Rohde, M., & Berthe-Corti, L. (2001). *Muricauda ruestringensis* gen. nov., sp. nov., a facultatively anaerobic, appendaged bacterium from German North Sea intertidal sediment. *Int J Syst Evol Microbiol*, 51(Pt 6), 1997–2006. doi:10.1099/00207713-51-6-1997

- Butcher, R. W. (1959). *An introductory account of the smaller algae of British coastal waters* (Vol. 1).
- Cai, Y. M. (2020). Non-surface Attached Bacterial Aggregates: A Ubiquitous Third Lifestyle. *Front Microbiol*, 11, 557035. doi:10.3389/fmicb.2020.557035
- Cepas, V., Lopez, Y., Gabasa, Y., Martins, C. B., Ferreira, J. D., Correia, M. J., . . . Soto, S. M. (2019). Inhibition of Bacterial and Fungal Biofilm Formation by 675 Extracts from Microalgae and Cyanobacteria. *Antibiotics (Basel)*, 8(2). doi:10.3390/antibiotics8020077
- Cepeda, C., Garcia-Marquez, S., Santos, Y. (2004). Improved growth of *Flavobacterium psychrophilum* using a new culture medium. *Aquaculture*, 238(1-4), 75–82.
- Charette, S. J. (2021). Microbe profile: *Aeromonas salmonicida*: an opportunistic pathogen with multiple personalities. *Microbiology (Reading)*, 167(5). doi:10.1099/mic.0.001052
- Chen, D., Yuan, X., Zheng, X., Fang, J., Lin, G., Li, R., . . . Xue, T. (2022). Multi-omics Analyses Provide Insight into the Biosynthesis Pathways of Fucoxanthin in *Isochrysis galbana*. *Genomics Proteomics Bioinformatics*, 20(6), 1138–1153. doi:10.1016/j.gpb.2022.05.010
- Chen Min, C. K., Palaniappan Krishnaveni, Ratner Anna, Huang Jinghua, Kyrpides Nikos. (2021). The IMG/M data management and analysis system v.6.0: new tools and advanced capabilities. *Nucleic Acids Research*, 49(D1), D751–D763. Retrieved from <https://doi.org/10.1093/nar/gkaa939>
- Chen, S., Zhou, Y., Chen, Y., Gu, J. (2018). fastp: an ultra-fast all-in-one FASTQ preprocessor. *Bioinformatics*, 34(17), i884–i890. doi:10.1093/bioinformatics/bty560
- Chiang, W. C., Nilsson, M., Jensen, P. O., Hoiby, N., Nielsen, T. E., Givskov, M., & Tolker-Nielsen, T. (2013). Extracellular DNA shields against aminoglycosides in *Pseudomonas aeruginosa* biofilms. *Antimicrob Agents Chemother*, 57(5), 2352–2361. doi:10.1128/AAC.00001-13
- Chodat, R. (1902). Algues vertes de la Suisse. Pleurococcoïdes - Chrooléoïdes. *Beiträge Kryptogamenflora der Schweiz*, 1(3), 1–373.
- Chopin, T., Sawhney, M. (2009). *Seaweed and their Mariculture* (J. Steele Ed.): Elsevier.
- Cirri, E., & Pohnert, G. (2019). Algae-bacteria interactions that balance the planktonic microbiome. *New Phytol*, 223(1), 100–106. doi:10.1111/nph.15765
- Cohen, P. A. (2018). Probiotic Safety-No Guarantees. *JAMA Intern Med*, 178(12), 1577–1578. doi:10.1001/jamainternmed.2018.5403
- Comolli, J. C., & Donohue, T. J. (2004). Differences in two *Pseudomonas aeruginosa* cbb3 cytochrome oxidases. *Mol Microbiol*, 51(4), 1193–1203. doi:10.1046/j.1365-2958.2003.03904.x
- Costerton, J. W., Stewart, P. S., & Greenberg, E. P. (1999). Bacterial biofilms: a common cause of persistent infections. *Science*, 284(5418), 1318–1322. doi:10.1126/science.284.5418.1318
- Czapinska, H., Kowalska, M., Zagorskaite, E., Manakova, E., Slyvka, A., Xu, S. Y., . . . Bochtler, M. (2018). Activity and structure of EcoKMcrA. *Nucleic Acids Res*, 46(18), 9829–9841. doi:10.1093/nar/gky731
- de Beer, D., Stoodley, P., Roe, F., & Lewandowski, Z. (1994). Effects of biofilm structures on oxygen distribution and mass transport. *Biotechnol Bioeng*, 43(11), 1131–1138. doi:10.1002/bit.260431118
- de la Fuente-Nunez, C., Reffuveille, F., Fernandez, L., & Hancock, R. E. (2013). Bacterial biofilm development as a multicellular adaptation: antibiotic resistance and new therapeutic strategies. *Curr Opin Microbiol*, 16(5), 580–589. doi:10.1016/j.mib.2013.06.013
- Declercq, A. M., Haesebrouck, F., Van den Broeck, W., Bossier, P., & Decostere, A. (2013). Columnaris disease in fish: a review with emphasis on bacterium-host interactions. *Vet Res*, 44(1), 27. doi:10.1186/1297-9716-44-27
- Defoirdt, T., Thanh, L., Delsen, B., Schryver, P., Sorgeloos, P., Boon, N., Bossier, P. (2011). N-acylhomoserine lactone-degrading *Bacillus* strains isolated from aquaculture animals. *Aquaculture*, 311(1-4), 258–260. doi:10.1016/j.aquaculture.2010.11.046

- Dong, Y. H., Xu, J. L., Li, X. Z., & Zhang, L. H. (2000). AiiA, an enzyme that inactivates the acylhomoserine lactone quorum-sensing signal and attenuates the virulence of *Erwinia carotovora*. *Proc Natl Acad Sci U S A*, 97(7), 3526–3531. doi:10.1073/pnas.97.7.3526
- Dorken, G., Ferguson, G. P., French, C. E., & Poon, W. C. (2012). Aggregation by depletion attraction in cultures of bacteria producing exopolysaccharide. *J R Soc Interface*, 9(77), 3490–3502. doi:10.1098/rsif.2012.0498
- Doroshenko, N., Tseng, B. S., Howlin, R. P., Deacon, J., Wharton, J. A., Thurner, P. J., . . . Stoodley, P. (2014). Extracellular DNA impedes the transport of vancomycin in *Staphylococcus epidermidis* biofilms preexposed to subinhibitory concentrations of vancomycin. *Antimicrob Agents Chemother*, 58(12), 7273–7282. doi:10.1128/AAC.03132-14
- Draganov, D. I., Teiber, J. F., Speelman, A., Osawa, Y., Sunahara, R., & La Du, B. N. (2005). Human paraoxonases (PON1, PON2, and PON3) are lactonases with overlapping and distinct substrate specificities. *J Lipid Res*, 46(6), 1239–1247. doi:10.1194/jlr.M400511-JLR200
- Eickhoff, M. J., & Bassler, B. L. (2018). SnapShot: Bacterial Quorum Sensing. *Cell*, 174(5), 1328–1328 e1321. doi:10.1016/j.cell.2018.08.003
- Engelbrecht, J., Nealson, K., & Silverman, M. (1983). Bacterial bioluminescence: isolation and genetic analysis of functions from *Vibrio fischeri*. *Cell*, 32(3), 773–781. doi:10.1016/0092-8674(83)90063-6
- Engelbrecht, J., & Silverman, M. (1984). Identification of genes and gene products necessary for bacterial bioluminescence. *Proc Natl Acad Sci U S A*, 81(13), 4154–4158. doi:10.1073/pnas.81.13.4154
- Evelyn, T. P. (1997). A historical review of fish vaccinology. *Dev Biol Stand*, 90, 3–12. Retrieved from <https://www.ncbi.nlm.nih.gov/pubmed/9270829>
- Ewing, W., McWhorter, A., Escobar, M., Lubin, A. (1965). *Edwardsiella*, a new genus of Enterobacteriaceae based on a new species, *E. tarda*. *International Journal of Systematic and Evolutionary Microbiology*, 15(1). doi:10.1099/00207713-15-1-33
- Fahy, P., Persley, G. (1983). *Plant bacterial diseases. A diagnostic guide*. Australia: Academic Press Australia.
- FAO. (2024). *The State of World Fisheries and Aquaculture 2024 – Blue Transformation in action*.
- Fawley, M. W. J., I.; Fawley, K. P. (2015). The phylogeny of the genus *Nannochloropsis* (Monodopsidaceae, Eustigmatophyceae), with descriptions of *N. australis* sp. nov. and *Microchloropsis* gen. nov. *Phycologia*, 54(5), 545–552. doi:10.2216/15-60.1
- Fei, Y., Chen, Z., Han, S., Zhang, S., Zhang, T., Lu, Y., . . . Yao, M. (2023). Role of prebiotics in enhancing the function of next-generation probiotics in gut microbiota. *Crit Rev Food Sci Nutr*, 63(8), 1037–1054. doi:10.1080/10408398.2021.1958744
- Feng, G. D., Zhang, X. J., Yang, S. Z., Li, A. Z., Yao, Q., & Zhu, H. (2020). Transfer of *Sphingorhabdus marina*, *Sphingorhabdus litoris*, *Sphingorhabdus flavimaris* and *Sphingorhabdus pacifica* corrig. into the novel genus *Parasphingorhabdus* gen. nov. and *Sphingopyxis baekryungensis* into the novel genus *Novosphingopyxis* gen. nov. within the family Sphingomonadaceae. *Int J Syst Evol Microbiol*, 70(3), 2147–2154. doi:10.1099/ijsem.0.004033
- Fetzner, S. (2015). Quorum quenching enzymes. *J Biotechnol*, 201, 2–14. doi:10.1016/j.jbiotec.2014.09.001
- Fisher, C. L., Fong, M. V., Lane, P. D., Carlson, S., & Lane, T. W. (2023). Storage and Algal Association of Bacteria That Protect *Microchloropsis salina* from Grazing by *Brachionus plicatilis*. *Microorganisms*, 11(3). doi:10.3390/microorganisms11030786
- Fleming, A. (1929). On the Antibacterial Action of Cultures of a *Penicillium*, with Special Reference to their Use in the Isolation of *B. influenzae*. *Br J Exp Pathol*, 10(3), 226–236.
- Flemming, H. C. (2008). *Biofilms*. *Wiley Online Library*. Retrieved from <https://doi.org/10.1002/9780470015902.a0000342.pub2>

- Flemming, H. C., van Hullebusch, E. D., Little, B. J., Neu, T. R., Nielsen, P. H., Seviour, T., . . . Wuertz, S. (2024). Microbial extracellular polymeric substances in the environment, technology and medicine. *Nat Rev Microbiol*. doi:10.1038/s41579-024-01098-y
- Flemming, H. C., & Wingender, J. (2010). The biofilm matrix. *Nat Rev Microbiol*, 8(9), 623–633. doi:10.1038/nrmicro2415
- Flemming, H. C., & Wuertz, S. (2019). Bacteria and archaea on Earth and their abundance in biofilms. *Nat Rev Microbiol*, 17(4), 247–260. doi:10.1038/s41579-019-0158-9
- Fuqua, W. C., Winans, S. C., & Greenberg, E. P. (1994). Quorum sensing in bacteria: the LuxR-LuxI family of cell density-responsive transcriptional regulators. *J Bacteriol*, 176(2), 269–275. doi:10.1128/jb.176.2.269-275.1994
- Furuhata, K., Edagawa, A., Miyamoto, H., Kawakami, Y., & Fukuyama, M. (2013). *Porphyrobacter colymbi* sp. nov. isolated from swimming pool water in Tokyo, Japan. *J Gen Appl Microbiol*, 59(3), 245–250. doi:10.2323/jgam.59.245
- Gao, R., & Stock, A. M. (2009). Biological insights from structures of two-component proteins. *Annu Rev Microbiol*, 63, 133–154. doi:10.1146/annurev.micro.091208.073214
- Gao, Z., Nie, P., Lu, J. F., Liu, L., Xiao, T., Liu, W., . . . Xie, H. X. (2015). Type III Secretion System Translocon Component EseB Forms Filaments on and Mediates Autoaggregation of and Biofilm Formation by *Edwardsiella tarda*. *Appl Environ Microbiol*, 81(17), 6078–6087. doi:10.1128/AEM.01254-15
- Garrrity, G. M. (2005). Class III. Gammaproteobacteria class. nov. *Bergeys Manual of Systematic Bacteriology*, 2, 1.
- Gauthier, M. J., Lafay, B., Christen, R., Fernandez, L., Acquaviva, M., Bonin, P., & Bertrand, J. C. (1992). *Marinobacter hydrocarbonoclasticus* gen. nov., sp. nov., a new, extremely halotolerant, hydrocarbon-degrading marine bacterium. *Int J Syst Bacteriol*, 42(4), 568–576. doi:10.1099/00207713-42-4-568
- Gibson, G. R., & Roberfroid, M. B. (1995). Dietary modulation of the human colonic microbiota: introducing the concept of prebiotics. *J Nutr*, 125(6), 1401–1412. doi:10.1093/jn/125.6.1401
- Gilbertie, J. M., Schnabel, L. V., Hickok, N. J., Jacob, M. E., Conlon, B. P., Shapiro, I. M., . . . Schaer, T. P. (2019). Equine or porcine synovial fluid as a novel ex vivo model for the study of bacterial free-floating biofilms that form in human joint infections. *PLoS One*, 14(8), e0221012. doi:10.1371/journal.pone.0221012
- Giovannoni, S. J., Tripp, H. J., Givan, S., Podar, M., Vergin, K. L., Baptista, D., . . . Mathur, E. J. (2005). Genome streamlining in a cosmopolitan oceanic bacterium. *Science*, 309(5738), 1242–1245. doi:10.1126/science.1114057
- Griffin, M. J., Reichley, S. R., Khoo, L. H., Ware, C., Greenway, T. E., Mischke, C. C., & Wise, D. J. (2014). Comparative susceptibility of Channel Catfish, Blue Catfish, and their hybrid cross to experimental challenge with *Bolbophorus damnificus* (Digenea: Bolbophoridae) cercariae. *J Aquat Anim Health*, 26(2), 96–99. doi:10.1080/08997659.2014.886636
- Guillard, R. R., & Ryther, J. H. (1962). Studies of marine planktonic diatoms. I. *Cyclotella nana* Hustedt, and *Detonula confervacea* (Cleve) Grun. *Can J Microbiol*, 8, 229–239. doi:10.1139/m62-029
- Guiry, M. D. G., G.M. (2023). AlgaeBase. Retrieved from <https://www.algaebase.org>
- Hahm, J. Y., Park, J., Jang, E. S., & Chi, S. W. (2022). 8-Oxoguanine: from oxidative damage to epigenetic and epitranscriptional modification. *Exp Mol Med*, 54(10), 1626–1642. doi:10.1038/s12276-022-00822-z
- Hall-Stoodley, L., Costerton, J. W., & Stoodley, P. (2004). Bacterial biofilms: from the natural environment to infectious diseases. *Nat Rev Microbiol*, 2(2), 95–108. doi:10.1038/nrmicro821
- Hall-Stoodley, L., & Stoodley, P. (2005). Biofilm formation and dispersal and the transmission of human pathogens. *Trends Microbiol*, 13(1), 7–10. doi:10.1016/j.tim.2004.11.004
- Hall, R. S., Fedorov, A. A., Marti-Arbona, R., Fedorov, E. V., Kolb, P., Sauder, J. M., . . . Raushel, F. M. (2010). The hunt for 8-oxoguanine deaminase. *J Am Chem Soc*, 132(6), 1762–1763. doi:10.1021/ja909817d

- Han, P., Lu, Q., Fan, L., & Zhou, W. (2019). A Review on the Use of Microalgae for Sustainable Aquaculture. *Applied Sciences*, 9(11), 2377. doi:10.3390/app9112377
- Harrison, J. J., Turner, R. J., & Ceri, H. (2005). Persister cells, the biofilm matrix and tolerance to metal cations in biofilm and planktonic *Pseudomonas aeruginosa*. *Environ Microbiol*, 7(7), 981–994. doi:10.1111/j.1462-2920.2005.00777.x
- Hartmann, R., Jeckel, H., Jelli, E., Singh, P. K., Vaidya, S., Bayer, M., . . . Drescher, K. (2021). Quantitative image analysis of microbial communities with BiofilmQ. *Nat Microbiol*, 6(2), 151–156. doi:10.1038/s41564-020-00817-4
- Hibberd, D. J. (1981). Notes on the taxonomy and nomenclature of the algal classes Eustigmatophyceae and Tribophyceae (synonym Xanthophyceae). *Journal of the Linnean Society of London, Botany*, 82, 93–119.
- Holmström, K. M., & Finkel, T. (2014). Cellular mechanisms and physiological consequences of redox-dependent signalling. *Nat Rev Mol Cell Biol*, 15(6), 411–421. doi:10.1038/nrm3801
- Horke, S., Xiao, J., Schutz, E. M., Kramer, G. L., Wilgenbus, P., Witte, I., . . . Teiber, J. F. (2015). Novel Paraoxonase 2-Dependent Mechanism Mediating the Biological Effects of the *Pseudomonas aeruginosa* Quorum-Sensing Molecule N-(3-Oxo-Dodecanoyl)-L-Homoserine Lactone. *Infect Immun*, 83(9), 3369–3380. doi:10.1128/IAI.00141-15
- Horswill, A. R., Stoodley, P., Stewart, P. S., & Parsek, M. R. (2007). The effect of the chemical, biological, and physical environment on quorum sensing in structured microbial communities. *Anal Bioanal Chem*, 387(2), 371–380. doi:10.1007/s00216-006-0720-y
- Huston, W. M., Jennings, M. P., & McEwan, A. G. (2002). The multicopper oxidase of *Pseudomonas aeruginosa* is a ferroxidase with a central role in iron acquisition. *Mol Microbiol*, 45(6), 1741–1750. doi:10.1046/j.1365-2958.2002.03132.x
- Hyeon, J. W., Jeong, S. E., Baek, K., & Jeon, C. O. (2017). *Roseitalea porphyridii* gen. nov., sp. nov., isolated from a red alga, and reclassification of *Hoeflea suaedae* Chung et al. 2013 as *Pseudohoeflea suaedae* gen. nov., comb. nov. *Int J Syst Evol Microbiol*, 67(2), 362–368. doi:10.1099/ijsem.0.001633
- Jahn, A., Griebe, T., Nielsen, P. H. (1999). Composition of *pseudomonas putida* biofilms: Accumulation of protein in the biofilm matrix. *Biofouling*, 14(1), 49–57. doi:10.1080/08927019909378396
- Ji, G., Beavis, R. C., & Novick, R. P. (1995). Cell density control of staphylococcal virulence mediated by an octapeptide pheromone. *Proc Natl Acad Sci U S A*, 92(26), 12055–12059. doi:10.1073/pnas.92.26.12055
- Ji, X., Li, H., Zhang, J., Saiyin, H., & Zheng, Z. (2019). The collaborative effect of *Chlorella vulgaris*-*Bacillus licheniformis* consortia on the treatment of municipal water. *J Hazard Mater*, 365, 483–493. doi:10.1016/j.jhazmat.2018.11.039
- Jones, D. T., Taylor, W. R., & Thornton, J. M. (1992). The rapid generation of mutation data matrices from protein sequences. *Comput Appl Biosci*, 8(3), 275–282. doi:10.1093/bioinformatics/8.3.275
- Juhas, M., Eberl, L., & Tummler, B. (2005). Quorum sensing: the power of cooperation in the world of *Pseudomonas*. *Environ Microbiol*, 7(4), 459–471. doi:10.1111/j.1462-2920.2005.00769.x
- Jumper, J., Evans, R., Pritzel, A., Green, T., Figurnov, M., Ronneberger, O., . . . Hassabis, D. (2021). Highly accurate protein structure prediction with AlphaFold. *Nature*, 596(7873), 583–589. doi:10.1038/s41586-021-03819-2
- Kanehisa, M., Furumichi, M., Sato, Y., Matsuura, Y., & Ishiguro-Watanabe, M. (2025). KEGG: biological systems database as a model of the real world. *Nucleic Acids Res*, 53(D1), D672–D677. doi:10.1093/nar/gkae909
- Katharios, P., Kalatzis, P. G., Kokkari, C., Pavlidis, M., & Wang, Q. (2019). Characterization of a Highly Virulent *Edwardsiella anguillarum* Strain Isolated From Greek Aquaculture, and a Spontaneously Induced Prophage Therein. *Front Microbiol*, 10, 141. doi:10.3389/fmicb.2019.00141
- Kavanagh, K., & Reeves, E. P. (2004). Exploiting the potential of insects for in vivo pathogenicity testing of microbial pathogens. *FEMS Microbiol Rev*, 28(1), 101–112. doi:10.1016/j.femsre.2003.09.002

- Kessler, E., & Czygan, F. C. (1970). Physiological and biochemical contributions to the taxonomy of the genus *Chlorella*. IV. Utilization of organic nitrogen compounds]. *Arch Mikrobiol*, 70(3), 211–216. Retrieved from <https://www.ncbi.nlm.nih.gov/pubmed/4245108>
- Kleerebezem, M., Quadri, L. E., Kuipers, O. P., & de Vos, W. M. (1997). Quorum sensing by peptide pheromones and two-component signal-transduction systems in Gram-positive bacteria. *Mol Microbiol*, 24(5), 895–904. doi:10.1046/j.1365-2958.1997.4251782.x
- Knupp, C., Soto, E., & Loch, T. P. (2024). Varying *Flavobacterium psychrophilum* shedding dynamics in three bacterial coldwater disease-susceptible salmonid (Family Salmonidae) species. *Microbiol Spectr*, 12(2), e0360123. doi:10.1128/spectrum.03601-23
- Kragh, K. N., Alhede, M., Rybtke, M., Stavnsberg, C., Jensen, P. O., Tolker-Nielsen, T., . . . Bjarnsholt, T. (2018). The Inoculation Method Could Impact the Outcome of Microbiological Experiments. *Appl Environ Microbiol*, 84(5). doi:10.1128/AEM.02264-17
- Kravchenko, V. V., Kaufmann, G. F., Mathison, J. C., Scott, D. A., Katz, A. Z., Grauer, D. C., . . . Ulevitch, R. J. (2008). Modulation of gene expression via disruption of NF-kappaB signaling by a bacterial small molecule. *Science*, 321(5886), 259–263. doi:10.1126/science.1156499
- Krieg, N. R. (2011). Class I. Bacteroidia class. nov. *Bergey's Manual of Systematic Bacteriology*, 4, 25.
- Krohn, I., Bergmann, L., Qi, M., Indenbirken, D., Han, Y., Perez-Garcia, P., . . . Streit, W. R. (2021). Deep (Meta)genomics and (Meta)transcriptome Analyses of Fungal and Bacteria Consortia From Aircraft Tanks and Kerosene Identify Key Genes in Fuel and Tank Corrosion. *Front Microbiol*, 12, 722259. doi:10.3389/fmicb.2021.722259
- Krohn, I., Menanteau-Ledouble, S., Hageskal, G., Astafyeva, Y., Jouannais, P., Nielsen, J. L., . . . Streit, W. R. (2022). Health benefits of microalgae and their microbiomes. *Microb Biotechnol*, 15(7), 1966–1983. doi:10.1111/1751-7915.14082
- Kumar, A., Pillay, B., & Olaniran, A. O. (2014). Two structurally different dienelactone hydrolases (TfdEI and TfdEII) from *Cupriavidus necator* JMP134 plasmid pJP4 catalyse cis- and trans-dienelactones with similar efficiency. *PLoS One*, 9(7), e101801. doi:10.1371/journal.pone.0101801
- Kumar, S., Stecher, G., Li, M., Knyaz, C., & Tamura, K. (2018). MEGA X: Molecular Evolutionary Genetics Analysis across Computing Platforms. *Mol Biol Evol*, 35(6), 1547–1549. doi:10.1093/molbev/msy096
- Kusada, H., Zhang, Y., Tamaki, H., Kimura, N., & Kamagata, Y. (2019). Novel N-Acyl Homoserine Lactone-Degrading Bacteria Isolated From Penicillin-Contaminated Environments and Their Quorum-Quenching Activities. *Front Microbiol*, 10, 455. doi:10.3389/fmicb.2019.00455
- Labrenz, M., Collins, M. D., Lawson, P. A., Tindall, B. J., Schumann, P., & Hirsch, P. (1999). *Roseovarius tolerans* gen. nov., sp. nov., a budding bacterium with variable bacteriochlorophyll a production from hypersaline Ekho Lake. *Int J Syst Bacteriol*, 49 Pt 1, 137–147. doi:10.1099/00207713-49-1-137
- Lade, H., Paul, D., & Kweon, J. H. (2014). Quorum quenching mediated approaches for control of membrane biofouling. *Int J Biol Sci*, 10(5), 550–565. doi:10.7150/ijbs.9028
- Lafferty, K. D., Harvell, C. D., Conrad, J. M., Friedman, C. S., Kent, M. L., Kuris, A. M., . . . Saksida, S. M. (2015). Infectious diseases affect marine fisheries and aquaculture economics. *Ann Rev Mar Sci*, 7, 471–496. doi:10.1146/annurev-marine-010814-015646
- Lawrence, J. R., Korber, D. R., Hoyle, B. D., Costerton, J. W., & Caldwell, D. E. (1991). Optical sectioning of microbial biofilms. *J Bacteriol*, 173(20), 6558–6567. doi:10.1128/jb.173.20.6558-6567.1991
- Lee, D. D., Galera-Laporta, L., Bialecka-Fornal, M., Moon, E. C., Shen, Z., Briggs, S. P., . . . Suel, G. M. (2019). Magnesium Flux Modulates Ribosomes to Increase Bacterial Survival. *Cell*, 177(2), 352–360 e313. doi:10.1016/j.cell.2019.01.042

- Lee, P. T., Yamamoto, F. Y., Low, C. F., Loh, J. Y., & Chong, C. M. (2021). Gut Immune System and the Implications of Oral-Administered Immunoprophylaxis in Finfish Aquaculture. *Front Immunol*, 12, 773193. doi:10.3389/fimmu.2021.773193
- Lesley, J. A., & Waldburger, C. D. (2001). Comparison of the *Pseudomonas aeruginosa* and *Escherichia coli* PhoQ sensor domains: evidence for distinct mechanisms of signal detection. *J Biol Chem*, 276(33), 30827–30833. doi:10.1074/jbc.M104262200
- Li, H., & Durbin, R. (2009). Fast and accurate short read alignment with Burrows-Wheeler transform. *Bioinformatics*, 25(14), 1754–1760. doi:10.1093/bioinformatics/btp324
- Li, W., & Zhang, G. (2022). Detection and various environmental factors of antibiotic resistance gene horizontal transfer. *Environ Res*, 212(Pt B), 113267. doi:10.1016/j.envres.2022.113267
- Liao, W., Huang, L., Han, S., Hu, D., Xu, Y., Liu, M., . . . Li, P. (2022). Review of Medicinal Plants and Active Pharmaceutical Ingredients against Aquatic Pathogenic Viruses. *Viruses*, 14(6). doi:10.3390/v14061281
- Liao, Y., Smyth, G. K., & Shi, W. (2014). featureCounts: an efficient general purpose program for assigning sequence reads to genomic features. *Bioinformatics*, 30(7), 923–930. doi:10.1093/bioinformatics/btt656
- Lin, G., Chai, J., Yuan, S., Mai, C., Cai, L., Murphy, R. W., . . . Luo, J. (2016). VennPainter: A Tool for the Comparison and Identification of Candidate Genes Based on Venn Diagrams. *PLoS One*, 11(4), e0154315. doi:10.1371/journal.pone.0154315
- Liu, R., Han, G., Li, Z., Cun, S., Hao, B., Zhang, J., & Liu, X. (2022). Bacteriophage therapy in aquaculture: current status and future challenges. *Folia Microbiol (Praha)*, 67(4), 573–590. doi:10.1007/s12223-022-00965-6
- Loenen, W. A., & Raleigh, E. A. (2014). The other face of restriction: modification-dependent enzymes. *Nucleic Acids Res*, 42(1), 56–69. doi:10.1093/nar/gkt747
- Lopez, Y., & Soto, S. M. (2019). The Usefulness of Microalgae Compounds for Preventing Biofilm Infections. *Antibiotics (Basel)*, 9(1). doi:10.3390/antibiotics9010009
- Love, M. I., Huber, W., & Anders, S. (2014). Moderated estimation of fold change and dispersion for RNA-seq data with DESeq2. *Genome Biol*, 15(12), 550. doi:10.1186/s13059-014-0550-8
- Lubis, A. R., Sumon, M. A. A., Dinh-Hung, N., Dhar, A. K., Delamare-Deboutteville, J., Kim, D. H., . . . Brown, C. L. (2024). Review of quorum-quenching probiotics: A promising non-antibiotic-based strategy for sustainable aquaculture. *J Fish Dis*, 47(7), e13941. doi:10.1111/jfd.13941
- Ma, J., Bruce, T. J., Jones, E. M., & Cain, K. D. (2019). A Review of Fish Vaccine Development Strategies: Conventional Methods and Modern Biotechnological Approaches. *Microorganisms*, 7(11). doi:10.3390/microorganisms7110569
- Macias-Valcayo, A., Staats, A., Aguilera-Correa, J. J., Brooks, J., Gupta, T., Dusane, D., . . . Esteban, J. (2021). Synovial Fluid Mediated Aggregation of Clinical Strains of Four Enterobacterial Species. *Adv Exp Med Biol*, 1323, 81–90. doi:10.1007/5584_2020_573
- Maguire, R., Duggan, O., & Kavanagh, K. (2016). Evaluation of *Galleria mellonella* larvae as an in vivo model for assessing the relative toxicity of food preservative agents. *Cell Biol Toxicol*, 32(3), 209–216. doi:10.1007/s10565-016-9329-x
- Malone, C. L., Boles, B. R., & Horswill, A. R. (2007). Biosynthesis of *Staphylococcus aureus* autoinducing peptides by using the *synechocystis* DnaB mini-intein. *Appl Environ Microbiol*, 73(19), 6036–6044. doi:10.1128/AEM.00912-07
- Manefield, M., Rasmussen, T. B., Henzter, M., Andersen, J. B., Steinberg, P., Kjelleberg, S., & Givskov, M. (2002). Halogenated furanones inhibit quorum sensing through accelerated LuxR turnover. *Microbiology (Reading)*, 148(Pt 4), 1119–1127. doi:10.1099/00221287-148-4-1119
- McCain, B. B. (1970). *The Oregon sockeye salmon virus: A. Biophysical biochemical characteristics B. Antigenic relationship to two other salmonid viruses*. (Doctoral Dissertation). Oregon State University, ScholarsArchive@OSU.
- McPhee, J. B., Lewenza, S., & Hancock, R. E. (2003). Cationic antimicrobial peptides activate a two-component regulatory system, PmrA-PmrB, that regulates resistance to

- polymyxin B and cationic antimicrobial peptides in *Pseudomonas aeruginosa*. *Mol Microbiol*, 50(1), 205–217. doi:10.1046/j.1365-2958.2003.03673.x
- Mikkelsen, H., Sivaneson, M., & Filloux, A. (2011). Key two-component regulatory systems that control biofilm formation in *Pseudomonas aeruginosa*. *Environ Microbiol*, 13(7), 1666–1681. doi:10.1111/j.1462-2920.2011.02495.x
- Mistry, J., Chuguransky, S., Williams, L., Qureshi, M., Salazar, G. A., Sonnhammer, E. L. L., . . . Bateman, A. (2021). Pfam: The protein families database in 2021. *Nucleic Acids Res*, 49(D1), D412–D419. doi:10.1093/nar/gkaa913
- Morohoshi, T., Inaba, T., Kato, N., Kanai, K., & Ikeda, T. (2004). Identification of quorum-sensing signal molecules and the LuxRI homologs in fish pathogen *Edwardsiella tarda*. *J Biosci Bioeng*, 98(4), 274–281. doi:10.1016/S1389-1723(04)00281-6
- Moser, G. A. O. B.-A., J.J.; Ortega, M.J. . (2022). Comparative characterization of three *Tetraselmis chui* (Chlorophyta) strains as sources of nutraceuticals. *J Appl Phycol* 34, 821–835. doi:10.1007/s10811-021-02675-x
- Moskowitz, S. M., Ernst, R. K., & Miller, S. I. (2004). PmrAB, a two-component regulatory system of *Pseudomonas aeruginosa* that modulates resistance to cationic antimicrobial peptides and addition of aminoarabinose to lipid A. *J Bacteriol*, 186(2), 575–579. doi:10.1128/JB.186.2.575-579.2004
- Mubashar, M., Zulekha, R., Cheng, S., Xu, C., Li, J., & Zhang, X. (2024). Carbon-negative and high-rate nutrient recovery from municipal wastewater using mixotrophic *Scenedesmus acuminatus*. *J Environ Manage*, 354, 120360. doi:10.1016/j.jenvman.2024.120360
- Mukherjee, S., & Bassler, B. L. (2019). Bacterial quorum sensing in complex and dynamically changing environments. *Nat Rev Microbiol*, 17(6), 371–382. doi:10.1038/s41579-019-0186-5
- Mulcahy, H., Charron-Mazenod, L., & Lewenza, S. (2008). Extracellular DNA chelates cations and induces antibiotic resistance in *Pseudomonas aeruginosa* biofilms. *PLoS Pathog*, 4(11), e1000213. doi:10.1371/journal.ppat.1000213
- Müller, M., Spiers, A. J., Tan, A., & Mujahid, A. (2023). Investigating quorum-quenching marine bacilli as potential biocontrol agents for protection of shrimps against Early Mortality Syndrome (EMS). *Sci Rep*, 13(1), 4095. doi:10.1038/s41598-023-31197-4
- Nealson, K. H., Platt, T., & Hastings, J. W. (1970). Cellular control of the synthesis and activity of the bacterial luminescent system. *J Bacteriol*, 104(1), 313–322. doi:10.1128/jb.104.1.313-322.1970
- Newman, J. N., Floyd, R. V., & Fothergill, J. L. (2022). Invasion and diversity in *Pseudomonas aeruginosa* urinary tract infections. *J Med Microbiol*, 71(3). doi:10.1099/jmm.0.001458
- Ngai, K. L., Schlomann, M., Knackmuss, H. J., & Ornston, L. N. (1987). Dienelactone hydrolase from *Pseudomonas* sp. strain B13. *J Bacteriol*, 169(2), 699–703. doi:10.1128/jb.169.2.699-703.1987
- Nickerson, R., Thornton, C. S., Johnston, B., Lee, A. H. Y., & Cheng, Z. (2024). *Pseudomonas aeruginosa* in chronic lung disease: untangling the dysregulated host immune response. *Front Immunol*, 15, 1405376. doi:10.3389/fimmu.2024.1405376
- Niederwieser, T., Kociolek, P., & Klaus, D. (2018). Spacecraft cabin environment effects on the growth and behavior of *Chlorella vulgaris* for life support applications. *Life Sci Space Res (Amst)*, 16, 8–17. doi:10.1016/j.lssr.2017.10.002
- Nielsen, H., Tsigos, K. D., Brunak, S., & von Heijne, G. (2019). A Brief History of Protein Sorting Prediction. *Protein J*, 38(3), 200–216. doi:10.1007/s10930-019-09838-3
- Nik Mohamad Nek Rahimi, N., Natrah, I., Loh, J. Y., Ervin Ranzil, F. K., Gina, M., Lim, S. E., . . . Chong, C. M. (2022). Phytocompounds as an Alternative Antimicrobial Approach in Aquaculture. *Antibiotics (Basel)*, 11(4). doi:10.3390/antibiotics11040469
- Notredame, C., Higgins, D. G., & Heringa, J. (2000). T-Coffee: A novel method for fast and accurate multiple sequence alignment. *J Mol Biol*, 302(1), 205–217. doi:10.1006/jmbi.2000.4042
- Novick, R. P., & Geisinger, E. (2008). Quorum sensing in staphylococci. *Annu Rev Genet*, 42, 541–564. doi:10.1146/annurev.genet.42.110807.091640
- Nwoko, E. Q. A., & Okeke, I. N. (2021). Bacteria autoaggregation: how and why bacteria stick together. *Biochem Soc Trans*, 49(3), 1147–1157. doi:10.1042/BST20200718

- Ocaranza, D., Balic, I., Bruna, T., Moreno, I., Diaz, O., Moreno, A. A., & Caro, N. (2022). A Modeled High-Density Fed-Batch Culture Improves Biomass Growth and beta-Glucans Accumulation in *Microchloropsis salina*. *Plants (Basel)*, 11(23). doi:10.3390/plants11233229
- Ock, C. Y., Kim, E. H., Choi, D. J., Lee, H. J., Hahm, K. B., & Chung, M. H. (2012). 8-Hydroxydeoxyguanosine: not mere biomarker for oxidative stress, but remedy for oxidative stress-implicated gastrointestinal diseases. *World J Gastroenterol*, 18(4), 302–308. doi:10.3748/wjg.v18.i4.302
- Oh, W. T., Jun, J. W., Kim, H. J., Giri, S. S., Yun, S., Kim, S. G., . . . Park, S. C. (2020). Characterization and Pathological Analysis of a Virulent *Edwardsiella anguillarum* Strain Isolated From Nile Tilapia (*Oreochromis niloticus*) in Korea. *Front Vet Sci*, 7, 14. doi:10.3389/fvets.2020.00014
- Okada, M., Sato, I., Cho, S. J., Iwata, H., Nishio, T., Dubnau, D., & Sakagami, Y. (2005). Structure of the *Bacillus subtilis* quorum-sensing peptide pheromone ComX. *Nat Chem Biol*, 1(1), 23–24. doi:10.1038/nchembio709
- Okocha, R. C., Olatoye, I. O., & Adediji, O. B. (2018). Food safety impacts of antimicrobial use and their residues in aquaculture. *Public Health Rev*, 39, 21. doi:10.1186/s40985-018-0099-2
- Paerl, H. W., & Otten, T. G. (2013). Harmful cyanobacterial blooms: causes, consequences, and controls. *Microb Ecol*, 65(4), 995–1010. doi:10.1007/s00248-012-0159-y
- Park, Y. J., Yoon, S. J., & Lee, H. B. (2010). A novel diene lactone hydrolase from the thermoacidophilic archaeon *Sulfolobus solfataricus* P1: purification, characterization, and expression. *Biochim Biophys Acta*, 1800(11), 1164–1172. doi:10.1016/j.bbagen.2010.07.006
- Parke, M. (1949). Studies on marine flagellates. *Journal of the Marine Biological Association of the United Kingdom*, 28, 255–288.
- Pathak, D., & Ollis, D. (1990). Refined structure of diene lactone hydrolase at 1.8 Å. *J Mol Biol*, 214(2), 497–525. doi:10.1016/0022-2836(90)90196-s
- Pearson, J. P., Gray, K. M., Passador, L., Tucker, K. D., Eberhard, A., Iglewski, B. H., & Greenberg, E. P. (1994). Structure of the autoinducer required for expression of *Pseudomonas aeruginosa* virulence genes. *Proc Natl Acad Sci U S A*, 91(1), 197–201. doi:10.1073/pnas.91.1.197
- Peix, A., Rivas, R., Trujillo, M. E., Vancanneyt, M., Velazquez, E., & Willems, A. (2005). Reclassification of *Agrobacterium ferrugineum* LMG 128 as *Hoeflea marina* gen. nov., sp. nov. *Int J Syst Evol Microbiol*, 55(Pt 3), 1163–1166. doi:10.1099/ijs.0.63291-0
- Peng, Y., Leung, H. C., Yiu, S. M., & Chin, F. Y. (2012). IDBA-UD: a de novo assembler for single-cell and metagenomic sequencing data with highly uneven depth. *Bioinformatics*, 28(11), 1420–1428. doi:10.1093/bioinformatics/bts174
- Pereira, W. A., Mendonca, C. M. N., Urquiza, A. V., Marteinsson, V., LeBlanc, J. G., Cotter, P. D., . . . Oliveira, R. P. S. (2022). Use of Probiotic Bacteria and Bacteriocins as an Alternative to Antibiotics in Aquaculture. *Microorganisms*, 10(9). doi:10.3390/microorganisms10091705
- Petrova, O. E., & Sauer, K. (2012). Sticky situations: key components that control bacterial surface attachment. *J Bacteriol*, 194(10), 2413–2425. doi:10.1128/JB.00003-12
- Pettersen, E. F., Goddard, T. D., Huang, C. C., Couch, G. S., Greenblatt, D. M., Meng, E. C., & Ferrin, T. E. (2004). UCSF Chimera--a visualization system for exploratory research and analysis. *J Comput Chem*, 25(13), 1605–1612. doi:10.1002/jcc.20084
- Pettersen, E. F., Goddard, T. D., Huang, C. C., Meng, E. C., Couch, G. S., Croll, T. I., . . . Ferrin, T. E. (2021). UCSF ChimeraX: Structure visualization for researchers, educators, and developers. *Protein Sci*, 30(1), 70–82. doi:10.1002/pro.3943
- Prieto-Barajas, M. (2018). Microbial mat ecosystems: Structure types, functional diversity, and biotechnological application. *Electronic Journal of Biotechnology*, 31, 48–56. doi:10.1016/j.ejbt.2017.11.001
- Purevdorj-Gage, B., Costerton, W. J., & Stoodley, P. (2005). Phenotypic differentiation and seeding dispersal in non-mucoid and mucoid *Pseudomonas aeruginosa* biofilms. *Microbiology (Reading)*, 151(Pt 5), 1569–1576. doi:10.1099/mic.0.27536-0

- Puri, P., Sharma, J. G., & Singh, R. (2022). Biotherapeutic microbial supplementation for ameliorating fish health: developing trends in probiotics, prebiotics, and synbiotics use in finfish aquaculture. *Anim Health Res Rev*, 23(2), 113–135. doi:10.1017/S1466252321000165
- Qin, Z., Babu, V. S., Li, N., Fu, T., Li, J., Yi, L., . . . Lin, L. (2018). Protective effects of chicken egg yolk immunoglobulins (IgY) against experimental *Aeromonas hydrophila* infection in blunt snout bream (*Megalobrama amblycephala*). *Fish Shellfish Immunol*, 78, 26–34. doi:10.1016/j.fsi.2018.04.001
- Randall, D., Tsui, T. (2002). Ammonia toxicity in fish. *Marine Pollution Bulletin*, 45(1-12), 17–23. doi:10.1016/S0025-326X(02)00227-8
- Rasmussen, B. (2000). Filamentous microfossils in a 3,235-million-year-old volcanogenic massive sulphide deposit. *Nature*, 405(6787), 676–679. doi:10.1038/35015063
- Rodrigue, A., Quentin, Y., Lazdunski, A., Mejean, V., & Foglino, M. (2000). Two-component systems in *Pseudomonas aeruginosa*: why so many? *Trends Microbiol*, 8(11), 498–504. doi:10.1016/s0966-842x(00)01833-3
- Rumbaugh, K. P., & Sauer, K. (2020). Biofilm dispersion. *Nat Rev Microbiol*, 18(10), 571–586. doi:10.1038/s41579-020-0385-0
- Sauer, K., Stoodley, P., Goeres, D. M., Hall-Stoodley, L., Burmolle, M., Stewart, P. S., & Bjarnsholt, T. (2022). The biofilm life cycle: expanding the conceptual model of biofilm formation. *Nat Rev Microbiol*, 20(10), 608–620. doi:10.1038/s41579-022-00767-0
- Schade, R., Calzado, E. G., Sarmiento, R., Chacana, P. A., Porankiewicz-Asplund, J., & Terzolo, H. R. (2005). Chicken egg yolk antibodies (IgY-technology): a review of progress in production and use in research and human and veterinary medicine. *Altern Lab Anim*, 33(2), 129–154. doi:10.1177/026119290503300208
- Schleheck, D., Barraud, N., Klebensberger, J., Webb, J. S., McDougald, D., Rice, S. A., & Kjelleberg, S. (2009). *Pseudomonas aeruginosa* PAO1 preferentially grows as aggregates in liquid batch cultures and disperses upon starvation. *PLoS One*, 4(5), e5513. doi:10.1371/journal.pone.0005513
- Schlömann, M., Ngai, K. L., Ornston, L. N., & Knackmuss, H. J. (1993). Dienelactone hydrolase from *Pseudomonas cepacia*. *J Bacteriol*, 175(10), 2994–3001. doi:10.1128/jb.175.10.2994-3001.1993
- Schlömann, M., Schmidt, E., & Knackmuss, H. J. (1990). Different types of dienelactone hydrolase in 4-fluorobenzoate-utilizing bacteria. *J Bacteriol*, 172(9), 5112–5118. doi:10.1128/jb.172.9.5112-5118.1990
- Schoch, C. L., Ciufo, S., Domrachev, M., Hottot, C. L., Kannan, S., Khovanskaya, R., . . . Karsch-Mizrachi, I. (2020). NCBI Taxonomy: a comprehensive update on curation, resources and tools. *Database (Oxford)*, 2020. doi:10.1093/database/baaa062
- Schroeter, J. (1872). Ueber einige durch Bakterien gebildete Pigmente. *Beiträge zur Biologie der Pflanzen*, 2(1), 109–129.
- Secor, P. R., Michaels, L. A., Ratjen, A., Jennings, L. K., & Singh, P. K. (2018). Entropically driven aggregation of bacteria by host polymers promotes antibiotic tolerance in *Pseudomonas aeruginosa*. *Proc Natl Acad Sci U S A*, 115(42), 10780–10785. doi:10.1073/pnas.1806005115
- Shao, S., Lai, Q., Liu, Q., Wu, H., Xiao, J., Shao, Z., . . . Zhang, Y. (2015). Phylogenomics characterization of a highly virulent *Edwardsiella* strain ET080813(T) encoding two distinct T3SS and three T6SS gene clusters: Propose a novel species as *Edwardsiella anguillarum* sp. nov. *Syst Appl Microbiol*, 38(1), 36–47. doi:10.1016/j.syapm.2014.10.008
- Sionov, R. V., & Steinberg, D. (2022). Targeting the Holy Triangle of Quorum Sensing, Biofilm Formation, and Antibiotic Resistance in Pathogenic Bacteria. *Microorganisms*, 10(6). doi:10.3390/microorganisms10061239
- Snyder, E. E., Kampanya, N., Lu, J., Nordberg, E. K., Karur, H. R., Shukla, M., . . . Sobral, B. W. (2007). PATRIC: the VBI PathoSystems Resource Integration Center. *Nucleic Acids Res*, 35(Database issue), D401–406. doi:10.1093/nar/gkl858
- Sommerset, I., Krossoy, B., Biering, E., & Frost, P. (2005). Vaccines for fish in aquaculture. *Expert Rev Vaccines*, 4(1), 89–101. doi:10.1586/14760584.4.1.89

- Stanier, R. Y., Kunisawa, R., Mandel, M., & Cohen-Bazire, G. (1971). Purification and properties of unicellular blue-green algae (order Chroococcales). *Bacteriol Rev*, 35(2), 171–205. doi:10.1128/br.35.2.171-205.1971
- Stewart, P. S., & Franklin, M. J. (2008). Physiological heterogeneity in biofilms. *Nat Rev Microbiol*, 6(3), 199–210. doi:10.1038/nrmicro1838
- Stock, A. M., Robinson, V. L., & Goudreau, P. N. (2000). Two-component signal transduction. *Annu Rev Biochem*, 69, 183–215. doi:10.1146/annurev.biochem.69.1.183
- Swift, S., Karlyshev, A. V., Fish, L., Durant, E. L., Winson, M. K., Chhabra, S. R., . . . Stewart, G. S. (1997). Quorum sensing in *Aeromonas hydrophila* and *Aeromonas salmonicida*: identification of the LuxRI homologs AhyRI and AsaRI and their cognate N-acylhomoserine lactone signal molecules. *J Bacteriol*, 179(17), 5271–5281. doi:10.1128/jb.179.17.5271-5281.1997
- Tamura, K., Stecher, G., & Kumar, S. (2021). MEGA11: Molecular Evolutionary Genetics Analysis Version 11. *Mol Biol Evol*, 38(7), 3022–3027. doi:10.1093/molbev/msab120
- Tao, S., Luo, Y., Bin, H., Liu, J., Qian, X., Ni, Y., & Zhao, R. (2016). Paraoxonase 2 modulates a proapoptotic function in LS174T cells in response to quorum sensing molecule N-(3-oxododecanoyl)-L-homoserine lactone. *Sci Rep*, 6, 28778. doi:10.1038/srep28778
- Tateda, K., Ishii, Y., Horikawa, M., Matsumoto, T., Miyairi, S., Pechere, J. C., . . . Yamaguchi, K. (2003). The *Pseudomonas aeruginosa* autoinducer N-3-oxododecanoyl homoserine lactone accelerates apoptosis in macrophages and neutrophils. *Infect Immun*, 71(10), 5785–5793. doi:10.1128/IAI.71.10.5785-5793.2003
- Tatusov, R. L., Koonin, E. V., & Lipman, D. J. (1997). A genomic perspective on protein families. *Science*, 278(5338), 631–637. doi:10.1126/science.278.5338.631
- Teitzel, G. M., Geddie, A., De Long, S. K., Kirisits, M. J., Whiteley, M., & Parsek, M. R. (2006). Survival and growth in the presence of elevated copper: transcriptional profiling of copper-stressed *Pseudomonas aeruginosa*. *J Bacteriol*, 188(20), 7242–7256. doi:10.1128/JB.00837-06
- Telford, G., Wheeler, D., Williams, P., Tomkins, P. T., Appleby, P., Sewell, H., . . . Pritchard, D. I. (1998). The *Pseudomonas aeruginosa* quorum-sensing signal molecule N-(3-oxododecanoyl)-L-homoserine lactone has immunomodulatory activity. *Infect Immun*, 66(1), 36–42. doi:10.1128/IAI.66.1.36-42.1998
- Thaden, J. T., Lory, S., & Gardner, T. S. (2010). Quorum-sensing regulation of a copper toxicity system in *Pseudomonas aeruginosa*. *J Bacteriol*, 192(10), 2557–2568. doi:10.1128/JB.01528-09
- Thore, E. S. J., Muylaert, K., Bertram, M. G., & Brodin, T. (2023). Microalgae. *Curr Biol*, 33(3), R91–R95. doi:10.1016/j.cub.2022.12.032
- Todorov, S. D., Lima, J. M. S., Bucheli, J. E. V., Popov, I. V., Tiwari, S. K., & Chikindas, M. L. (2024). Probiotics for Aquaculture: Hope, Truth, and Reality. *Probiotics Antimicrob Proteins*, 16(6), 2007–2020. doi:10.1007/s12602-024-10290-8
- Trego, A. (2020). Granular biofilms: Function, application, and new trends as model microbial communities. *Critical Reviews in Environmental Science and Technology*, 51(15), 1702–1725. doi:10.1080/10643389.2020.1769433
- Tseng, B. S., Zhang, W., Harrison, J. J., Quach, T. P., Song, J. L., Penterman, J., . . . Parsek, M. R. (2013). The extracellular matrix protects *Pseudomonas aeruginosa* biofilms by limiting the penetration of tobramycin. *Environ Microbiol*, 15(10), 2865–2878. doi:10.1111/1462-2920.12155
- UniProt, C. (2025). UniProt: the Universal Protein Knowledgebase in 2025. *Nucleic Acids Res*, 53(D1), D609–D617. doi:10.1093/nar/gkae1010
- Vinoth Arul Raj, J., Praveen Kumar, R., Vijayakumar, B., Gnansounou, E., & Bharathiraja, B. (2021). Modelling and process optimization for biodiesel production from *Nannochloropsis salina* using artificial neural network. *Bioresour Technol*, 329, 124872. doi:10.1016/j.biortech.2021.124872
- Vishwakarma, V. (2020). Impact of environmental biofilms: Industrial components and its remediation. *J Basic Microbiol*, 60(3), 198–206. doi:10.1002/jobm.201900569

- Waite, R., Beveridge, M., Brummett, R., Castine, S., Chaiyawannakarn, N., Kaushik, S., Mungkung, R., Nawapakpilai, S., Phillips, M. (2014). *Improving productivity and environmental performance of aquaculture*: World resources institute.
- Wei, Q., & Ma, L. Z. (2013). Biofilm matrix and its regulation in *Pseudomonas aeruginosa*. *Int J Mol Sci*, 14(10), 20983–21005. doi:10.3390/ijms141020983
- Whitchurch, C. B., Tolker-Nielsen, T., Ragas, P. C., & Mattick, J. S. (2002). Extracellular DNA required for bacterial biofilm formation. *Science*, 295(5559), 1487. doi:10.1126/science.295.5559.1487
- Woese, C. R., Stackebrandt, E., Weisburg, W. G., Paster, B. J., Madigan, M. T., Fowler, V. J., . . . Fox, G. E. (1984). The phylogeny of purple bacteria: the alpha subdivision. *Syst Appl Microbiol*, 5, 315–326. doi:10.1016/s0723-2020(84)80034-x
- Yanong, R., Francis-Floyd, R., Petty, B. (2021). Bacterial Diseases in Aquaculture. *MSD Manual*. Retrieved from <https://www.msdsvetmanual.com/exotic-and-laboratory-animals/aquaculture/bacterial-diseases-in-aquaculture>
- Yuan, D., Wang, L., Wang, H., Miao, R., Wang, Y., Jin, H., . . . Gong, Y. (2023). Application of microalgae *Scenedesmus acuminatus* enhances water quality in rice-crayfish culture. *Front Bioeng Biotechnol*, 11, 1143622. doi:10.3389/fbioe.2023.1143622
- Zaharik, M. L., & Finlay, B. B. (2004). Mn²⁺ and bacterial pathogenesis. *Front Biosci*, 9, 1035–1042. doi:10.2741/1317
- Ziarati, M., Zorriehzahra, M. J., Hassantabar, F., Mehrabi, Z., Dhawan, M., Sharun, K., . . . Shamsi, S. (2022). Zoonotic diseases of fish and their prevention and control. *Vet Q*, 42(1), 95–118. doi:10.1080/01652176.2022.2080298

8 Supplemental

Table S1: Overall numbers of sequences and contigs generated for microbial consortia of algae. Assembled by IDBA

Parameter	Value
<i>Tetraselmis chui</i>	
Reads Illumina (filtered)	
Total no.	86,604,623
Average length (bp)	138.14
Duplicates (%)	48
Fails (%)	0
GC (%)	53
Contigs-assembly	
No.	176,777
Total length (bp)	245,460,098
No. contigs \geq 1000 bp	71,834
N50 size (bp)	1,698
Largest contig (bp)	949,877
GC (%)	52.33
<i>Isochrysis galbana</i>	
Reads Illumina (filtered)	
Total no.	80,579,167
Average length (bp)	141.10
Duplicates (%)	59
Fails (%)	18
GC (%)	61
Contigs-assembly	
No.	38,923
Total length (bp)	148,274,405
No. contigs \geq 1000 bp	19,948
N50 size (bp)	25,184
Largest (bp)	586,992
GC (%)	59.52
<i>Nannochloropsis salina</i>	
Reads Illumina (filtered)	
Total no.	79,761,293
Average length (bp)	138.91
Duplicates (%)	50
Fails (%)	23
GC (%)	57
Contigs-assembly (Spades)	
No.	38,159
Total length (bp)	172,907,087
No. \geq 1000 bp	17,787
N50 size (bp)	39,825
Largest (bp)	773,946
GC (%)	55.20

Parameter	Value
<i>Chlorella vulgaris</i>	
Reads Illumina (filtered)	
Total no.	78,796,023
Average length (bp)	139,85
Duplicates (%)	51
Fails (%)	27
GC (%)	61
Contigs-assembly	
No.	10,784
Total length (bp)	97,230,463
No. contigs \geq 1000 bp	8,190
N50 size (bp)	35,138
Largest (bp)	602,241
GC (%)	61.87
<i>Isochrysis spec.</i>	
Reads Illumina (filtered)	
Total no.	74,094,374
Average length (bp)	138.42
Duplicates (%)	56
Fails (%)	9
GC (%)	55
Contigs-assembly	
No.	18,665
Total length (bp)	112,201,420
No. contigs \geq 1000 bp	9,197
N50 size (bp)	48,522
Largest (bp)	916,017
GC (%)	53.70
<i>Scenedesmus acuminatus</i>	
Reads Illumina (filtered)	
Total no.	58,809,470
Average length (bp)	139.68
Duplicates (%)	44
Fails (%)	9
GC (%)	58
Contigs-assembly	
No.	16,806
Total length (bp)	109,460,776
No. contigs \geq 1000 bp	12,506
N50 size (bp)	13,732
Largest (bp)	544405
GC (%)	56.31

Table S2: FastP report of *E. anguillarum* transcriptome in presence of Dlh3 or PBS as control

Parameter	Value
General information	
fastp version:	0.21.0 (https://github.com/OpenGene/fastp)
sequencing:	single end (75 cycles)
mean length before filtering:	75bp
mean length after filtering:	74bp
duplication rate:	43.026844%43.854266% (may be overestimated since this is SE data)
Ea_DLH3_1_S5_R1_001	
After filtering	
total reads:	10.053648 M
total bases:	753.963162 M
Q20 bases:	727.772544 M (96.526274%)
Q30 bases:	714.104725 M (94.713477%)
GC content:	55.870085%
Filtering result	
reads passed filters:	10.053648 M (99.544972%)
reads with low quality:	38.332000 K (0.379540%)
reads with too many N:	127 (0.001257%)
reads too short:	7.497000 K (0.074231%)
Ea_DLH3_2_S6_R1_001	
After filtering	
total reads:	9.610773 M
total bases:	720.778033 M
Q20 bases:	695.949531 M (96.555319%)
Q30 bases:	683.039891 M (94.764249%)
GC content:	55.806640%
Filtering result	
reads passed filters:	9.610773 M (99.570586%)
reads with low quality:	33.549000 K (0.347578%)
reads with too many N:	96 (0.000995%)
reads too short:	7.803000 K (0.080841%)
Ea_DLH3_3_S7_R1_001	
After filtering	
total reads:	9.695770 M
total bases:	727.159625 M
Q20 bases:	701.458722 M (96.465576%)
Q30 bases:	688.179332 M (94.639376%)
GC content:	56.491569%
Filtering result	
reads passed filters:	9.695770 M (99.529625%)
reads with low quality:	36.168000 K (0.371274%)
reads with too many N:	107 (0.001098%)
reads too short:	9.547000 K (0.098002%)

Parameter	Value
Ea_PBS_4_S8_R1_001	
After filtering	
total reads:	9.677038 M
total bases:	725.748962 M
Q20 bases:	701.214482 M (96.619426%)
Q30 bases:	688.422133 M (94.856785%)
GC content:	56.516431%
Filtering result	
reads passed filters:	9.677038 M (99.597648%)
reads with low quality:	34.473000 K (0.354802%)
reads with too many N:	128 (0.001317%)
reads too short:	4.492000 K (0.046232%)
Ea_PBS_5_S9_R1_001	
After filtering	
total reads:	9.790316 M
total bases:	734.219251 M
Q20 bases:	708.656118 M (96.518324%)
Q30 bases:	695.374515 M (94.709382%)
GC content:	55.711214%
Filtering result	
reads passed filters:	9.790316 M (99.538832%)
reads with low quality:	40.079000 K (0.407486%)
reads with too many N:	119 (0.001210%)
reads too short:	5.161000 K (0.052472%)
Ea_PBS_6_S10_R1_001	
After filtering	
total reads:	9.527850 M
total bases:	714.501052 M
Q20 bases:	690.150782 M (96.591990%)
Q30 bases:	677.458642 M (94.815626%)
GC content:	54.916653%
Filtering result	
reads passed filters:	9.527850 M (99.532395%)
reads with low quality:	38.532000 K (0.402523%)
reads with too many N:	114 (0.001191%)
reads too short:	6.116000 K (0.063891%)

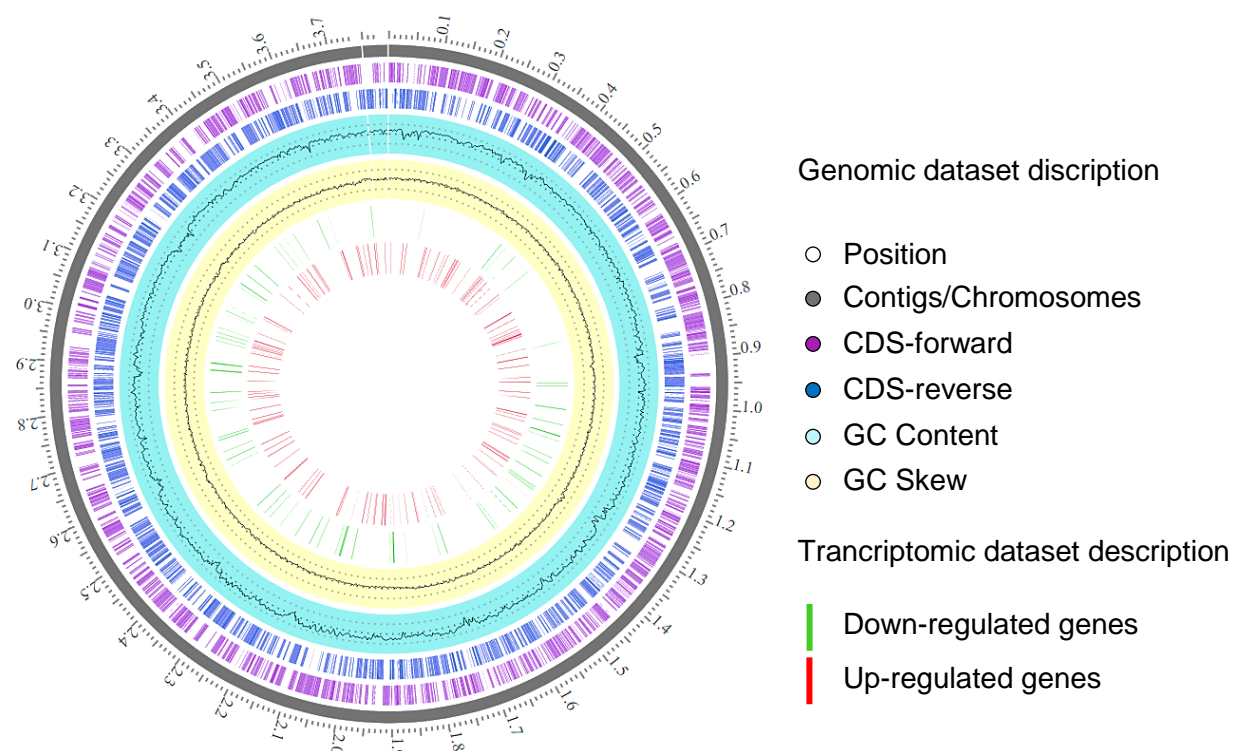


Figure S1: Circular genome map of transcriptomic data of *E. anguillarum* incubated with Dlh3. Moving inward, the subsequent two rings show CDSs in forward (magenta) and reverse (blue) strands. Cyan and yellow plots indicate GC content and a GC skew $[(GC)/(G+C)]$. Transcriptomic dataset description; red: up-regulated genes, green: down-regulated genes. Circular genome map provided by Dr. Yekaterina Astafyeva (Bergmann et al., 2024).

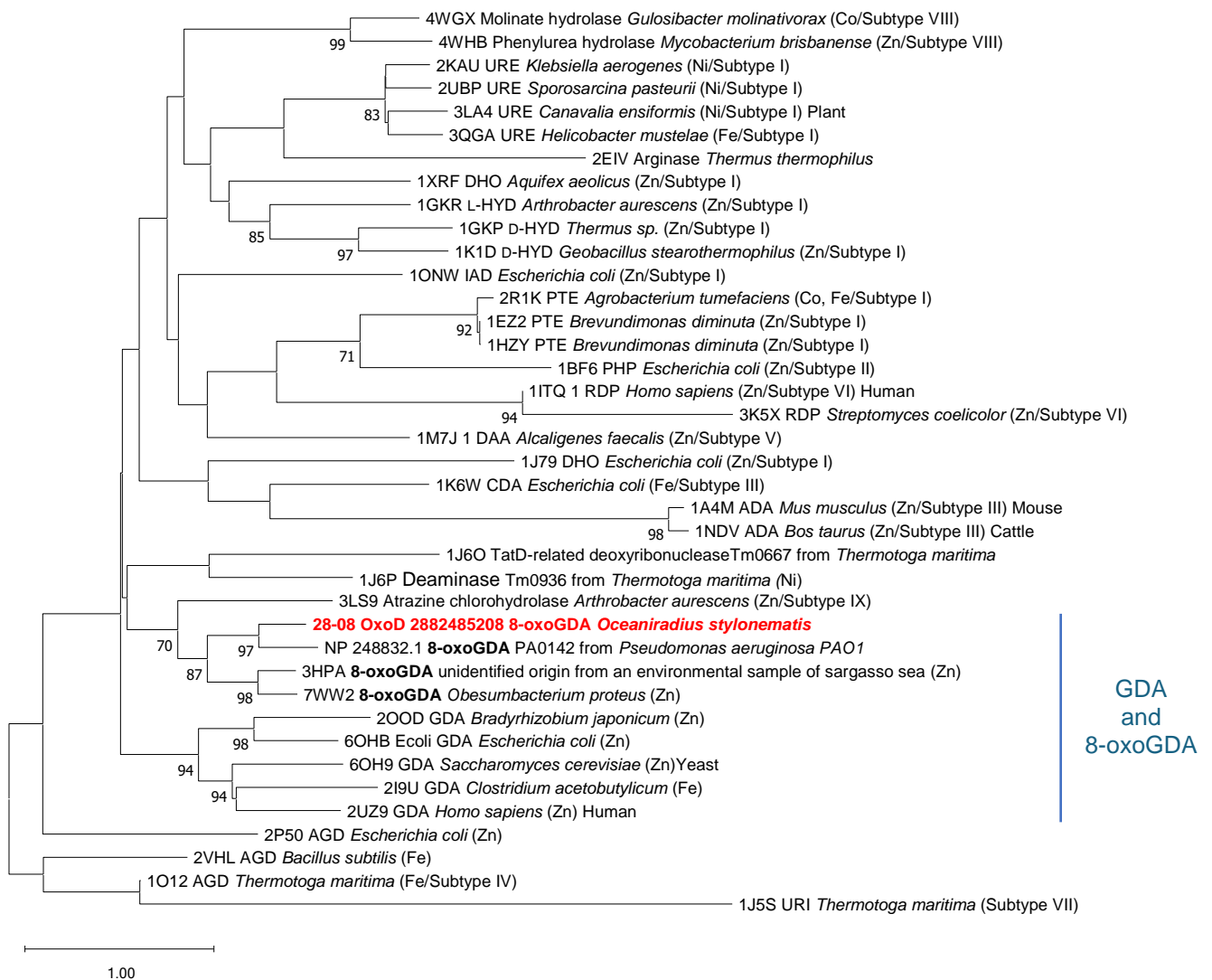


Figure S2: Phylogenetic tree of enzymes of the Amidohydrolase family. 28-08 OxoD clusters with Guanine deaminases (GDA) and 8-oxoguanine deaminases (8-oxoGDA). The phylogenetic tree was constructed with MEGA11 (Tamura, Stecher, & Kumar, 2021) based on the Neighbor-joining method and JTT matrix-based model with 1000 bootstrap replications after multiple alignments with T-Coffee (Notredame et al. 2000), friendly provided by Dr. Yuchen Han.

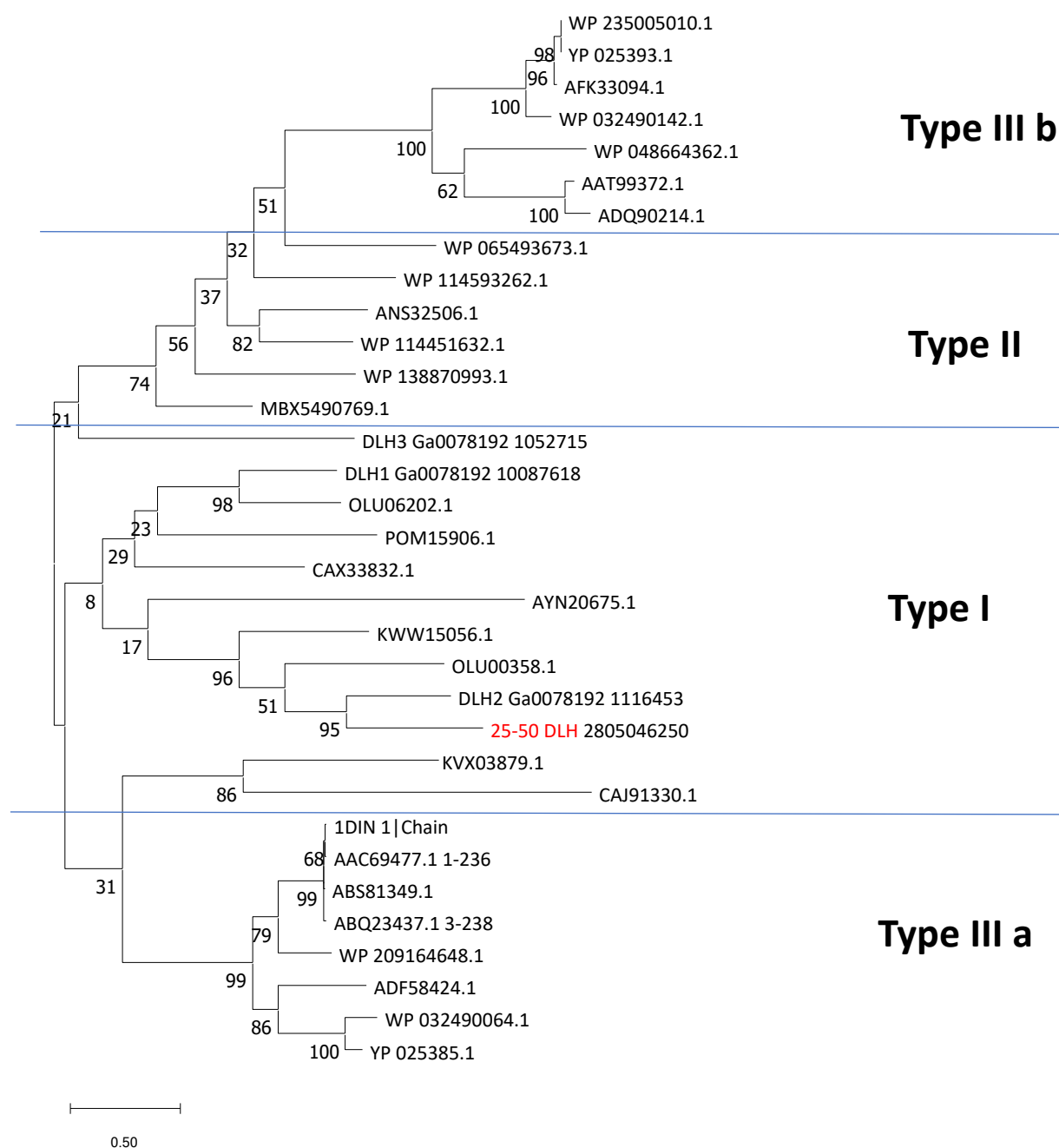


Figure S3: Phylogenetic tree of enzymes of the Dienelactone hydrolase family

The phylogenetic tree was constructed with MEGA11 (Tamura et al. 2021) based on the Neighbor-joining method and JTT matrix-based model with 1000 bootstrap replications after multiple alignments with T-Coffee (Notredame et al. 2000). 28-50 Dlh clusters within Type I Dlh, expecting *trans*-dienelactone hydrolysing activity for 28-50 Dlh. The phylogenetic tree was provided by Dr. Yuchen Han.

9 Acknowledgements

The years spent in AG Streit will always be the most valuable experiences of my working life. Thank you, Prof. Dr. Wolfgang Streit and PD Dr. Ines Krohn for placing your trust in me for the work on projects and with students. As supervisors of this thesis, you have been a great source of inspiration, support and professional exchange. My deepest thanks go to the great team of AG Streit. From group organization, technical survival, keeping chambers running and freezers filled – feel embraced Regina, Nurjan, Angela, Martina and Inka - up to scientific input and open ears for all between questions and despair – I am looking at you Ifey, Pablo, Christel, Eva and Gabi - you all are **the** group! My sincerest thanks go to Yuchen. You combine expertise, kindness and patience in a way, that has been of invaluable help for me and will always be my inspiration. All you folks who walked in and out of lab 3.115, PhD-, M.Sc.-, B.Sc.- students – Lena, Sarah, Marno, Yekaterina, Jascha, Madeleine, Maxime, Lena (W.), Lisa and Johannes - you made my days with your freaky, joyous and nerdy pleasure to create knowledge but not forgetting fun anytime. My heartfelt thanks go to the co-writers of all published papers and those in draft for discussion, exchange, expanding the laboratory repertoire and your hospitality with special regards to Gunhild and Simone.

Finally, nothing would have been possible without my most beloved family. You gave me roots, you gave me courage, it was all worth it – because of you.